ANALYSIS AND COMPARISON OF THE CONTRAST ENHANCEMENT TECHNIQUES FOR INFRARED IMAGES

A THESIS SUBMITTED TO
THE GRADUATE SCHOOL OF NATURAL AND APPLIED SCIENCES
OF
MIDDLE EAST TECHNICAL UNIVERSITY

BY

ARIF ERGÜN TURAN

IN PARTIAL FULFILLMENT OF THE REQUIREMENTS
FOR
THE DEGREE OF MASTER OF SCIENCE
IN
ELECTRICAL AND ELECTRONICS ENGINEERING

FEBRUARY 2012

Approval of the thesis:

ANALYSIS AND COMPARISON OF THE CONTRAST ENHANCEMENT TECHNIQUES FOR INFRARED IMAGES

submitted by **ARİF ERGÜN TURAN** in partial fulfillment of the requirements for the degree of **Master of Science in Electrical and Electronics Engineering Department, Middle East Technical University** by,

Prof. Dr. Canan ÖZGEN _____
Dean, Graduate School of **Natural and Applied Sciences**

Prof. Dr. İsmet ERKMEN _____
Head of Department, **Electrical and Electronics Engineering**

Prof. Dr. Gözde B. AKAR _____
Supervisor, **Electrical and Electronics Eng. Dept., METU**

Examining Committee Members:

Prof. Dr. Aydın ALATAN _____
Electrical and Electronics Engineering Dept., METU

Prof. Dr. Gözde B. AKAR _____
Electrical and Electronics Engineering Dept., METU

Prof. Dr. Tolga ÇİLOĞLU _____
Electrical and Electronics Engineering Dept., METU

Assist. Prof. Dr. Ahmet Oğuz AKYÜZ _____
Computer Engineering Dept., METU

Lütfi Murat GEVREKCİ, PhD. _____
MGEO, ASELSAN

Date: 06.02.2012

I hereby declare that all information in this document has been obtained and presented in accordance with academic rules and ethical conduct. I also declare that, as required by these rules and conduct, I have fully cited and referenced all material and results that are not original to this work.

Name, Last Name : Arif Ergün TURAN

Signature :

ABSTRACT

ANALYSIS AND COMPARISON OF THE CONTRAST ENHANCEMENT TECHNIQUES FOR INFRARED IMAGES

Turan, Arif Ergün
M.Sc., Department of Electrical and Electronics Engineering
Supervisor: Prof. Dr. Gözde B. Akar

February 2012, 126 pages

Today, infrared cameras are used especially for target tracking and surveillance operations. However, they have a high dynamic range output, and the standard display devices cannot handle them. In order to show them on common devices, the dynamic range is cropped. Thus, the contrast of the image is reduced. This is called as the High Dynamic Range (HDR) Compression. Although several algorithms have been proposed for preserving details during the HDR compression process, it cannot be used to enhance the local contrasts of image contents.

In this thesis, we compare the performances of contrast enhancement techniques, which are suitable for real time applications. The methods experimented are generally histogram based methods. Some modifications are also proposed in order to reduce computational complexity of the process. Performances of these methods are compared with common objective quality metrics on different image sets.

Keywords: Infrared, Contrast Enhancement, High Dynamic Range Compression

ÖZ

KIZILÖTESİ GÖRÜNTÜLER İÇİN KONTRAST ZENGİNLEŞTİRME TEKNİKLERİNİN ANALİZİ VE KARŞILAŞTIRILMASI

Turan, Arif Ergün
Yüksek Lisans, Elektrik-Elektronik Mühendisliği Bölümü
Tez Yöneticisi: Prof. Dr. Gözde B. Akar

Şubat 2012, 126 sayfa

Günümüzde, kızılötesi kameralar özellikle hedef takibi ve gözetimi işlemleri için kullanılmaktadır. Fakat bu cihazlar yüksek dinamik aralıkta çıkış verdikleri için standart görüntüleme cihazları bu çıkışları işleyemez. Bu çıkışları standart cihazlarda gösterebilmek için dinamik aralıkları kesilmektedir. Böylece görüntünün kontrastı azaltılmaktadır. Bu işleme Yüksek Dinamik Aralık Sıkıştırma adı verilmektedir. Yüksek Dinamik Aralık Sıkıştırma işlemi esnasında detayın korunması için birçok yöntem önerilmesine rağmen bu işlemler yerel kontrastı zenginleştirmek için kullanılamaz.

Bu tezde, performansları açısından gerçek zamanlı uygulamalara uygun karşıtlık zenginleştirme tekniklerini karşılaştırıyoruz. İncelenen metodlar genellikle histogram tabanlı metodlardır. Ayrıca işlemlerin sayısal karmaşıklığını azaltmak için bazı değişiklikler önerilmiştir. Bu metodların performansı nesnel test metrikleri ile karşılaştırılmıştır.

Anahtar Kelimeler: Kızılötesi, Kontrast İyileştirme, Yüksek Dinamik Aralık Sıkıştırma

To My Parents …

ACKNOWLEDGEMENTS

Firstly, I wish to express my deepest gratitude to my supervisor Prof. Dr. Gözde B. AKAR for her guidance, advice, criticism, encouragements and insight throughout my thesis research.

I also express my sincere gratitude to my managers and my colleagues from ASELSAN INC. and ASELSAN INC. itself, for their initiative ideas and guidance that helped to construct this work.

I wish to thank to my friends, who never stop their encouragement and always continue to motivate me.

I would like to express my greatest thanks to my parents Şenol Turan and Erol Turan, my brother Ç. Kaan Turan and my sister Gülsen Turan for their endless support and patience through my education.

TABLE OF CONTENTS

LIST OF FIGURES

FIGURES

LIST OF TABLES

TABLES

LIST OF ABBREVIATONS

AMBE	: Absolute Mean Brightness Error
AMHE	: Adaptively Modified Histogram Equalization
BCLAHE	: Balanced Contrast Limited Adaptive Histogram Equalization
BG	: Background
BR	: Border Region
CDF	: Cumulative Distribution Function
CLAHE	: Contrast Limited Adaptive Histogram Equalization
CR	: Corner Region
DE	: Discrete Entropy
DPS	: Detail-Preserving Stretching
DRC	: Dynamic Range Compression
EUBC	: Entropy Used by Chen
EWLFC	: Enhancement with Local Frequency Cues
EWLFC-KM	: Distance matrix calculation is replaced with KMeans operation in EWLFC
EWLFC-KMMSD	: Enhancement with mean and standard deviation by using KMeans operation
EWLFC-M-SD	: Frequency information is replaced with mean and standard deviation in EWLFC
EWLFC-WTC	: Frequency information is replaced with Wavelet Transform coefficient in EWLFC
FIR	: Far Infrared
HDR	: High Dynamic Range
HE	: Histogram Equalization
HEBMs	: Histogram Equalization Based Methods
HM	: Histogram Matching
HVS	: Human Visual System

ICUBC	: Intensity Contrast Used by Chen
IR	: Infrared
LDR	: Low Dynamic Range
LWIR	: Longwave Infrared
MI	: Mutual Information
MWIR	: Midwave Infrared
NEDT	: Noise Equivalent Temperature Difference
NIR	: Near Infrared
PDF	: Probability Density Function
PHE	: Plateau Histogram Equalization
RE	: Relative Entropy
SSIM	: Structural Similarity
SWIR	: Shortwave Infrared
TPHE	: Tail-less Plateau Histogram Equalization
TRC	: Tone Reproduction Curve
TRO	: Tone Reproduction Operator
UIQI	: Universal Image Quality Index
UMBMs	: Unsharp-Masking Based Methods

CHAPTER 1

INTRODUCTION

Human Visual System (HVS) is a good perception system with the aid of brain in the visible spectrum. However, this system also has its limits at night, and in adverse weather conditions. There are a lot of efforts in different areas to compensate this problem. For example, night vision and infrared systems are developed for improving the perception and data gathering in place of the human visual systems in such conditions. These systems operate in different spectral bands and have superior performance. Especially, infrared imaging systems have the tasks of target acquisition and tracking. These systems consist of sensors and digitalizing units. Sensors receive continuous heat radiation from the surface and target to produce electrical outputs. Digitalizing units produce pixel values at the output.

Although infrared systems provide thermal information, which is impossible for human perception, they also have limitations. Thermal radiation from an object is affected from scattering due to the atmospheric conditions [1, 2]. Scattering decreases the radiation received by a detector. The net effect is the low visibility of scene and reduced contrast. The high dynamic range requirement of the infrared systems is another problem for standard display devices. These displays generally have 8-bit output dynamic range and cannot show raw infrared images.

Dynamic range compression and contrast enhancement techniques are the main solution to the problems associated with IR images. Dynamic range compression

is performed in order to reduce bit size to the standard display level. These techniques are generally divided into two main branches. These are tone reproduction curve (TRC) and tone reproduction operator (TRO) methods [5]. TRC methods use a simple transformation curve to obtain final pixel values while TRO methods use different transformation curves for the same pixel intensity depending on its neighbors or spatial location. TRC based methods are used in this thesis for their real time performance and low computational complexity.

Contrast enhancement is a crucial operation for IR images due to their reduced contrast because of the scattering. These operations improve overall contrast and visibility of the details. In the literature, there are lots of contrast enhancement operations. They are divided into categories [9]. Histogram based methods use an input histogram to improve visibility and detail information. Unsharp masking based methods only improve edge details in given images, and so they are unsuitable for IR images, which already suffer from reduced visibility. They can be used as post-processing methods. There are also methods, which do not fit in these two categories. Enhancement with local frequency cues is proposed in [5], and authors tried enhancement of the target region determined with clustering operation based on the frequency information.

1.1 Scope of the Thesis

This thesis investigates histogram based enhancement techniques and enhancement with local frequency cues for infrared images. Histogram based techniques are preferred for their popularity, performance and computational complexity. They are ideal for real time applications. Modifications are also proposed for some of these methods in order to improve performance and solve problems associated with the local enhancement.

Dynamic range compression is performed in order to reduce bit size to the standard display level. Contrast enhancement methods are applied to improve

visibility and detail information in 8-bit images after dynamic range compression operation.

Different image sets are used to experiment on these techniques, and results are compared according to the objective quality metrics. All enhancement methods and quality metrics are implemented in Matlab environment.

There are investigations in the literature in this area. However, none of them investigates all the enhancement techniques in this thesis with detail.

1.2 Thesis Outline

This thesis is composed of six chapters. Chapter 1 explains the general information about the necessity of contrast enhancement in infrared imaging and scope of the thesis. Chapter 2 gives brief information about infrared imaging and high dynamic range compression techniques. Chapter 3 covers contrast enhancement techniques. These techniques are summarized, and sample output images are presented for each algorithm. Some modification schemes are suggested in Chapter 4. In Chapter 5, brief information about objective quality metrics is given with experiment results. Chapter 6 gives a summary of this thesis with possible future studies and works.

CHAPTER 2

INFRARED IMAGING AND HIGH DYNAMIC RANGE COMPRESSION

2.1 Infrared Imaging Systems

Human visual system (HVS) is a good sensor in the visible spectrum with aid of the brain. However, this system cannot adapt well to all environment conditions. Infrared imaging (IR) systems have satisfying performance at night, and in adverse weather conditions. They have the tasks of target acquisition and tracking in place of the human visual system in such conditions.

IR imaging systems operate in a different spectral band than the human visual system. It is called infrared spectral band. It extends from 0.7 to 300 μm and can be divided into several imaging bands. They are presented in Table 2-1. Generally, three spectral bands are used for IR imaging. These are shortwave, midwave and longwave bands. IR detectors are available for these separate ranges. Each of them operates on one specific range due to the restrictions. These restrictions come out from the amount of thermal radiation, emissivity and transmission of atmosphere [1].

Table 2-1 Infrared Imaging Bands

Spectral Band	Symbol	Wavelength Range (μm)
Near infrared	NIR	0.7-1
Shortwave infrared	SWIR	1-3
Midwave infrared	MWIR	3-5
Longwave infrared	LWIR	8-12
Far Infrared	FIR	>12

2.2 Infrared Thermal Imaging Parameters

Infrared spectrum bands are selected according to the specific application types. There are factors, which affect this choice [1]. These are:

- Thermal Radiation
- Emissivity
- Atmospheric transmittance

2.2.1 Thermal Radiation

Thermal radiation is the continuous emission of energy from a surface [2]. The emitted energy depends upon the surface temperature and surface characteristics. Any object which is at a temperature above absolute zero temperature (0°K) emits thermal radiation [2].

Thermal radiation from an object is attenuated via absorption or scattering, and then it is received by Infrared (IR) detectors. Apart from the object of interest, the atmosphere and warm objects in the background also emit radiation into the direction of IR detector. This radiation creates a varying electrical signal in the detector array. It is amplified to create a visible image at the output of the imaging system.

2.2.2 Emissivity and Kirchhoff's Law

The thermal radiation is very important for imaging systems because it defines the signal quality at the output of an imaging system. The amount of thermal radiation emitted is defined with emissivity. For example, blackbody is called as the perfect emitter of thermal radiation. It can absorb incident radiation in any case and emits more radiation than any surface. Its absorption is independent of wavelength and direction. Therefore, emissivity is described with aid of blackbody. Emissivity of

an object is the ratio of the amount of radiation emitted from a surface and absorbed by blackbody at the same temperature [1].

Emissivity can be expressed with different parameters. Kirchhoff's Law states the equality of the amount of radiation emitted and absorbed by the same object [1]. It is expressed as follows:

$$\in = \alpha \,, \tag{2.1}$$

where $\in$ denotes the emissivity and α denotes the absorptivity. According to the energy conservation law, any radiation incident on any object is either reflected, transmitted or absorbed [1]. It is expressed as follows:

$$1 = r + t + \alpha \,, \tag{2.2}$$

where r denotes reflectance, t denotes transmittance. They are the fractions of radiance, which are reflected and transmitted respectively. Equations (2.1) and (2.2) are combined as follows:

$$\in = 1 - (r + t) \tag{2.3}$$

Emissivity is expressed with the reflectance and transmittance. Clearly, emissivity is equal to 1 for reflectance and transmittance of 0. Infrared defectors have an average emission value for their respective spectral bands. They can operate at wider wavelength ranges to detect more object radiance. However, this will cause the problem for average emission value selection. Therefore, they use smaller spectral bands to define better emissivity value.

2.2.3 Atmospheric Transmittance

The atmosphere is composed of numerous gases and aerosols. These constituents absorb and scatter radiation in its transmission path from target to IR system. Thus, thermal energy is reduced. This reduction in radiation is the result of atmospheric transmittance [2]. These constituents are at ambient temperature, and they also radiate energy. The radiation accumulated along the line of sight is called path radiance, and it prevents the visibility of the objects of interest in adverse weather conditions [2]. The effect of the low visibility is the reduced contrast in IR sensor.

Atmospheric transmittance is a function of path length. It causes problems over a long distance due to the high reduction in the radiance, and so IR system will generate a low system response. If this response is lower than the system noise level, then the signal will be lost.

Atmospheric conditions also affect IR system performance. For example, high humidity reduces atmospheric transmittance by causing aerosols to grow. Aerosols are invisible particles in the air, and they consist of dust, dirt, carbon, minute organism, sea salt, water droplets and, etc. Concentration of these particles differs from place to place. Scattering is directly proportional to the ratio of particle diameter to the wavelength. Scattering is minimum when the ratio is low and vice versa. This ratio increases with high humidity. Thus, it can lead a low IR system performance, although the weather is clear and visibility is high according to the human visual system (HVS).

2.3 Imaging System Output

Infrared systems consist of sensors and digitalizing units to produce pixel values at the output. Irradiance falling on a sensor is directly proportional to the scene radiance and produces electrical outputs [3]. The digitalizing units take these

analog signals and convert them to digital outputs. However, some restrictions are placed on the sensing devices. Sensing elements generally do not produce the same output value for the same image irradiance. This non uniformity is corrected for a specific sensing element with the formulation below.

$$P(x, y, t) = g \times I(x, y, t) + \emptyset + n(x, y, t)\,, \tag{2.4}$$

where I and n are the irradiance falling on the sensing element and noise introduced by IR system at time t respectively; g is the gain, and ∅ is the offset values at pixel location (x, y).

2.4 High Dynamic Range IR Imaging

The real world exhibits a wide range of luminance values. The ratio between the maximum and minimum intensity values of the world scene image is called as high dynamic range. The main reason for using the HDR imaging is to show low and high contrast objects to the human observer simultaneously. Many system designs use the HDR imaging principles to produce output with competitive performance to the human visual system.

Dynamic range is a very important problem for infrared imaging because the temperature difference between the target and background is a decisive parameter for system design. Both background and target radiate large amount of energy. If a low dynamic range (LDR) system is used for imaging, then the intensity difference between them will be low at the output. This leads to serious problems and requires careful settings of both gain and offset values to compensate [2]. Thus, HDR imaging is the main preference for many IR system designs.

Another reason to use such a high dynamic range for IR imaging is to record more detailed temperature measurement for the analysis. It is a very important process to measure thermal sensitivity. Thermal sensitivity is the smallest differential

temperature which can be detected by the IR detector [2]. It is also called noise equivalent temperature difference (NEDT). If more levels are assigned to the noise measurement, then detail information will be lost for low dynamic range images. Therefore, output is expressed with more bits to examine all detail information. For example, the dynamic range of an 8-bit system with NETD value 0.1℃ is calculated as follows [2]:

$$Dynamic\ Range = 256\left(\frac{0.1}{4}\right) = 6.4℃ \tag{2.5}$$

In this example, the NETD range is divided into four levels for accurate noise measurement. The resulted output temperature range is insufficient for IR imaging. Therefore, more bits are assigned to the system.

2.5 High Dynamic Range Compression

High dynamic range imaging systems have resolutions between 12 and 16 bit. However, standard display devices generally use very low dynamic ranges. These devices are used in many areas by the human observers. This is possible due to the sensitivity of the human eye to the relative intensity changes rather than the amount of intensity changes. Figure 2-1 shows the dynamic range compression operation. There are lots of algorithms to reduce high dynamic range to the standard display level. They can be collected in two categories. These are tone reproduction curve (TRC) and tone reproduction operator (TRO) methods [5, 7].

The TRC methods use a simple transformation curve to obtain final pixel values. They are also called global high dynamic range compression methods. These operations compress high input dynamic range to narrower ones at the output. The transformation is applied to each pixel independently, and so operation can be performed with a lookup table. The general formulation for an input image I and output image O is set up as follows:

$$O = T(I)\,, \tag{2.6}$$

where T is the one to one and monotonic tone reproduction curve. Curve function must be monotonic, or else it will change the color of the image parts such as edges. Traditional TRC curves can be implemented to all HDR images with single parameter changing.

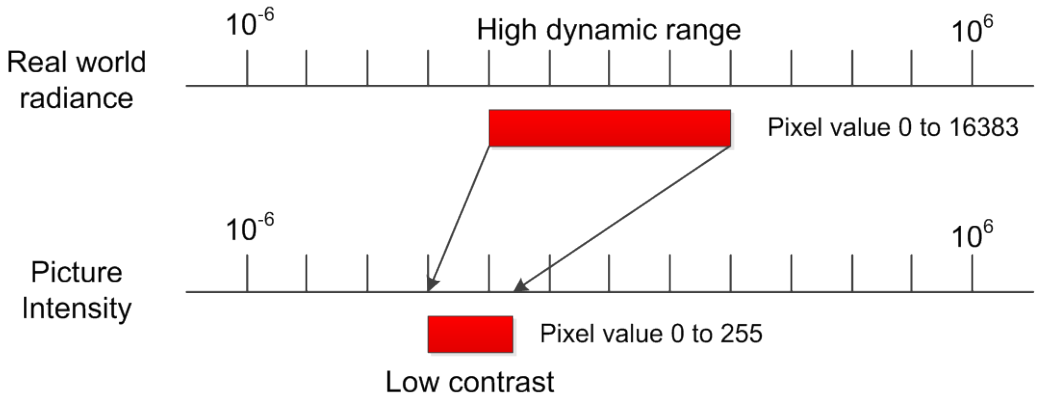

Figure 2-1 Dynamic Range Compression Operation

Tone reproduction operations transform same pixel intensities to the different values depending on the spatial location and neighboring pixels. They are also called local high dynamic range compression methods. This transformation operation has several curves to produce display intensity values, and so it is not one to one. However, the TRO methods usually behave like TRC operations on small local regions. These methods use a model to express HDR images. The general concept of the model is formulated for an input image I as follows:

$$I(x,y) = L(x,y)R(x,y), \tag{2.7}$$

where L and R are the illumination and scene reflectance components respectively. Illumination is the amount of light source incident on the scene

viewed, and scene reflectance is the amount of light source reflected by the objects [6]. Scene reflectance has low dynamic range in the absence of wide illumination variations. It contains all detail information about scene and determined by the characteristics of the objects. On the other hand, illumination is determined by the light source. Therefore, the main concern of TRO methods is to extract these two parts and then generate LDR image with reducing the dynamic range of illumination component.

Computational complexities of these two methods are different. TRC methods use simple transformation curves to calculate LDR images, and their computational complexities are very simple. TRO methods use spatial processing and are computationally expensive.

HDR compression is a step applied to obtain low dynamic range images before contrast enhancement operations, and HDR compression methods were not compared in this thesis. There are two types of dynamic range compression techniques used to obtain 8-bit images. These are:

- HDR compression techniques used in contrast enhancement operation
- HDR compression techniques applied before contrast enhancement operations

Some contrast enhancement techniques have dynamic range compression operations merged with their algorithm. These types of enhancement methods generally use TRC based methods to compress high dynamic range of an input image. Balanced CLAHE method used in this thesis also has this feature [19]. This method is explained in Chapter 3. In this thesis, TRC based methods are used for other contrast enhancement techniques to obtain LDR images before enhancement procedures due to their performances and computational complexities.

There are also methods merging the properly exposed parts of the same scene to obtain a better result after dynamic range compression. This is accomplished by using the shorter or longer exposure times. Shorter exposure times give the details of bright parts of the image while longer exposure times give the details of darker parts. However, this process requires image fusion operation, and so these methods are out of scope for this thesis.

2.5.1 HDR Compression Techniques Used In Thesis

In the literature, there are lots of techniques to compress high dynamic range [7, 8, 10]. Some of them are used in this thesis to produce LDR images before contrast enhancement operations. The operations used are:

- Linear Scaling
- Non-Linear Scaling
- Histogram Adjustment

2.5.1.1 Linear Scaling

Linear scaling is a global operator and can be used to compress high dynamic range [7]. It is the simplest way to create a LDR image from HDR one. High input luminance value is linearly scaled to the lower output dynamic range. This is accomplished as follows:

$$I' = k\left(\frac{I(x,y) - I_{min}}{I_{max} - I_{min}}\right), \tag{2.8}$$

where k is the maximum intensity value of the display device; I_{max} and I_{min} are the maximum and minimum intensity values of an input image. IR images use only a small partition of the input dynamic range. However, histogram of an IR image generally has a noise component, which spreads to the dynamic range. It creates

confusion about the global maximum and minimum values of the given image. Therefore, linear scaling generates low contrast images. This problem leads to undesirable effects such as flattened structures. Images, which contain satisfying overall contrast, are achieved with introducing a clipping operation to this method. It forces the frequency values at the beginning and end of the histogram to zero. In other words, it forces the cumulative distribution function to saturation at these regions. This operation prevents the effect of noise component over linear scaling. The results of linear scaling with and without a clipping operation are presented in Figure 2-2. Clip limit is selected as 1% for both upper and lower partition of the histogram.

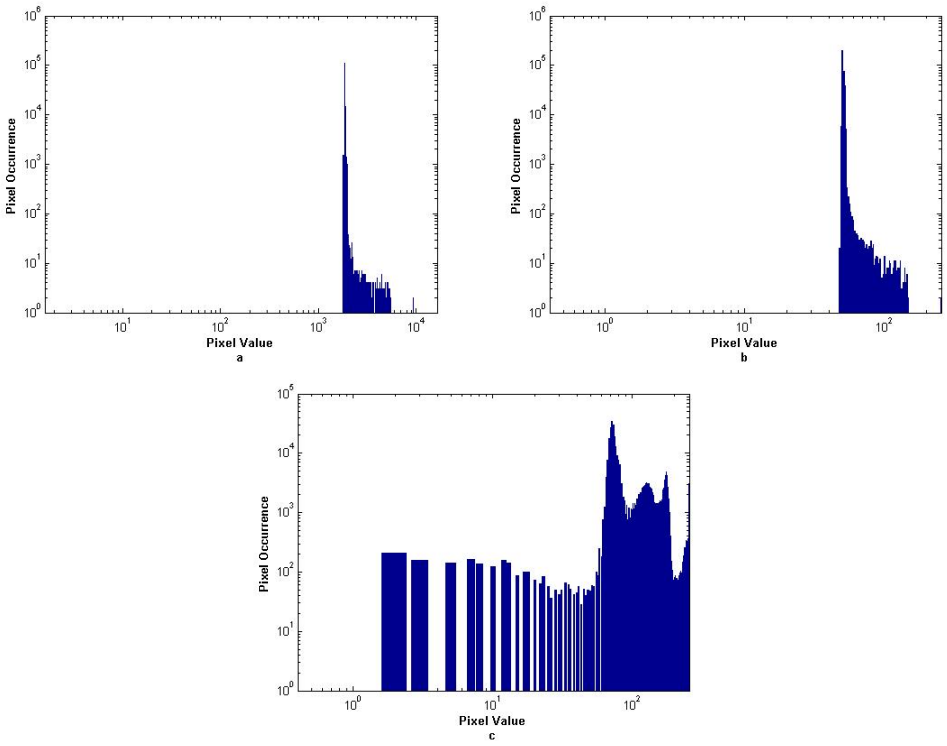

Figure 2-2 Output Histograms of High Dynamic Range Compression with Linear Scaling (a) Original Histogram, (b) Final Histogram without a clipping operation, (c) Final Histogram with a clipping operation

2.5.1.2 Non-Linear Scaling

Non-Linear scaling is another one to one and monotonic global operator for high dynamic range compression. This method compresses an input image with an exponent value. It either compresses the lower or higher end of the image histogram while the other parts have low compression [7]. Non-Linear scaling is achieved with gamma value γ as follows:

$$I' = k\left(\frac{I(x,y) - I_{min}}{I_{max} - I_{min}}\right)^{\gamma}, \tag{2.9}$$

where k is the maximum intensity value of the display device; I_{max} and I_{min} are the maximum and minimum intensity values of an input image. If gamma value is smaller than 1, then bright pixel values are amplified. If gamma value is greater than 1, then dark pixel values are amplified. Clipping operation can be used in non-linear scaling in order to suppress noise components in the histogram. The results of non-linear scaling with and without a clipping operation are presented in Figure 2-3. Clip limit is selected as 1% for both upper and lower partition of the histogram.

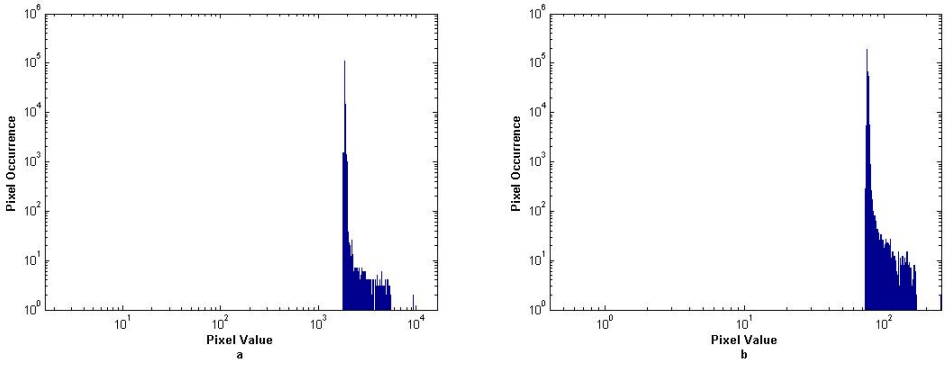

Figure 2-3 Output Histograms of High Dynamic Range Compression with Non-Linear Scaling (a) Original Histogram, (b) Final Histogram without a clipping operation (gamma=0.75)

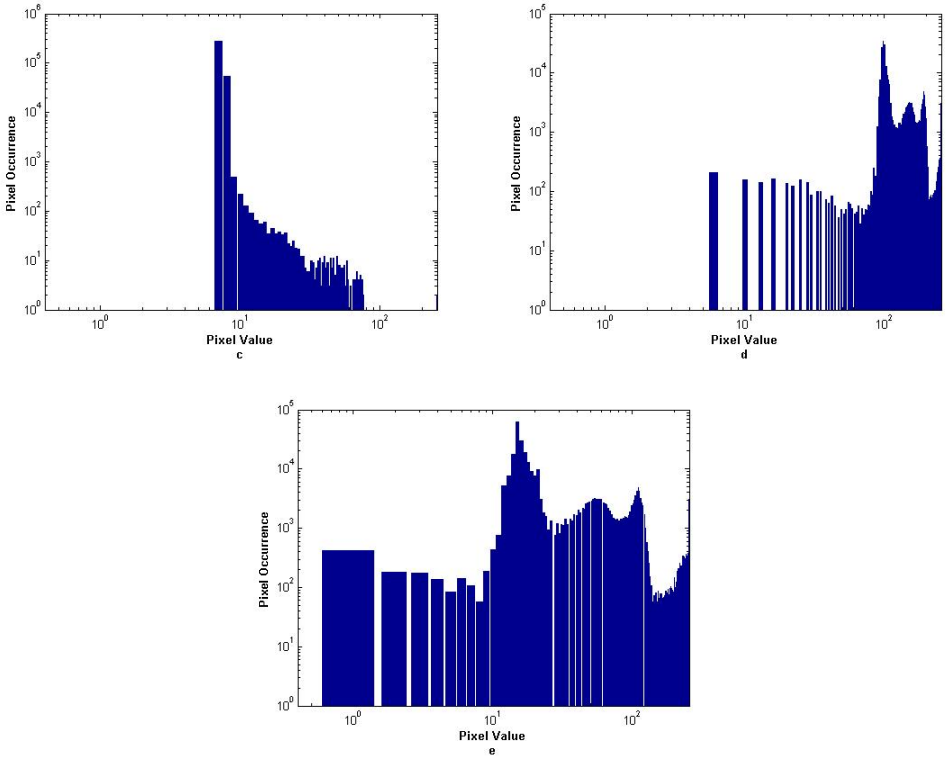

Figure 2-3 Output Histograms of High Dynamic Range Compression with Non-Linear Scaling (c) Final Histogram without a clipping operation (gamma=2.2), (d) Final Histogram with a clipping operation (gamma=0.75), (e) Final Histogram with a clipping operation (gamma=2.2) (continued)

2.5.1.3 Histogram Adjustment

Ward proposed a technique to compress high dynamic range images with a modified histogram equalization based method [8]. Histogram is used as a starting point to preserve contrast difference in the image after high dynamic range compression.

Firstly, this method calculates the histogram and cumulative distribution functions from the original HDR image. Histogram is taken between the maximum and minimum intensity values. 100 histogram bins were found sufficient for the experiments of Ward. Cumulative distribution function is calculated from the frequency counts of the histogram as follows:

$$CDF(x) = \frac{\sum_{i<x} p(i)}{T}, \tag{2.10}$$

where T is the total number of frequency counts, and it is calculated as follows:

$$T = \sum_{x=1}^{N} p(x) \tag{2.11}$$

In this formulation, N is the number of histogram bins and p(x) is the frequency count corresponding to the pixel value x. Cumulative distribution function is an integration function, and histogram equals to its derivative with appropriate normalization factor. It is calculated by Ward as follows:

$$\frac{\partial CDF(x)}{\partial x} = \frac{p(x)}{T\Delta x}, \qquad \Delta x = \frac{(log(L_{wmax}) - log(L_{wmin}))}{N}, \tag{2.12}$$

where L_{wmax} and L_{wmin} are the maximum and minimum world luminance values for the scene respectively. Step size Δx is calculated at the logarithmic scale. It is same for each histogram bin because histogram values with equal probabilities are desired at the output. Display luminance values are calculated with cumulative distribution function at the logarithmic scale. It is:

$$\log\big(L_d(x)\big) = \log(L_{dmin}) + [\log(L_{dmax}) - \log(L_{dmin})]CDF\big(\log\big(L_w(x)\big)\big), \tag{2.13}$$

where L_{dmax} and L_{dmin} are the maximum and minimum display luminance values. Equation (2.13) causes over enhancement at large object areas due to the property of histogram equalization. Histogram equalization technique is mentioned briefly in Chapter 3. Over enhancement is suppressed with a proper threshold value. Clearly, derivative of display luminance with respect to the real-world luminance is not greater than their ratio. Threshold value is found with this equation. It is:

$$\frac{\partial L_d}{\partial L_w} \leq \frac{L_d}{L_w}, \tag{2.14}$$

where L_d and L_w are display and real-world luminance values respectively. Equation (2.13) is placed in (2.14), and the new equation is:

$$e^{\log(L_d)} \frac{p(L_w)}{T\Delta x} \frac{[\log(L_{dmax}) - \log(L_{dmin})]}{L_w} \leq \frac{L_d}{L_w} \tag{2.15}$$

This equation is reduced to a simpler form as follows:

$$p(L_w) \leq \frac{T\Delta x}{\log(L_{dmax}) - \log(L_{dmin})} \tag{2.16}$$

Equation (2.16) defines a restriction for histogram adjustment operation with a threshold. If all histogram frequency counts of HDR image are smaller or equal to the right side of this equation, then final histogram will not cause over enhancement. Ward's method continues to iterate until fewer than 2.5 percent of the histogram frequencies exceed the threshold value. Output of histogram adjustment method is shown with different clipping percentages in Figure 2-4.

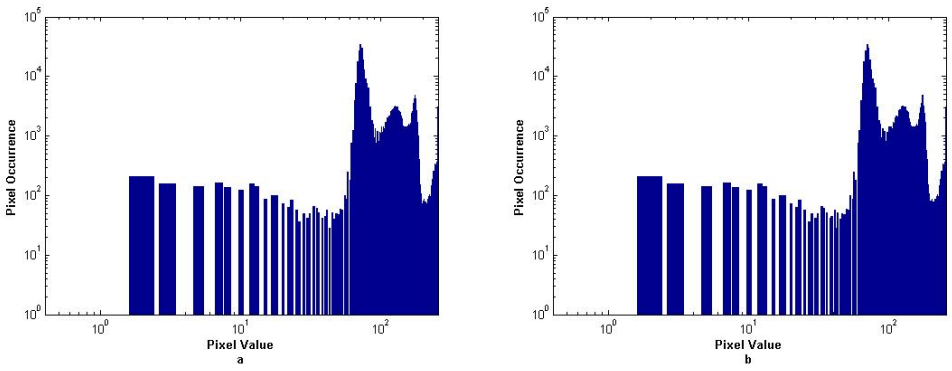

Figure 2-4 Output Histograms of High Dynamic Range Compression with Histogram Adjustment (a) Final Histogram with 2.5% threshold, (b) Final Histogram with 10% threshold

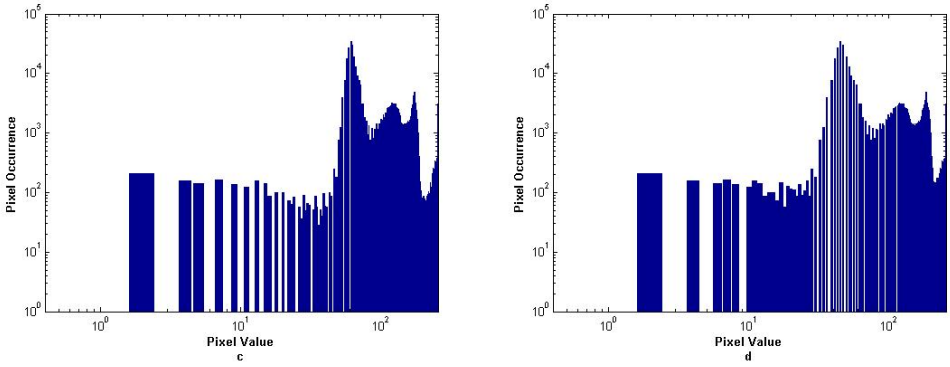

Figure 2-4 Output Histograms of High Dynamic Range Compression with Histogram Adjustment (c) Final Histogram with 20% threshold, (d) Final Histogram with 40% threshold (continued)

This method gives similar results to the linear scaling for small clipping percentages. If this value is increased, then the final histogram will spread more to the entire display range.

CHAPTER 3

CONTRAST ENHANCEMENT METHODS

3.1 Introduction

High Dynamic Range Compression (HDRC) method reduces the perception of small targets or details. This result prevents the good understanding of the scene. The method which is used to improve visibility is called contrast enhancement. There are several algorithms in the literature for contrast enhancement. They can be grouped under three main branches [12]. These methods are:

- Histogram equalization based methods HEBMs
- Unsharp-masking-based methods UMBMs
- Methods, which do not belong to any of these two categories

HEBMs use the image statistics for contrast enhancement. Image histogram, probability density function (pdf), and cumulative distribution function (cdf) are the most-used parameters for these types of operations. These methods are very fast and have wide application areas. For example, a general framework based on histogram equalization is presented in [23] and authors proposed an enhancement technique based on histogram modification.

UMBMs use the high and low frequency components of an input image. The general structure of these methods is represented as follows [12]:

$$I^{out}(x,y) = I^{in}(x,y) + \propto \left[I^{in}(x,y) - I^{in}_{avg}(x,y)\right] \quad (3.1)$$

In this formula, I^{in} and I^{out} denote the input and output images respectively; I_{avg}^{in} denotes the average image obtained by filtering the input image with smoothing filter. The primary objective of these methods is to enhance detail information rather than improving the visibility.

3.2 Contrast Enhancement Methods

Contrast enhancement methods used in this thesis are selected by considering the real time implementations. Therefore, some computationally complex methods are ignored and HEBMs are generally selected. The implemented methods are: Histogram Equalization Method [6], Histogram Matching (Histogram Specification) Method [6], Plateau Histogram Equalization Method [14], Tail-less Plateau Histogram Equalization Method [12], Adaptively Modified Histogram Equalization Method [15], Detail-Preserving Stretching Method [17], Contrast Limited Adaptively Modified Histogram Equalization (CLAHE) Method [18], Balanced Contrast Limited Adaptive Histogram Equalization Method [19], Detail Enhancement Method with Local Frequency Cues [24].

3.2.1 Histogram Equalization Method

This method uses the concept of spreading pixel values in the given image to the entire histogram more uniformly [6]. This way, the unseen scene details are more visible to the observer. This method uses the histogram of the input image and brings it to its ideal uniform form. Histogram is constructed by calculating the pixel frequencies for the entire dynamic range of the input image. Pixel frequency represents the number of times a gray level seen in the input image. This frequency can be interpreted as the probability density function (pdf). It is calculated as follows:

$$PDF(k) = \frac{p_k}{p} \qquad 0 \leq k \leq 2^m - 1 \qquad (3.2)$$

In this formulation, p_k represents the frequency of the pixel level k with image depth m, and p is the total number of pixels in the input image. Pixel values in the input image are random variables. Thus, the probability of the pixel value k in the given image is less than or equal to the sum of probability density function up to pixel level k. This operation is called as cumulative distribution function (cdf) and it is calculated as follows:

$$CDF(k) = \sum_{l=0}^{k} PDF(l) \qquad 0 \leq k \leq 2^m - 1 \qquad (3.3)$$

Finally, the transformation of the pixel value from input to output is calculated as follows:

$$k' = (2^n - 1) \times CDF(k) \qquad 0 \leq k \leq 2^m - 1\,, \qquad (3.4)$$

where k' denotes the value corresponding to the pixel value k in the enhanced image with depth n.

The histogram equalization method has less computational complexity. However, it is also clear that this method converts the pixel values with higher-frequency counts to the very large gray level intervals. This means that small details disappear between the objects with high frequencies (background, large objects, etc.) at the output image. A sample input image and the output of histogram equalization operation can be seen in Figure 3-1.

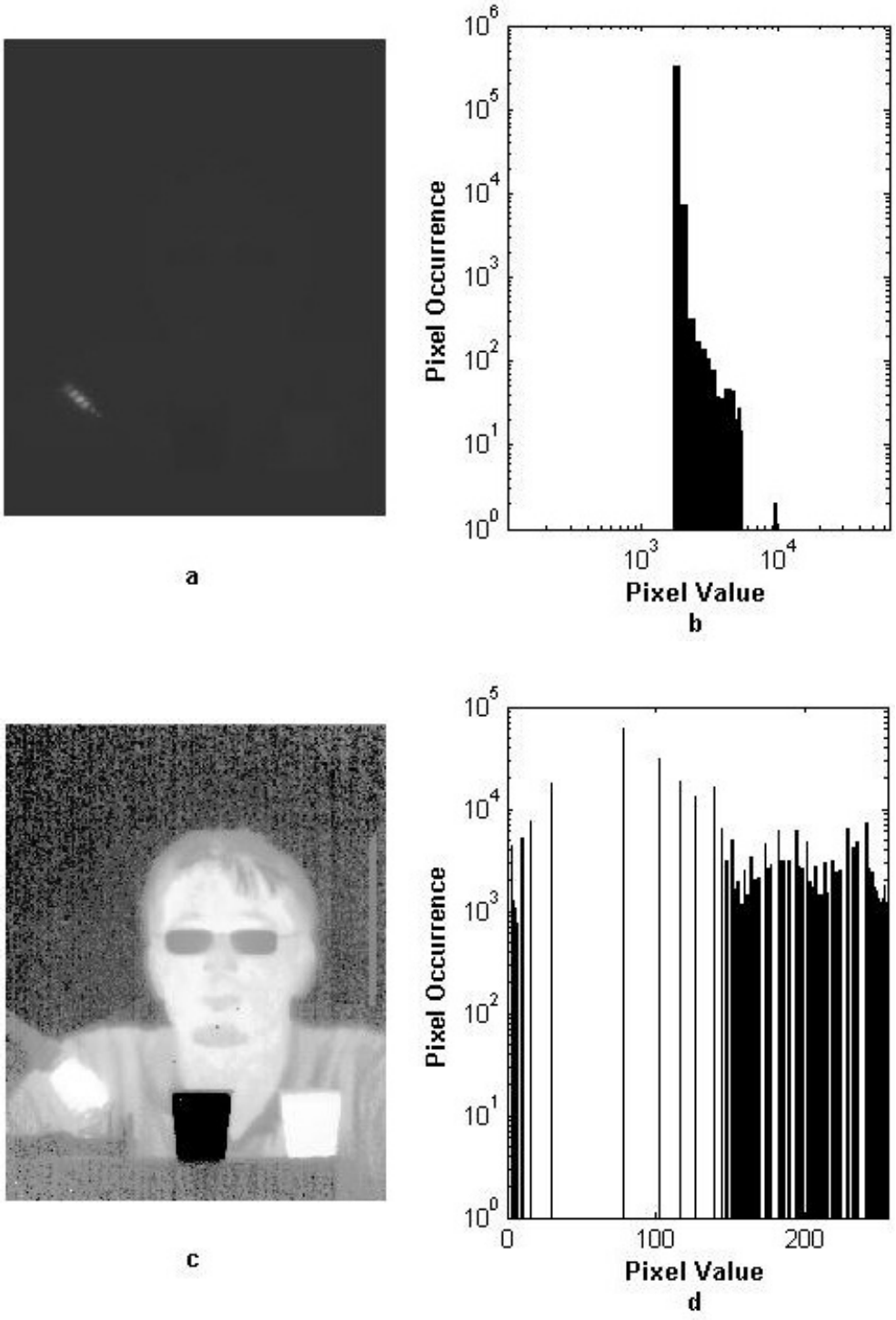

Figure 3-1 Input and Output of Histogram Equalization Method (a) 14-bit Input, (b) Histogram of The Input Image, (c) 8-bit Output, (d) Histogram of The Output Image

3.2.2 Histogram Matching (Histogram Specification) Method

This method produces an output image for applications, which needs a specific histogram distribution scheme. The histogram of an input image is converted to the desired output with matching of the histograms [6]. This method achieves its purpose with two-stage transformation. There are two values k and z, which correspond to the intensity values of the input and enhanced images respectively. The first step of the algorithm is to calculate the transformation function for input image. PDF_I denotes the probability density function of the input image; CDF_I denotes the cumulative distribution function of the input image, and T denotes the transformation function.

$$PDF_I(k) = \frac{p_k}{p} \qquad 0 \le k \le 2^m - 1 \tag{3.5}$$

$$CDF_I(k) = \sum_{l=0}^{k} PDF_I(l) \qquad 0 \le k \le 2^m - 1 \tag{3.6}$$

$$T(k) = (2^m - 1) \times CDF_I(k) \qquad 0 \le k \le 2^m - 1 \tag{3.7}$$

The second step of the algorithm is to calculate the transformation function for the output image. PDF_O denotes the probability density function of the output image; CDF_O denotes the cumulative distribution function of the output image, and G denotes the transformation function for the desired output image.

$$PDF_O(z) = \frac{p_z}{p} \qquad 0 \le z \le 2^n - 1 \tag{3.8}$$

$$CDF_O(z) = \sum_{l=0}^{z} PDF_O(l) \qquad 0 \le z \le 2^n - 1 \tag{3.9}$$

$$G(z) = (2^n - 1) \times CDF_O(z) \qquad 0 \le z \le 2^n - 1 \tag{3.10}$$

The final step of the algorithm is to obtain the output image with inverse transformation. It is realized as follows:

$$z = G^{-1}\big(T(k)\big) \tag{3.11}$$

The output of histogram matching method applied to the image in Figure 3-1 (a), and the histogram of the output can be seen in Figure 3-2. The output in (a) has pixel intensity values in the range [30,220] while the output in (c) has pixel intensity values in the range [50,150].

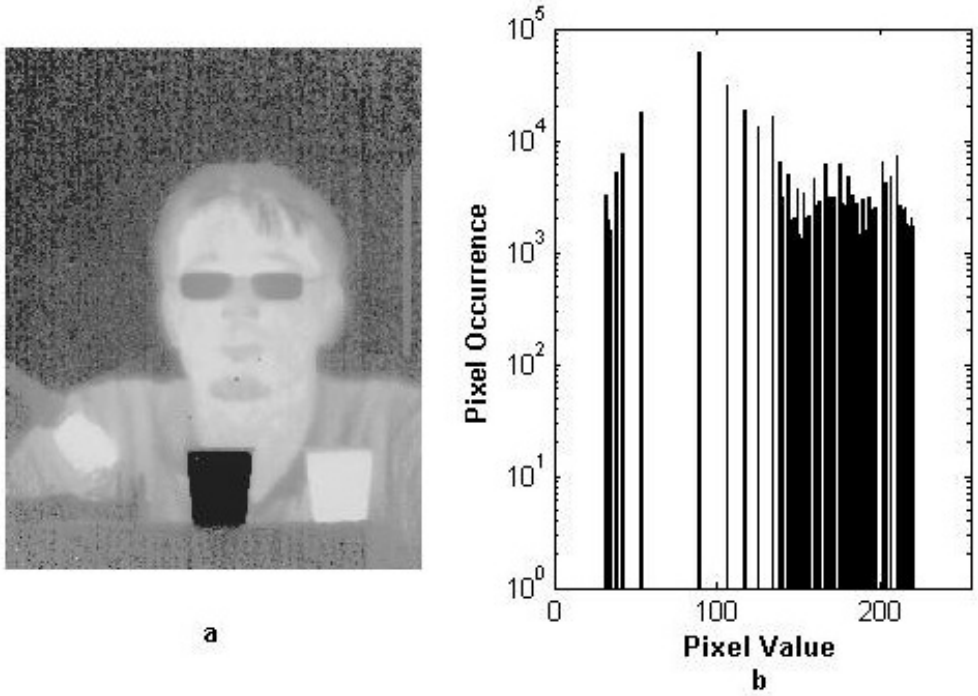

Figure 3-2 Output of Histogram Matching Method (a) 8-bit output with Interval [30,220], (b) Histogram of The Output in (a)

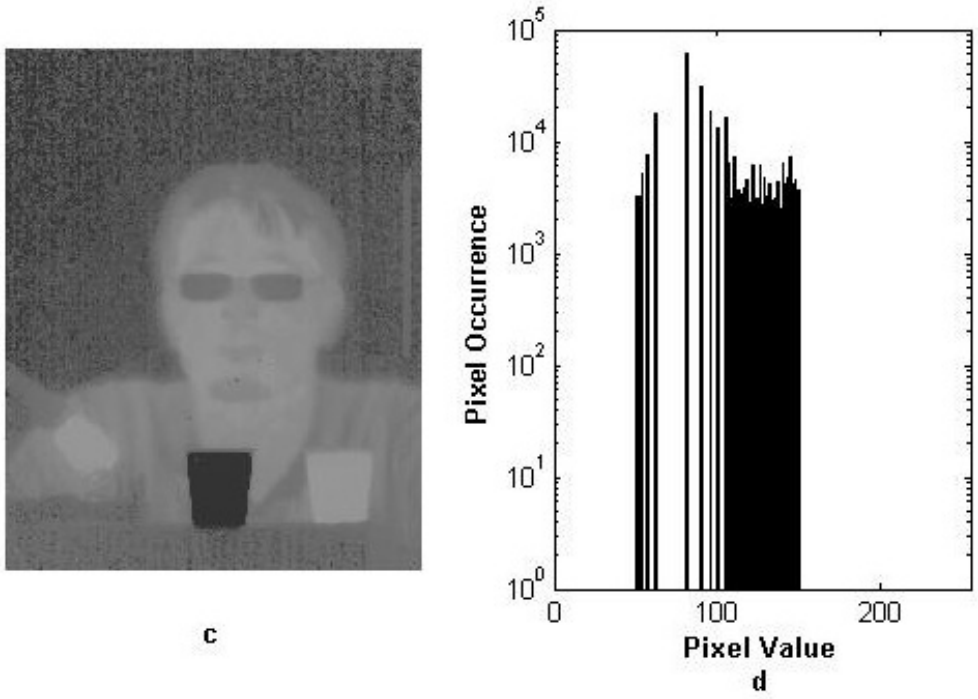

Figure 3-2 Output of Histogram Matching Method (c) 8-bit Output with Interval [50,150], (d) Histogram of The Output in (c) (continued)

The primary aim of this method is to obtain uniform gray level distribution between the upper and lower limits. However, it gives similar results to the histogram equalization, because there is no control over higher histogram frequencies. Therefore, over enhancement is introduced at the final image.

3.2.3 Plateau Histogram Equalization Method

This method is the modified version of the histogram equalization. Histogram equalization method covers the entire dynamic range of the output histogram. Therefore, it provides a fine contrast enhancement. However, histogram equalization method assigns a large gray level interval to the objects with high frequencies (background, large objects, etc.). This method introduces a plateau threshold value to the histogram equalization algorithm in order to suppress over enhancement in the final image [14].

If the frequency of an object background is limited to a threshold value, then the gray level spectrum of the object background will be less than the expected values. This process provides better enhancement of the targets in the final image.

An appropriate threshold value T is used to limit the frequencies of the objects in the input histogram. Any frequency which is greater than the threshold value T is made equal to T. If it is smaller than T, then it is left unchanged. It is implemented in the probability density function as follows:

$$PDF_T(k) = \begin{cases} PDF(k), PDF(k) \leq T \\ T, PDF(k) > T \end{cases} \qquad 0 \leq k \leq 2^m - 1\,, \qquad (3.12)$$

where k denotes the pixel value in the input image; PDF(k) denotes the occurrence value of pixel level k in the original histogram, and $PDF_T(k)$ denotes the probability density function after thresholding operation. The cumulative distribution function is calculated as follows:

$$CDF(k) = \sum_{l=0}^{k} PDF_T(l) \qquad 0 \leq k \leq 2^m - 1\,, \qquad (3.13)$$

where k' denotes the value corresponding to the k in the enhanced image, and it is calculated as follows:

$$k' = \left(\frac{(2^n - 1) \times CDF(k)}{CDF(2^m - 1)} \right) \quad 0 \leq k \leq 2^m - 1 \ \ and \ 0 \leq k' \leq 2^n - 1 \quad (3.14)$$

3.2.3.1 Selection of the Threshold Value

The threshold value of the plateau histogram equalization affects the output performance of the algorithm. It is very clear that this algorithm turns into the histogram projection if T equals to 1, and it turns to histogram equalization if T equals to the maximum frequency value in the histogram. It is very likely that this

maximum value corresponds to the background of the image because the background generally has the higher frequency in the original histogram. An appropriate threshold value prevents the excessive gray level stretching for background area. Therefore, objects in the original image will be enhanced greatly while suppressing the object background.

Apart from a manual threshold selection, an adaptive method for the calculation of the threshold value T is proposed in [14]. The processes of this algorithm are as follows:

- Histogram is calculated from the input image.
- Median filter is applied to the histogram for the window size 3. This operation smooths the rapid frequency change in the histogram.
- Nonzero histogram values are obtained from the smoothed histogram.
- F(l) denotes the nonzero frequency value in the histogram, and L denotes the total number of nonzero frequencies. Local minimum values are calculated as follows:

$$Fdif(l) = F(l) - F(l-1) \qquad 0 \le l \le L \qquad (3.15)$$

$$|Fmin(l)| = min\{Fdif(l), Fdif(l+1)\} \qquad 0 \le l \le L \qquad (3.16)$$

- The median value of the local minimum vector is selected as the threshold value.

The output of plateau histogram equalization method applied to the image in Figure 3-1 (a) with an adaptive threshold value and the histogram of the output can be seen in Figure 3-3.

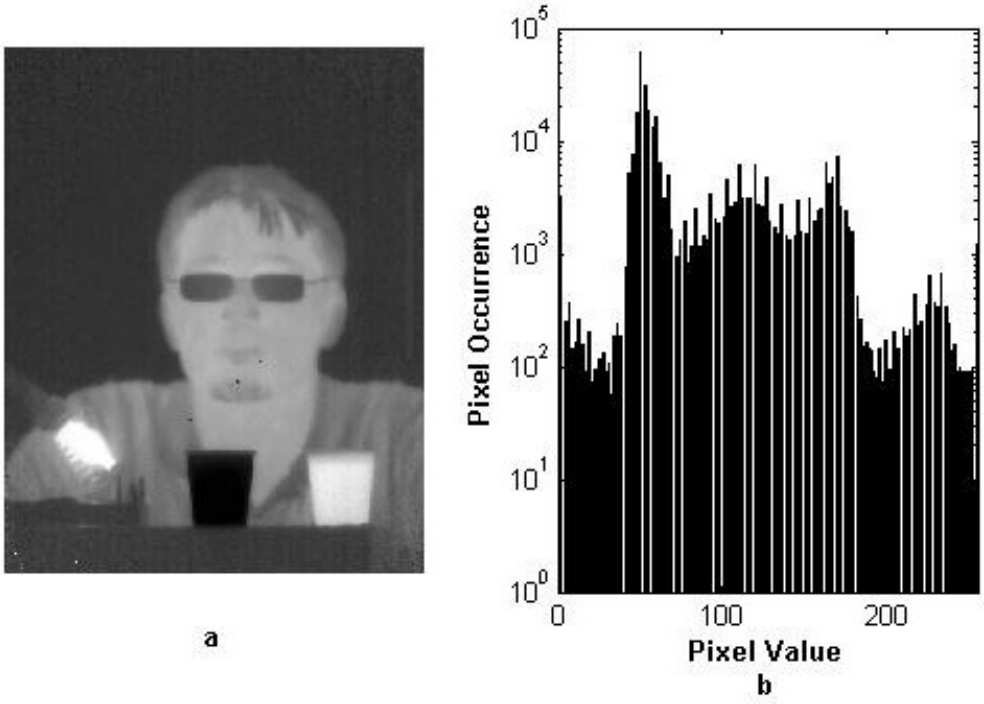

Figure 3-3 Output of Plateau Histogram Equalization Method (a) 8-bit Output, (b) Histogram of The Output

3.2.4 Tail-less Plateau Histogram Equalization Method

This method is the modified version of the plateau histogram equalization. It forces the frequency values at the beginning and end of the histogram to zero, thus forces the cumulative distribution function to saturation [12]. Therefore, resulting histogram gives a better dynamic range for the remaining input values and further enhances the image compared to the plateau histogram equalization method. The performance of this operation depends on the clipping percentage. This percentage, t_{max}, takes a value between 0 and 0.5. $PDF_T(k)$ denotes the frequency value in the histogram after the plateau threshold value is applied, and $CDF_T(k)$ denotes the cumulative distribution value corresponding to the $PDF_T(k)$. This operation is applied as follows:

$$PDF_T(k) = \begin{cases} PDF_T(k), & CDF_T(k) \in [t_{max}, 1 - t_{max}] \\ 0, & otherwise \end{cases} \qquad 0 \leq k \leq 2^m - 1 \quad (3.17)$$

The output of tail-less plateau histogram equalization method applied to the image in Figure 3-1 (a), and the histogram of the output can be seen in Figure 3-4. The output images are calculated for the clipping percentages 0.05, 0.1 and 0.17. This method uses the same adaptive threshold value with plateau method.

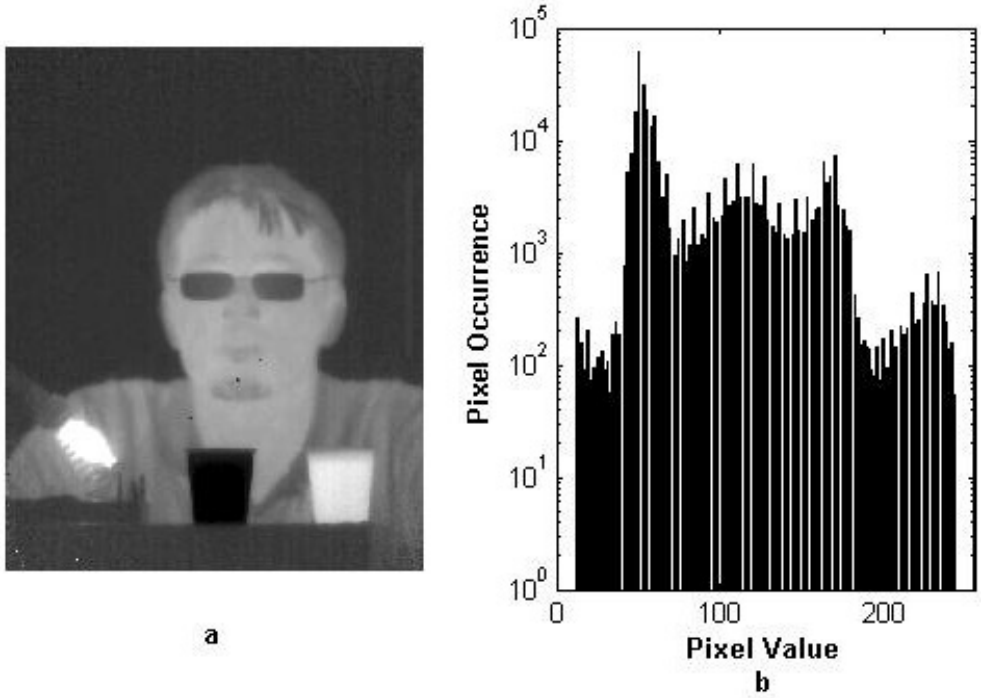

Figure 3-4 Output of Tail-Less Plateau Histogram Equalization Method (a) 8-bit Output with clipping percentage 0.05, (b) Histogram of The Output in (a)

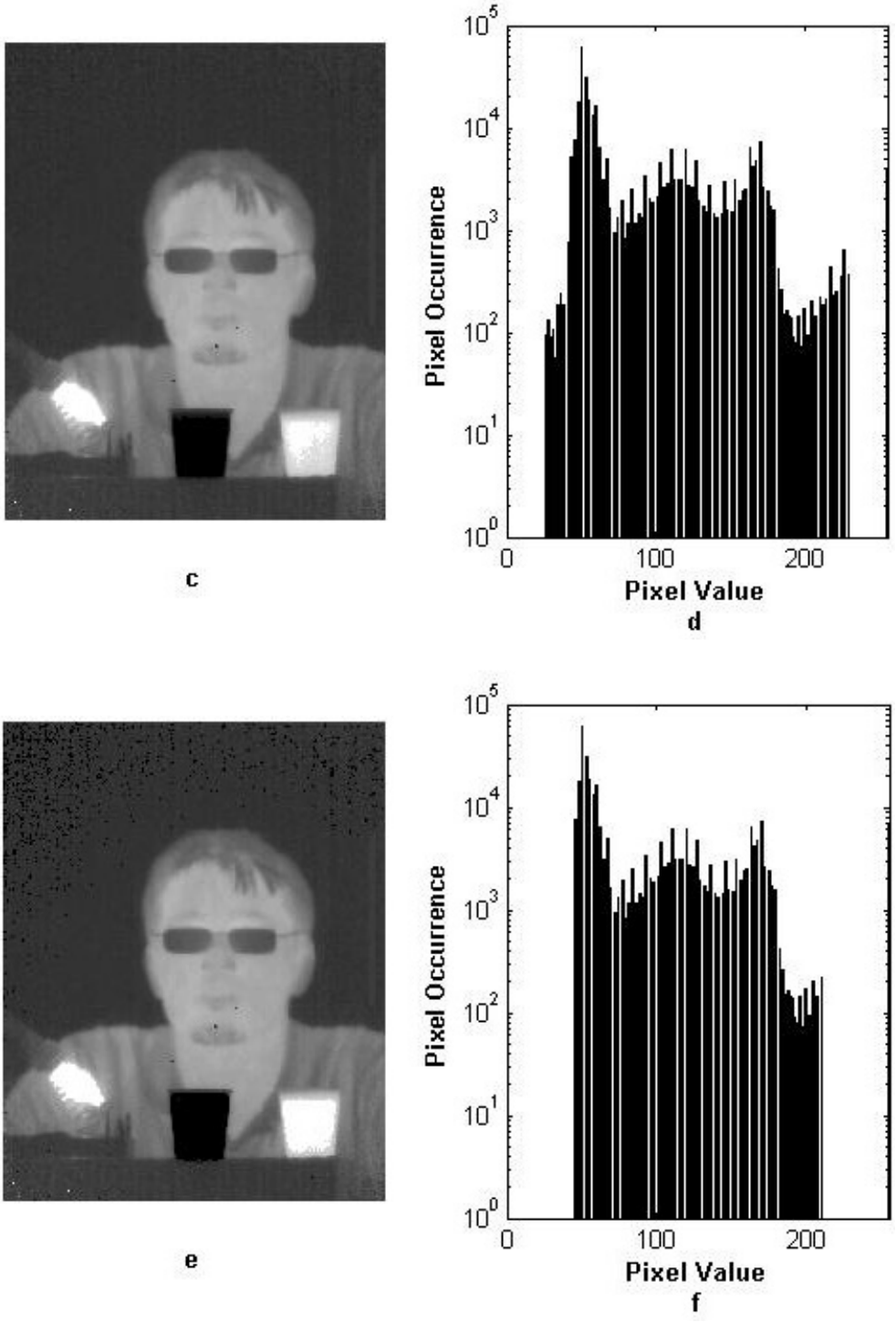

Figure 3-4 Output of Tail-Less Plateau Histogram Equalization Method (c) 8-bit Output with clipping percentage 0.1, (d) Histogram of The Output in (c), (e) 8-bit Output with clipping percentage 0.17, (f) Histogram of The Output in (e) (continued)

It is clear from the Figure 3-4 (e) that high clipping percentages damage the natural structure of the image. Therefore, an appropriate clipping percentage can be selected with experiments.

3.2.5 Adaptively Modified Histogram Equalization Method

A method is proposed in [15] to control enhancement rate and preserve the shape of the histogram. This method is named as Adaptively Modified Histogram Equalization. PDF denotes the probability density function of the input image. The length of the PDF function depends on the depth of an input image. Minimum, maximum and mean frequency values of the PDF function are found as follows:

$$PDF_{MAX} = \max(PDF) \tag{3.18}$$

$$PDF_{MIN} = \min(PDF) \tag{3.19}$$

$$PDF_{MEAN} = \frac{PDF_{MAX} + PDF_{MIN}}{2} \tag{3.20}$$

This mean PDF value is used to divide an image into two sub images. After this, new PDF function is calculated by modifying the upper and lower sub images with their gradient information. The probability density function of the input image is modified as follows:

$$PDF_{AHME}(k) = \begin{cases} \mathrm{PDF}_{MEAN} + \alpha \times \frac{(PDF(k) - PDF_{MEAN})^2}{(PDF_{MAX} - PDF_{MEAN})}, & PDF(k) > PDF_{MEAN} \\ \mathrm{PDF}_{MEAN} - \alpha \times \frac{(PDF_{MEAN} - PDF(k))^2}{(PDF_{MEAN} - PDF_{MIN})}, & otherwise \end{cases} \tag{3.21}$$

The variable α determines the enhancement rate, and it is calculated adaptively. Mean frequency count also corresponds to the mean pixel intensity value. Therefore, these sub images contain intensity values, which are smaller and

greater than the mean intensity value (k_m) of the input image respectively. α is calculated for these two sub images as follows:

$$\alpha = \frac{k_m - k_{ml}}{k_{mu} - k_{ml}}, \qquad 0 \le k \le k_m \tag{3.22}$$

$$\alpha = \frac{k_{mu} - k_m}{k_{mu} - k_{ml}}, \qquad k_m < k \le 2^m - 1 \tag{3.23}$$

The constants k_{mu} and k_{ml} denote the mean values of the first and second sub images respectively. Clearly, the variable has a value for each half of image.

The modified pdf function is set to zero when the equation is negative. The cumulative distribution function (cdf) and final mapping are obtained as follows:

$$CDF_{AHME}(k) = \sum_{l=0}^{k} PDF_{AHME}(l), \qquad 0 \le k \le 2^m - 1 \tag{3.24}$$

$$k' = \frac{CDF_{AHME}(k)}{CDF_{AHME}(2^m - 1)} \times (2^n - 1), \qquad 0 \le k' \le 2^n - 1, \tag{3.25}$$

where k' denotes the value corresponding to the k in the enhanced image. The constants m and n represents the depth of input and output images respectively.

AMHE method divides an input image to two sub images based on the mean histogram frequency value and enhances them separately. It can enhance contrast by preventing the significant change in gray level. This method has better output performance compared to HE. However, it has a higher computational load. The output of AMHE method applied to the image in Figure 3-1 (a) and histogram of the output can be seen in Figure 3-5.

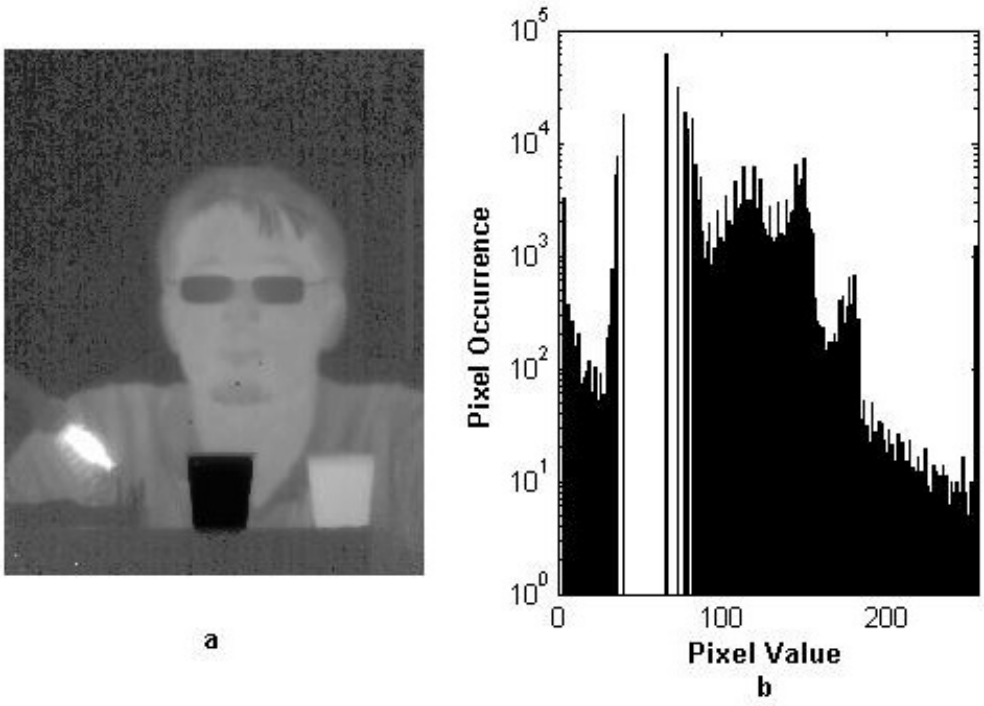

Figure 3-5 Output of AHME Method (a) 8-bit Output, (b) Histogram of The Output

3.2.6 Detail-Preserving Stretching Method

This operation combines the contrast stretching and gradient domain processing operations to obtain a better contrast enhancement scheme for IR images. Contrast stretching is an easy method to apply any input image. However, stretching operation causes to the loss of detail information. Gradient domain processing compensates this problem. This method has two stages of operation [17], and it is explained below.

The output of detail-preserving stretching method applied to the image in Figure 3-1 (a) and histogram of the output can be seen in Figure 3-7.

3.2.6.1 Contrast Stretching Operation

The contrast stretching operation uses a piecewise straight transformation operation. This is shown in the Figure 3-6. The straight-line segments show the transformation from input image to the output image. These lines are modified in order to change the mapping operation. The region which contains the detail information is given a large gray level interval and the region which contains less detail information is given a small grey level interval. The values k1, k2, s1 and s2 determines the shape and position of the lines, and they are constants.

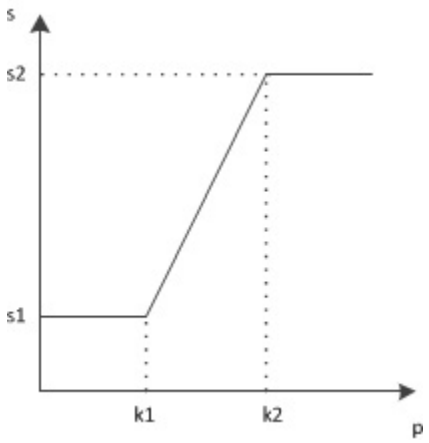

Figure 3-6 Contrast Streching Operation

Detail-Preserving Stretching method uses the mean based stretching operation for contrast enhancement. The mean based stretching uses mean and standard deviation values of the input image to find k1 and k2 values. They are calculated as follows:

$$k1 = m - \alpha \times \sigma \tag{3.26}$$

$$k2 = m + \beta \times \sigma \tag{3.27}$$

In this formula, m denotes the mean and σ denotes the standard deviation of the input image. α and β are the coefficients, which are used to calculate k1 and k2. They are determined according to the experiment results and selected as 3 for Figure 3-7. The complete operation for the contrast stretching is defined as follows:

$$s(k) = \begin{cases} s1, & p(k) < k1 \\ s2, & p(k) > k2 \\ K \times [p(k) - k1] + s1, & otherwise \end{cases} \tag{3.28}$$

In this formula, s(k) denotes the output pixel value and p(k) denotes the input pixel value. The constants s1 and s2 denote the lower and upper saturation limits for the output histogram. K is the stretching gain, and it is calculated adaptively as follows:

$$K = \frac{s2 - s1}{k2 - k1} \tag{3.29}$$

3.2.6.2 Gradient Domain Process

The low and high partitions of the histograms are saturated with contrast stretching operation. Thus, the details at these parts are not visible anymore. Gradient domain approach uses the gradient information of the original image, and the stretching gain K obtained by mean based contrast stretching. It is a local approach with gradient information extracted from pixel locations and their neighbors. The gradient of the stretched image is equal to the gradient of input image multiplied by K for the pixel values between [k1,k2]. It is either zero or smaller than the gradient of input image multiplied by K for the pixel values excluding the interval [k1,k2]. This causes a loss of information at the output image. Therefore, the gradient of the output image is made equal to the gradient of the input image multiplied by K. This causes the output image to differ from stretched image. An additional constraint is added to compensate for this

difference. This constraint is placed to minimize the difference between contrast stretched image v and output image f. The minimization function is set up as follows:

$$\sum_{k\in f} E = \sum_{k\in f} (E_d + E_g) \tag{3.30}$$

In this formula, E is the energy function; E_d is the data cost function and E_g is the gradient cost function. The data and gradient cost functions are defined as follows:

$$E_d = \lambda_d (f - v)^2 \tag{3.31}$$

$$E_g = \lambda_g [(f_x - G_x)^2 + \left(f_y - G_y\right)^2] \tag{3.32}$$

In these formulas, f_x and f_y are the horizontal and vertical derivatives of the output image f; λ_d and λ_g are the weight values; G_x and G_y are the horizontal and vertical parts of the gradient of the input image multiplied by K. This energy function satisfies the Euler-Lagrance equation [17].

$$\frac{\partial E}{\partial f} - \frac{\partial}{\partial x}\frac{\partial E}{\partial f_x} - \frac{\partial}{\partial y}\frac{\partial E}{\partial f_y} = 0 \tag{3.33}$$

The final equation is represented as follows.

$$\frac{\lambda_d}{\lambda_g} f - \left(f_{xx} + f_{yy}\right) = \frac{\lambda_d}{\lambda_g} v - (G_x + G_y) \tag{3.34}$$

In this final formula, f_{xx} and f_{yy} are the horizontal and vertical components of the Laplacian operator. Therefore, this formula can be expressed as follows:

$$\frac{\lambda_d}{\lambda_g} f - \nabla^2 f = \frac{\lambda_d}{\lambda_g} v - \nabla G \tag{3.35}$$

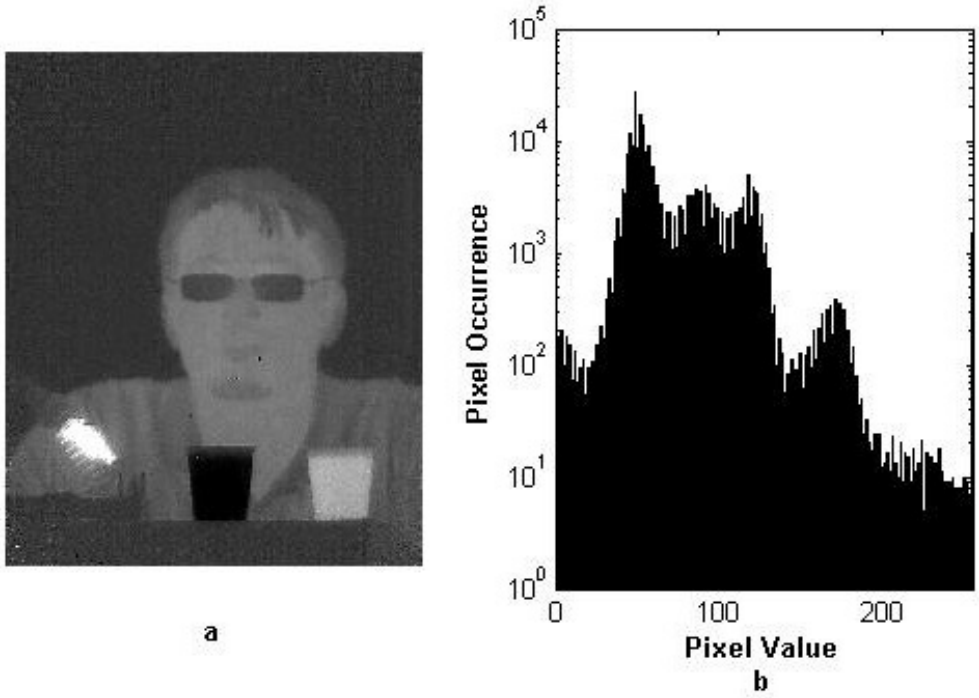

Figure 3-7 Output of Detail-Preserving Stretching Method (a) 8-bit Output, (b) Histogram of The Output

In equation (3.35), weight values are generally set to 1 by authors to get affordable visual quality.

3.2.7 Contrast Limited Adaptively Modified Histogram Equalization (CLAHE) Method

This method uses the same principle with plateau method. Background or large objects have bigger intensity intervals at the output due to their high-frequency counts in the input histogram. The plateau method uses a thresholding operation to limit frequencies of these regions. The excess frequency counts are not used. Thus, over enhancement of the background or large objects are prevented. However, Plateau method does not generate a uniform distribution. Because the input values are spread over to the whole available dynamic range after thresholding operation.

The CLAHE method calculates the histogram of the whole image, and then the histogram is clipped according to the threshold value [18]. After this, it uses the excess frequency counts and distributes them uniformly over the input histogram interval. This operation adds the unused histogram bins of the input image to the mapping calculation and limits the enhancement operation. This way, the resulting image looks more natural.

3.2.7.1 Local Approach

In Local CLAHE operation, the input image is divided into several non-overlapping regions. The histogram of each region is calculated, and these histograms are clipped according to the appropriate threshold value. The clipped frequency values are stored for each region and then redistributed to their histograms. This operation is done in a way that it does not exceed the threshold value. Therefore, resulting histogram will be more linear due to the uniform distribution of the excess pixels. Finally, cumulative distribution function (cdf) is calculated by using the resulting histogram. This cdf is used to calculate pixel mapping function of the respective block. The pixels are mapped to their final value in each block by using the pixel mapping functions of its neighbors. However, there are some special considerations for these mapping operations, and they will be explained later.

The output of CLAHE method applied to the image in Figure 3-1 (a) and histogram of the output can be seen in Figure 3-8. The input image is divided into four blocks in (a), and the threshold value is selected as 27.5% of the total pixels. In other words, 72.5% of the total pixels are trimmed, and they are treated as excess pixels. 16 blocks is used in Figure 3-8 (c). The threshold value selected as 24% of the total pixels. Clearly, local contrast improves with the increment of the block number. However, further increment of the block number causes problem

for CLAHE method. Main problem is the over enhancement of the noise component in the blocks.

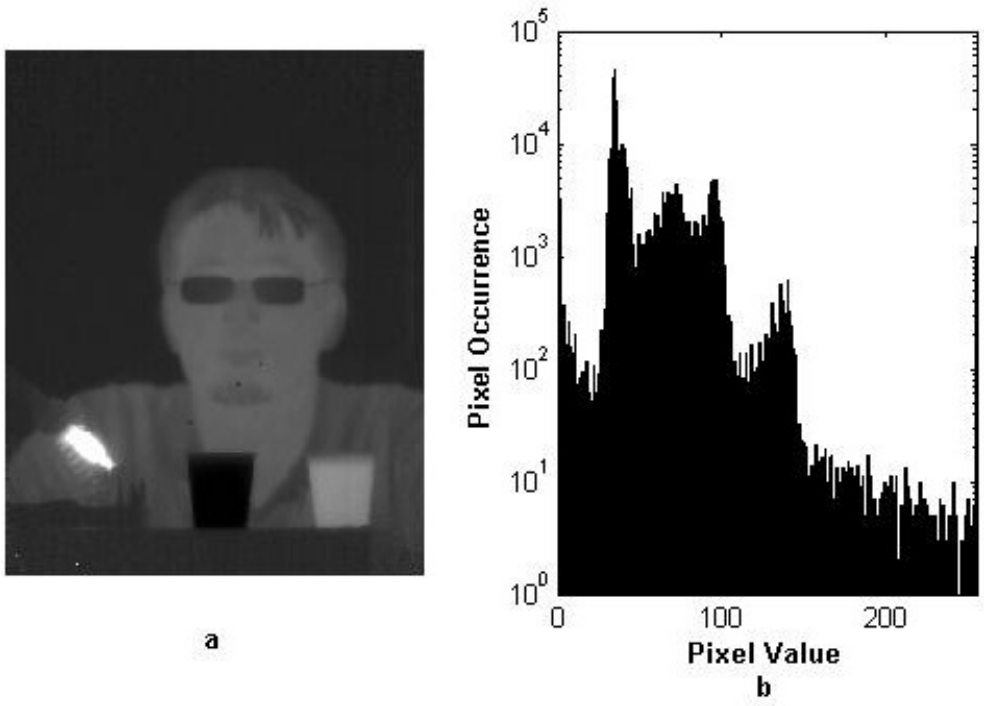

Figure 3-8 Output of CLAHE Method (a) 8-bit Output with 4 block, (b) Histogram of The Output in (a)

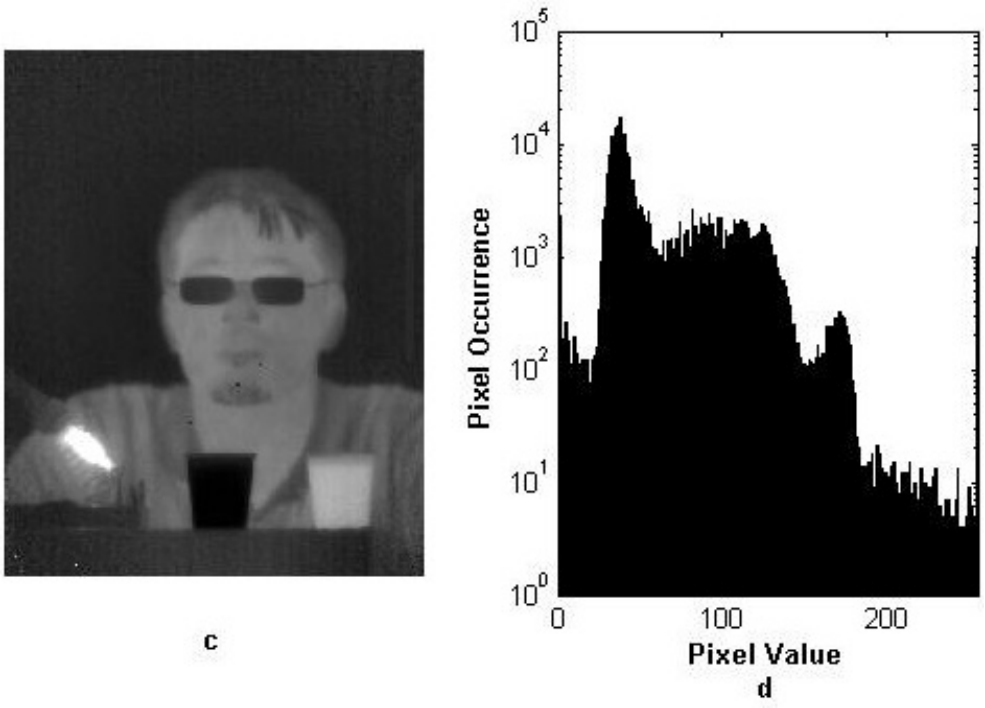

Figure 3-8 Output of CLAHE Method (c) 8-bit Output with 16 block, (d) Histogram of The Output in (c) (continued)

3.2.8 Balanced Contrast Limited Adaptive Histogram Equalization

This method uses an improved version of CLAHE approach. CLAHE method uses a threshold value to limit enhancement of the large objects. It uses the excess frequency counts to limit the spreading of the histogram. However, CLAHE method also distributes excess pixels to the unused histogram bins. This operation limits the enhancement of important details while suppressing background. Balanced CLAHE method makes an improvement to solve this problem. This method distributes excess pixels to the nonzero histogram bins according to the percentage which they have in the histogram after clipping operation. Therefore, shape of the original histogram is preserved. Algorithm ensures that no histogram bin exceed the threshold value. This operation improves the detail enhancement

while suppressing over enhancement of the objects like background, which have less information, to get more intensity intervals. This method uses an approach which is a combination of the histogram and unsharp masking based methods [19].

Firstly, histogram of each block is calculated, and then it is clipped with the threshold T. The formula for this operation is set up as follows:

$$h^{clipped}(k) = \begin{cases} h(k), & h(k) < T \\ T, & h(k) > T \end{cases} \qquad 0 \le k \le 2^m - 1 \qquad (3.36)$$

The excess frequency counts of the histogram are stored and then the contributions of each nonzero block in the clipped histogram are calculated. After this operation, new histogram is calculated with adding excess frequency counts to the histogram with the percentage of each block in the histogram.

$$p(k) = \frac{h(k)}{\sum_{k \in C} h(k)}, C = \{k: h^{clipped}(k) < T\} \qquad (3.37)$$

$$h^{new}(k) = \begin{cases} h^{clipped}(k) + p(k) \times E, & h(k) < T \\ h^{clipped}(k), & h(k) > T \end{cases} \qquad (3.38)$$

In this formula, h^{new} denotes the final histogram and E denotes the total sum of the excess frequency counts after the threshold is applied. If new histogram value exceeds the threshold T again, the algorithm will continue to run in order to prevent this condition. This is one of the main drawbacks of this method. The output of Balanced CLAHE method applied to the image in Figure 3-1 (a) and the histogram of the output can be seen in Figure 3-9. The input image is divided into four blocks, and the threshold value is selected as 21.5% of the total pixels. Further increment of the block number causes problems for Balanced CLAHE method. These problems are explained in Chapter 4.

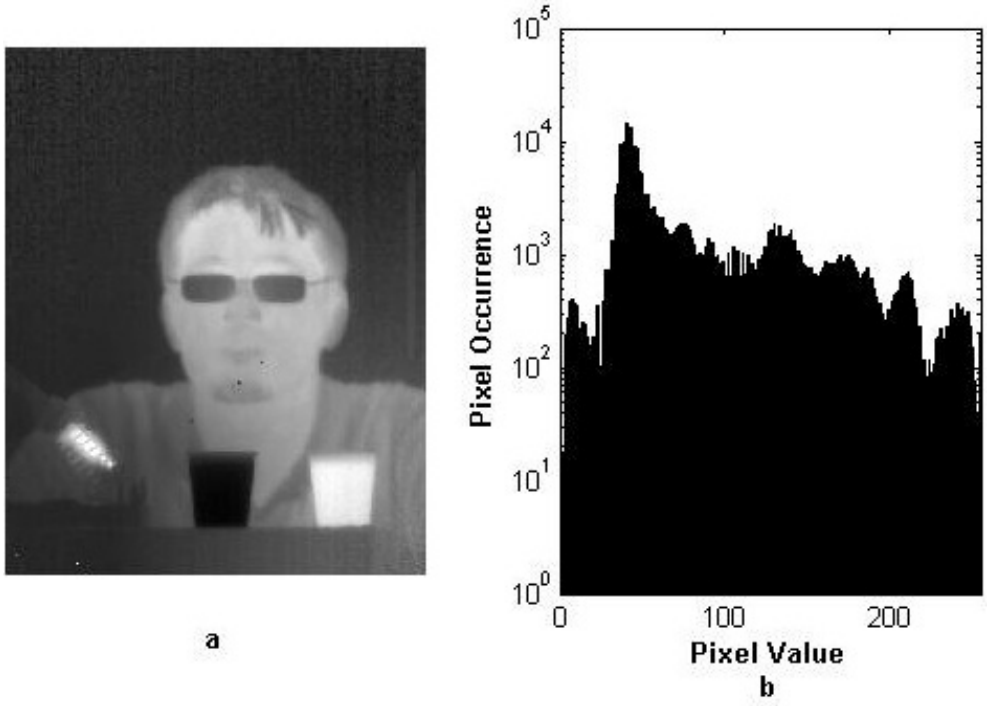

Figure 3-9 Output of Balanced CLAHE Method (a) 8-bit Output, (b) Histogram of The Output

3.2.8.1 Dynamic Range Compression with Balanced CLAHE Method

In this method, Balanced CLAHE operation performs high dynamic range compression task besides contrast enhancement. IR image is concentrated on a small partition of the input histogram. Balanced CLAHE operation is applied to this region. The cumulative distribution function takes the value of zero before this region and the value of 1 after this region. It is used to calculate final pixel mapping function with the aid of further enhancement determined with the ratio of input image and its average version. This ratio improves edge details. These two components constitute a transformation function to scale input dynamic range to the standard display level. The transformation curve takes several shapes depending on $\propto$. The formulation for this operation is set up as follows [19]:

$$f^{out} = p\left(f^{in}(x,y)\right) x \left[\frac{f^{in}(x,y)}{f_M^{in}(x,y)}\right]^{\propto} \tag{3.39}$$

This formula is the linear version. f_{in} and f_{out} denote the input and output images of the algorithm. f_M^{in} is the average image obtained by filtering the input image with an averaging filter. p denotes the non-decreasing linear version of the Balanced CLAHE operation. The logarithm of this formula is obtained as follows:

$$F^{out}(x,y) = P\left(F^{in}(x,y)\right) + \propto \times \left[F^{in}(x,y) - F_M^{in}(x,y)\right] \qquad (3.40)$$

The capital letters represent the logarithmic versions of input image, output image, average image and contrast enhancement method. This representation resembles to the unsharp-masking based methods. The high-frequency component (detail image) is added to the enhanced image with factor $\propto$. This operation further enhances the detail information.

3.2.8.2 Local Approach

In local Balanced CLAHE operation, the input image is divided into several non-overlapping regions. The histogram of each region is calculated. These histograms are clipped according to the appropriate threshold value. The clipped histogram frequency values are stored for each region, and then redistributed to the nonzero bins of the histogram according to their contribution. This operation is done in a way that it does not exceed the threshold value. Operation is repeated until this condition is satisfied. Finally, cumulative distribution function of each region is calculated by using the resulting histogram. This cdf is used to calculate a transformation curve for each block. All regions are merged with the transformation functions of their neighbors to prevent blocking artifacts.

3.2.9 Detail Enhancement with Local Frequency Cues

This method mainly focuses on the detail enhancement operation rather than the contrast enhancement [24]. The input image is divided into the smaller blocks, and each block is labeled as either target or background region according to the

clustering operation. The clusters are separated according to the frequency-domain information of each block.

Firstly, this method divides an input image with dimensions M and N into reasonable b blocks. B1 and B2 are x and y dimensions of each block. After this operation, the Discrete Fourier Transform of each block is computed as follows [24]:

$$F_i(u,v) = \frac{1}{B1 \times B2} \sum_{x=0}^{B1-1} \sum_{y=0}^{B2-1} I_i(x,y) e^{j2\pi[(ux/B1)+(vy/B2)]} \qquad (3.41)$$

The background region has a more smooth frequency response than the target region. The target region has a different frequency response due to its detail information. After the calculation of DFT data, the distances of each block from others are calculated according to the Fourier transform matrix. The cost of this operation is very high. It is also clear that the Fourier transform is a symmetric operation. Therefore, the half of Fourier transform data is used for distance calculation operation. For this purpose, F_i matrix is converted to the 1-D vector by zigzag scanning. Zigzag scanning converts a two-dimensional matrix to one-dimensional vector. It is a very useful technique to convert Fourier transform matrix to one-dimensional vector. The zero-frequency component is shifted to center of the spectrum before this operation. The example of zigzag scanning, which converts 8x8 matrix to the 1x64 vector is shown at Figure 3-10.

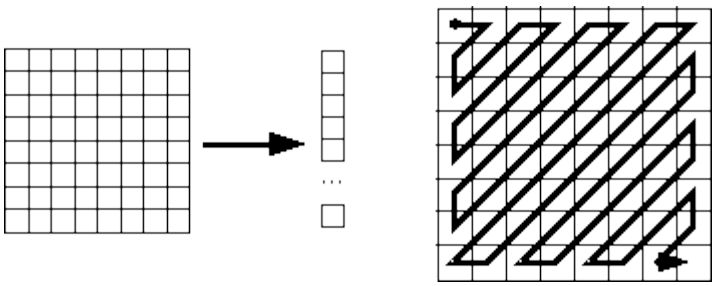

Figure 3-10 Mapping of 8 x 8 matrix to a 1 x 64 vector

The next operation is clustering, and it is done according to the cluster tree. This tree is constructed with the nearest distance as follows:

$$d_{rs} = (V_r - V_s)(V_r - V_s)^T \tag{3.42}$$

In this equation, d_{rs} denotes the distance from the block r to block s, and V_i denotes the 1-D Fourier transform with half-length corresponding to the block i. The distance of each block from the others is calculated and then a distance matrix is constructed with these values. This distance matrix is used to find specified number of clusters. Clusters are groups, which contain similar elements to each other in some sense. In this method, similarity is measured by the frequency difference. If the frequency difference is small between two blocks, then they are grouped under same cluster.

Secondly, cluster centers are computed by averaging 1-D vectors, which belong to the same cluster. After this operation, normalized cluster centers are calculated with the median filtering. Normalization is done with the energy of each cluster. The median filtering with window size 3 is used for noise reduction. The formulas for these operations are described as follows:

$$TE_j = \sum_{n=1}^{B1B2/2} [CC_j(n)]^2 \tag{3.43}$$

$$\overline{CC_j}(n) = \frac{[CC_j(n-1)]^2 + [CC_j(n)]^2 + [CC_j(n+1)]^2}{TE_j} \tag{3.44}$$

In these equations, j denotes the cluster number. CC_j and $\overline{CC_j}(n)$ denote the cluster center and normalized cluster center respectively. Then, a weight for each cluster is calculated using the equation as follows:

$$w_j = \sum_{n=1}^{B1B2/2} \overline{CC_j}(n) \times n \tag{3.45}$$

It can be seen from the above equation that the weight is increased for high-frequency components by multiplying them with high values of n, since they have most of the detail information about targets. Then, these weight values are used to decide target and background regions and assigned to the blocks at each cluster. Each block will have the weight value of the cluster which it belongs. The blocks with low weight values are labeled as background while blocks with high weight values are labeled as targets. After that, a gain matrix is calculated from these weight values. Gain matrix has the same dimensions with input image. Each member of the gain matrix is found by using its distance to all block centers with distance transformation operation. This operation ensures that each block has contributions from its neighbors to decide its final gain value. This results in smooth transition from one block to another. It is performed as follows:

$$D_k(x,y) = \frac{1}{\sqrt{(BW_k(x_c) - x)^2 + (BW_k(y_c) - y)^2} + \in} \tag{3.46}$$

$$G(x,y) = \sum_{k=1}^{b} \frac{D_k(x,y)}{\sum_{l=1}^{b} D_l(x,y)} BW(k)\,, \tag{3.47}$$

where x_c and y_c are the center coordinates of the blocks; BW_k is the weight value of the kth block, and b denotes the number of blocks. The small variable $\in$ is used to prevent division by zero at the cluster centers. The gain matrix is used to calculate two different matrices. These matrices are constructed with the equations below:

$$G_{mid}(x,y) = \frac{(G(x,y) - G_{min}) \propto_{mid}}{(G_{max} - G_{min})} + \beta_{mid} \tag{3.48}$$

$$G_{high}(x,y) = \frac{(G(x,y) - G_{min}) \propto_{high}}{(G_{max} - G_{min})} + \beta_{high} \quad (3.49)$$

G_{max} and G_{min} are the maximum and minimum values of the gain matrix G respectively. $\propto_{mid}$, $\propto_{high}$, β_{mid} and β_{high} are coefficients used to calculate gain matrices. Matrices in equation (3.48) and (3.49) denote enhancement factors of the mid-frequency and high-frequency partitions of the input image. They are used for the calculation of the final image as follows:

$$I_{final} = I_{low} + G_{mid}(x,y) \times I_{mid}(x,y) + G_{high}(x,y) \times I_{high}(x,y) \quad (3.50)$$

In this formulation, I_{low} denotes the average image. It is calculated by passing the original image from 25x25 averaging filter. I_{high} denotes the high-frequency image. It is calculated by first passing input image from 5x5 averaging filter and then subtracting the resulted image from the input. The mid-frequency image I_{mid} is calculated according to the equation (3.51) as follows:

$$I_{mid} = I_{original} - I_{low} - I_{high} \quad (3.51)$$

Finally, the values of the output image, which are outside the output dynamic range, are set to either 0 or 255. The output of this method for the image in Figure 3-1 (a) is presented in Figure 3-11. Additionally, the input and output of this method for another image can be seen in Figure 3-12. B1 and B2 are both selected as 25. The cluster number is selected as 2. Experiments showed that 0.5, 3, 0.5, 0.5 were good approximations for $\propto_{mid}$, $\propto_{high}$, β_{mid} and β_{high}. Clearly, this operation only improves edge details. The overall contrast of the image does not change.

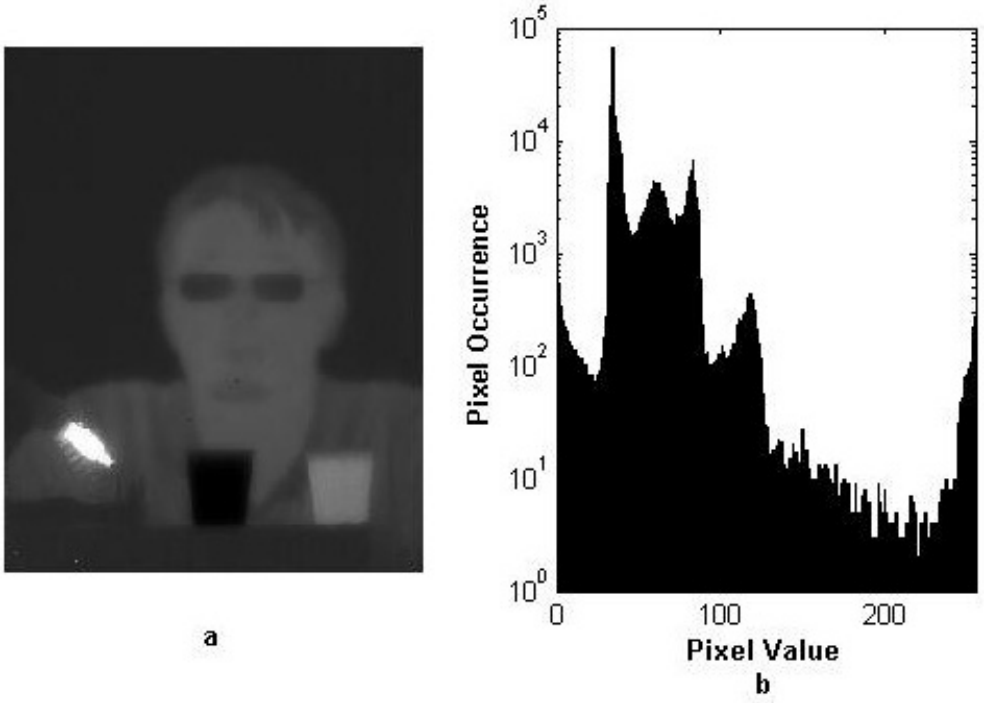

Figure 3-11 Output of Enhancement with Local Frequency Cues Method (a) Output Image, (b) Output Histogram

a

Figure 3-12 Output of Enhancement with Local Frequency Cues Method (a) Input Image

b

Figure 3-12 Output of Enhancement with Local Frequency Cues Method (b) Output Image (continued)

3.3 Contrast Enhancement Operations Before High Dynamic Range Compression

In this thesis, contrast enhancement operations are performed after high dynamic range compression operation. Therefore, enhancement operations are used to improve visual quality of 8-bit IR images. These operations can be performed on 14-bit IR images. However, there is one special consideration for them.

IR systems exhibit random temperature fluctuations in their histogram due to the heat exchange in the environment. This is known as thermal noise. A clipping operation is performed in order to suppress this noise component and give a better dynamic range for the middle pixel values. Percentages of the histogram from beginning and end are saturated. Contrast enhancement operations can be performed in this new image. After this, linear scaling can be used to obtain a 8-

bit image for standard display devices. An example operation can be seen in Figure 3-13. Standard CLAHE operation with 4 blocks is selected as the contrast enhancement operation, and it is applied to the image in Figure 3-1 (a). Linear scaling is used to obtain a 8-bit image after contrast enhancement.

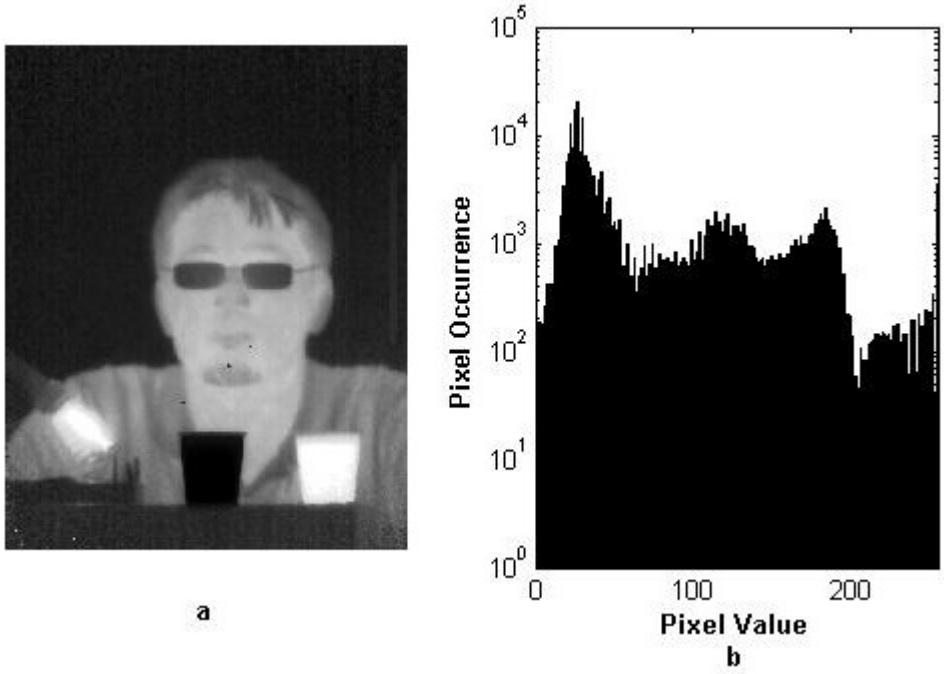

Figure 3-13 Output of CLAHE Method on IR Image with 14-bit Depth (a) Output Image, (b) Output Histogram

Clearly, this image has more contrast compared to the CLAHE operation performed on 8-bit image. However, detail information is flattened in some regions due to the linear scaling operation. Because contrast enhancement is performed to improve flattened detail information after linear scaling operation, Figure 3-8 has more detail information compared to Figure 3-13. Therefore, a better HDRC method can be used to improve output performance.

Contrast enhancement operations, which are performed on 8-bit images, are preferred to get more detail information. Real time considerations are another reason for this selection. Histogram calculations will be performed on 14-bit depth histogram instead of 8-bit depth, and storage problems will arise. External storage devices can be used to store image statistics like histogram, pdf, and cdf. However, this will increase operation time of the contrast enhancement algorithm.

3.4 Distance Transformation Function

Local contrast enhancement methods use a block based approach. This results in a better enhancement for images. These methods can be implemented with a sliding window approach. However, this will lead a higher computational load for real time systems. Thus, the nonoverlapped block based approach is developed in the literature to decrease computation time [29]. This operation divides an input image to blocks, which do not cross each other. Then, the final mapping function is calculated for each block by using its own pixels. The neighboring blocks have different mapping functions, and discontinuities will appear at the borders between blocks. This is named as blocking effect.

Blocking effect has a great impact on the output image quality, and it can be prevented by distance transformation operations. These operations merge adjacent blocks in a way that there is no clear boundary between them. It is accomplished by changing the image pixel values in order to create smooth transition between block boundaries. Block centers have their original pixel values. However, the pixel values use the gray level mapping function of their neighbors when they move away from the pixel centers. The contributions of neighbors are determined according to the distance of current pixel location to all block centers [27]. It is calculated as follows:

$$M_f\big(I(x,y)\big) = \frac{\sum_{i=1}^{B} \frac{1}{d_i(x,y)} M_i\big(I(x,y)\big)}{\sum_{i=1}^{B} \frac{1}{d_i(x,y)}}, \tag{3.52}$$

where M_f is the weighted average mapping function obtained with distance transformation operation; B is the total number of the blocks and d is the distance value between pixel location and corresponding block center. There are several methods used for this purpose. Experimented methods are:

- Chessboard distance transformation
- Cityblock distance transformation
- Euclidean distance transformation

These methods are experimented to find the best one for elimination of the block boundaries.

3.4.1 Chessboard Distance Transformation

Chessboard distance transformation assumes an image as a chess board. It calculates the horizontal and vertical distances between a block center and a pixel location. Then, the maximum of these two values is assigned as the distance between them. It is calculated as follows [26]:

$$x = |x_p - x_c|\,,\ y = |y_p - y_c| \tag{3.53}$$

$$d = \max(x,y) + \in \tag{3.54}$$

In this formulation, x_p and y_p denote the horizontal and vertical positions of the pixel; x_c and y_c denote the horizontal and vertical positions of the block centers; d is the chessboard distance between pixel and block center, and $\in$ is a small constant to prevent division by zero at the block center. The distance calculation

for 5x5 image with the center located at location (3,3) is shown in Figure 3-14, and its two-dimensional representation is shown in Figure 3-15.

2	2	2	2	2
2	1	1	1	2
2	1	ε	1	2
2	1	1	1	2
2	2	2	2	2

Figure 3-14 Chessboard Distance Transformation Calculation for 5x5 Image

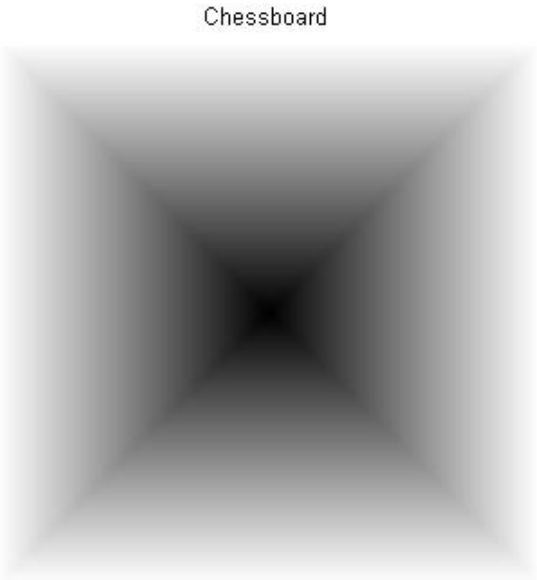

Figure 3-15 2D Representation of Chessboard Distance Transformation

It is clear from Figure 3-15 that this transformation does not show the true distance at diagonal locations. Therefore, the final mapping has errors at these locations. These locations do not merge well with their surrounding pixels.

3.4.2 City-Block Distance Transformation

City-Block distance transformation is also known as Manhattan distance. It calculates the distance between two points by adding the absolute differences of their coordinates. It is calculated as follows [26]:

$$d = |x_p - x_c| + |y_p - y_c| + \in \tag{3.55}$$

In this formulation, x_p and y_p denote the horizontal and vertical positions of the pixel; x_c and y_c denote the horizontal and vertical positions of the block centers; d is the city-block distance between pixel and block center, and $\in$ is a small constant to prevent division by zero at the block center. The distance calculation for 5x5 image with the center located at location (3,3) is shown in Figure 3-16, and its two-dimensional representation is shown in Figure 3-17.

4	3	2	3	4
3	2	1	2	3
2	1	ε	1	2
3	2	1	2	3
4	3	2	3	4

Figure 3-16 City-Block Distance Transformation Calculation for 5x5 Image

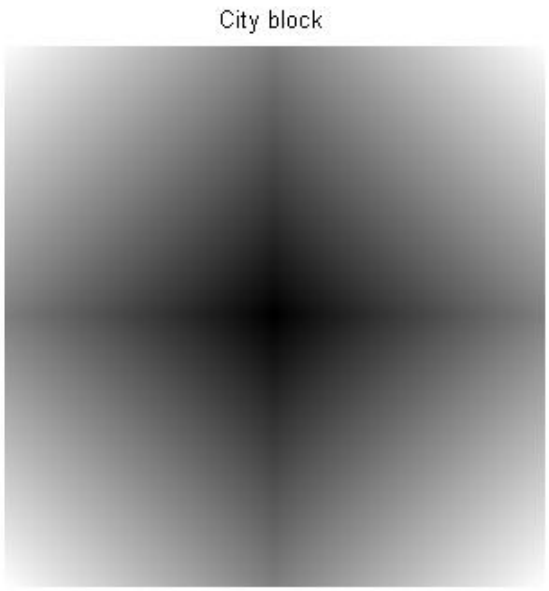

Figure 3-17 2D Representation of City-Block Distance Transformation

It is clear from Figure 3-17 that the distance matrix saturates rapidly at the locations excluding the horizontal and vertical locations starting from the block center due to the sum of horizontal and vertical locations. This causes an error at the distance matrix.

3.4.3 Euclidean Distance Transformation

Euclidean distance transformation calculates the distance between two points by adding the squared differences of their coordinates [30]. It is calculated as follows:

$$d = \left|x_p - x_c\right|^2 + \left|y_p - y_c\right|^2 + \in \tag{3.56}$$

In this formulation, x_p and y_p denote the horizontal and vertical positions of the pixel; x_c and y_c denote the horizontal and vertical positions of the block centers; d

is the euclidean distance between pixel and block center, and ∈ is a small constant to prevent division by zero at the block center. The distance calculation for 5x5 image with the center located at location (3,3) is shown in Figure 3-18, and its two-dimensional representation is shown in Figure 3-19.

8	5	4	5	8
5	4	1	4	5
4	1	ε	1	4
5	4	1	4	5
8	5	4	5	8

Figure 3-18 Euclidean Distance Transformation Calculation for 5x5 Image

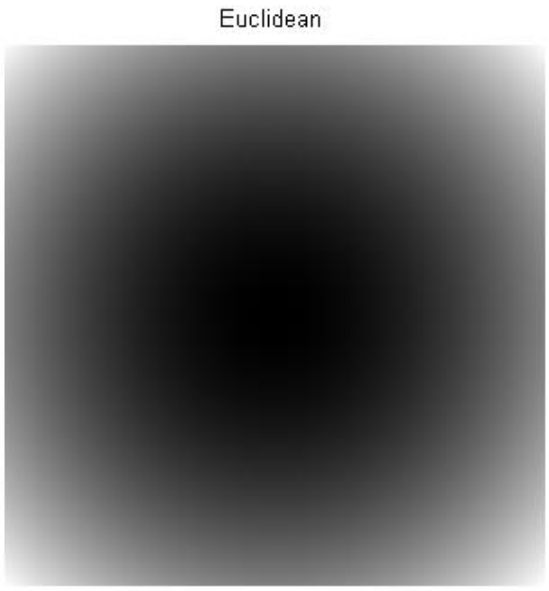

Figure 3-19 2D Representation of Euclidean Distance Transformation

It is clear from Figure 3-19 that the distance matrix saturates more uniformly with a circular approach. This produces a more smooth estimation for the mapping of pixel values. In this thesis, Euclidean distance transform is used to merge nonoverlapping blocks of the local enhancement methods.

CHAPTER 4

IMPROVEMENTS FOR CONTRAST ENHANCEMENT OPERATIONS

4.1 Introduction

There are two types of implementations for contrast enhancement operation. These are global and local implementations. The global implementation handles an input image as a whole while the local implementation divides the image to smaller sub regions. These regions generally have same dimensions. The local approach is more convenient to extract details in the smaller regions. However, it suffers from several aspects. Thus, some modifications are experimented to improve output image quality.

4.2 Problems in Balanced Contrast Limited Adaptive Histogram Equalization (BCLAHE) Method

Balanced CLAHE method is based on the histogram modification of an input image. The authors tried this algorithm with a block based approach to improve local image quality. It is very important to determine the appropriate number of blocks which the input image is divided, because some quality problems arise from the image under operation. The most important problem is the block size. The block size which is determined for one image may not be appropriate for one other. Thus, some regions contain only background information after the input image is divided into several sub regions. These regions do not have any information about the target such as edges or details. Histogram is modified using only the background information. Therefore, all gray level intervals are assigned to the background and natural texture of the image is damaged. Figure 4-2 (c) is

an example of the background region for the image in Figure 4-1 (c). Clearly, there is no target information in this region and noise information is amplified.

Clearly, the background partition of the image at Figure 4-1 (c) is mapped to a more whitish gray level interval, and the transition between the two adjacent regions is not smooth. Intensity change between the two regions is obvious, and it spreads to a very large area. This leads to a clear separation between two backgrounds at the top right side. The natural look is damaged at this image. Several methods are proposed and experimented in the thesis to prevent this situation.

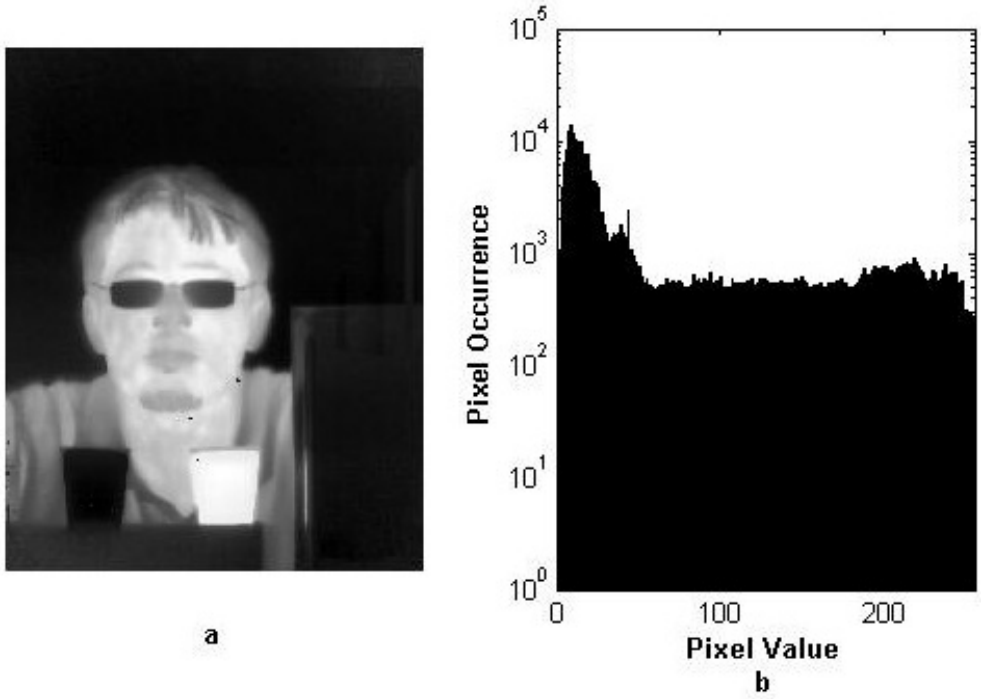

Figure 4-1 Output Images and Histograms for Balanced CLAHE Method (a) Output Image with 4 Block, (b) Output Histogram with 4 Block

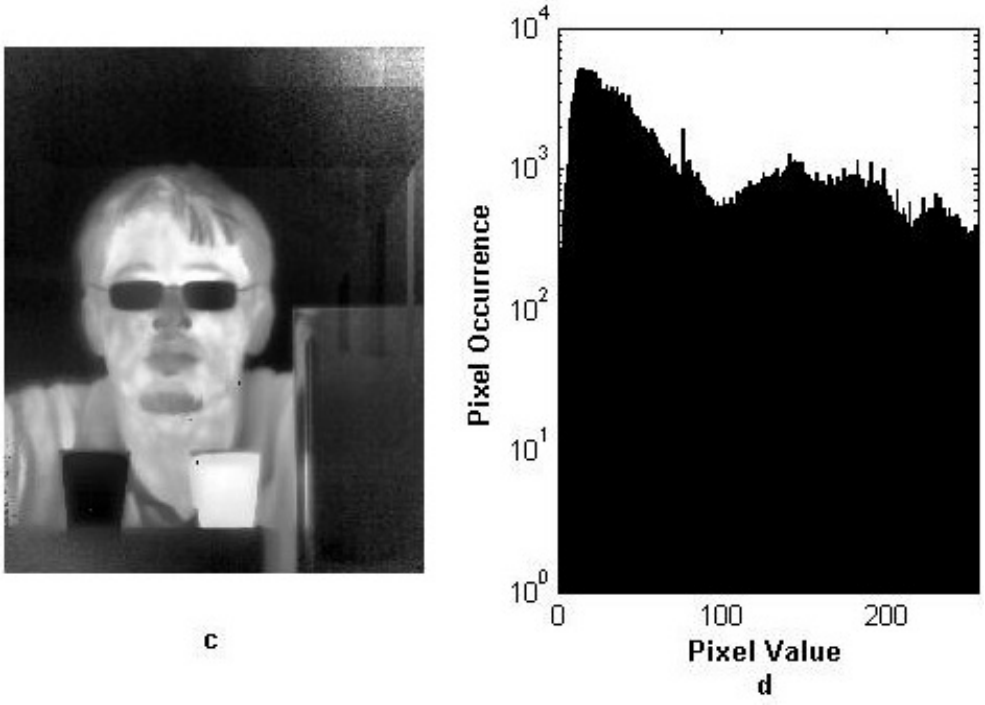

Figure 4-1 Output Images and Histograms for Balanced CLAHE Method (c) Output Image with 9 Block, (d) Output Histogram with 9 Block (continued)

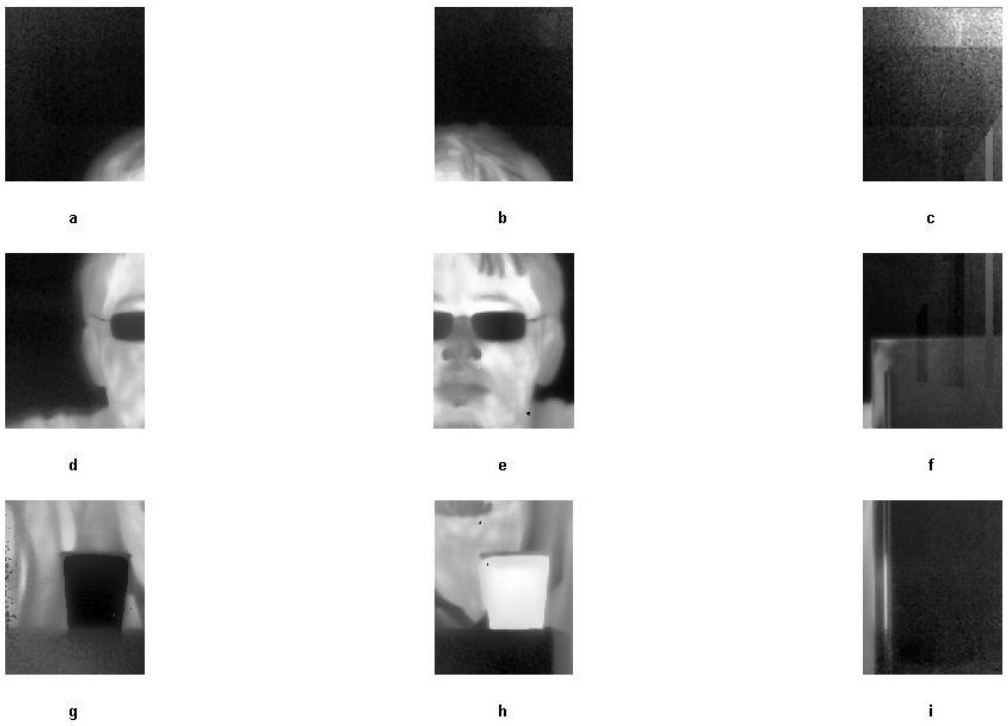

Figure 4-2 Block Representation of The Image in Figure 4-1

Proposed modifications are:

- Modification 1: Changing the contrast enhancement method of background region
- Modification 2: Changing the mapping function of background region

4.2.1 Proposed Modification 1

First modification proposed in this thesis is to change the contrast enhancement method of background region. A different mapping function is used to prevent over enhancement of this region. The standard CLAHE operation is suitable for this operation. Because, it distributes the clipped frequency values to all available output values in order to generate a uniform distribution. This prevents over enhancement of the background. The main problem is to determine which regions to apply this method. It is determined by the nonzero frequency counts of the region histograms before contrast enhancement operations. This value shows the spread of the pixel values and can be interpreted as contrast information of the region. The background has smaller contrast compared to the target region due to its uniform nature. This assumption leads to the conclusion that the blocks with fewer nonzero histogram bins are the background regions, and the others are the object regions. The background region is also assumed darker than the target region for infrared images because infrared radiation emitted from the background is smaller than the target region.

First, nonzero histogram bins are calculated for each region and then a small percentage of the nonzero bins of original image is assigned as the image contrast threshold. Experiments show that 25% is a good assumption to detect background regions. After this, standard CLAHE or other contrast enhancement operations are applied to the regions, which have lower nonzero histogram bins than the specified threshold value. This operation improves the enhancement of

background with its approach. However, experiments show that its effect is limited. Some of the experimented images suffer from the same problem, but the contrast difference is smaller than the previous case. This operation improves the natural appearance of the output image. However, problem is unsolved for some images.

An example of this operation is presented in Figure 4-3 for image in Figure 4-1. Balanced CLAHE operation is applied for 9 blocks with threshold value of 200, and outputs are presented. Top right part of the image is marked as the background region. Different methods are applied to this region to improve contrast. Best approach is the standard CLAHE operation in Figure 4-3 (d).

a b

Figure 4-3 Output Images for Balanced CLAHE Method (a) Fault Locations Enhanced with Histogram Equalization Method, (b) Fault Locations Enhanced with Plateau Histogram Equalization Method

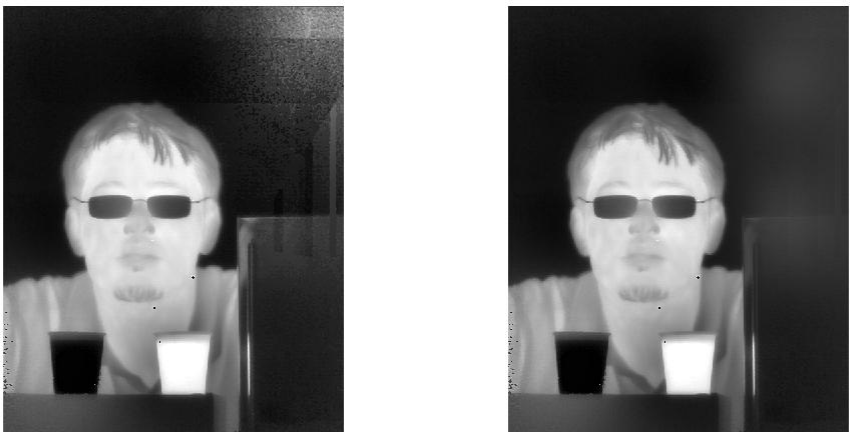

c d

Figure 4-3 Output Images for Balanced CLAHE Method (c) Fault Locations Enhanced with Tail-Less Plateau Histogram Equalization Method, (d) Fault Locations Enhanced with CLAHE Method (continued)

4.2.2 Proposed Modification 2

The other method to improve natural looking of the image is to change mapping function of the background region. Over enhancement problem can be solved by replacing the final mapping function of the background region with its neighbors. However, this neighbor should have more contrast.

Firstly, the image is divided into the blocks with same dimensions, and these regions are classified according to their positions in the image. These are:

- Corner regions (CR) are the four blocks on the image corners.
- Border regions (BR) consist of all blocks on the image border, excluding the corner regions.
- Inner regions (IR) consist of the remaining blocks.

Its example is shown for 16 blocks in Figure 4-4.

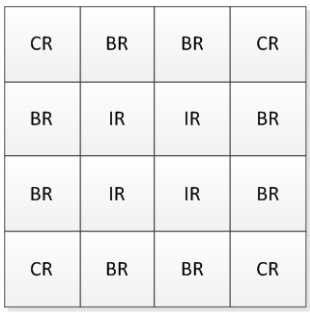

Figure 4-4 Image Regions for 16 Blocks

After this, the blocks with lower nonzero frequencies are marked as the background region. Background selection method is same with the previous method. Then, the mapping functions of these blocks are replaced with the neighbors with more contrast. In other words, mapping function of fault block is replaced with the region, which has higher nonzero frequencies. Algorithm searches at the three neighbors of the corner region, five neighbors of the border region or eight neighbors of the inner region depending on the situation. It is shown in Figure 4-5. The yellow regions show the example of search areas on the image for three classes, and BG denotes the background region. If some neighbors of the background region are also labeled as background, then the mapping functions of these blocks are replaced with the neighbor of them with more contrast. An example of this situation is shown at Figure 4-6.

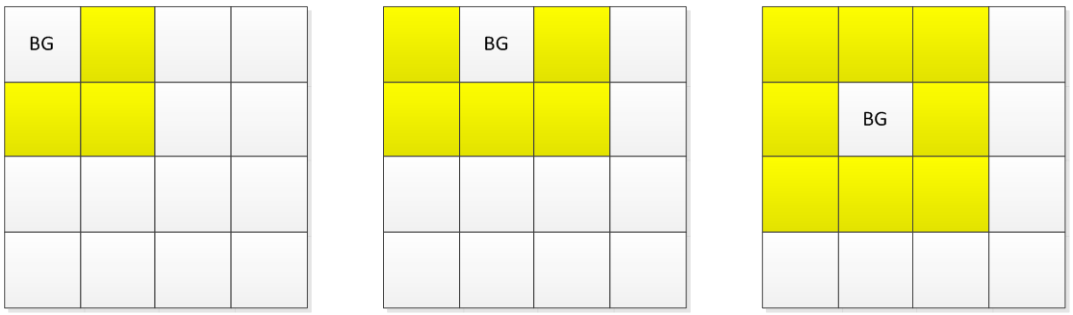

Figure 4-5 Search Areas for Single Background

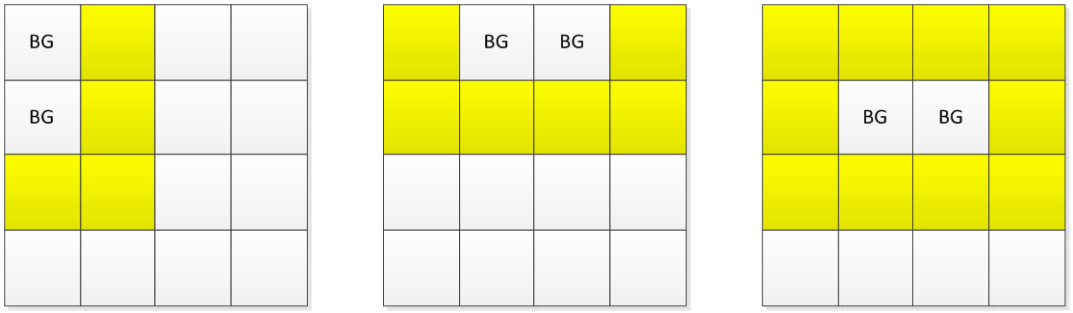

Figure 4-6 Search Areas for Two Backgrounds

Second, all image blocks are merged with the distance calculation methods in order to prevent blocking effect at the final image. An example of this operation is presented in Figure 4-7 for the image in Figure 4-1. Same parameters are used with method 1 to obtain this result.

Experiments showed that this method has more promising results compared to the previous one. Its outputs have natural look, and no blocking artifacts are presented. Clearly, output in Figure 4-7 also has more local contrast than the four-block approach.

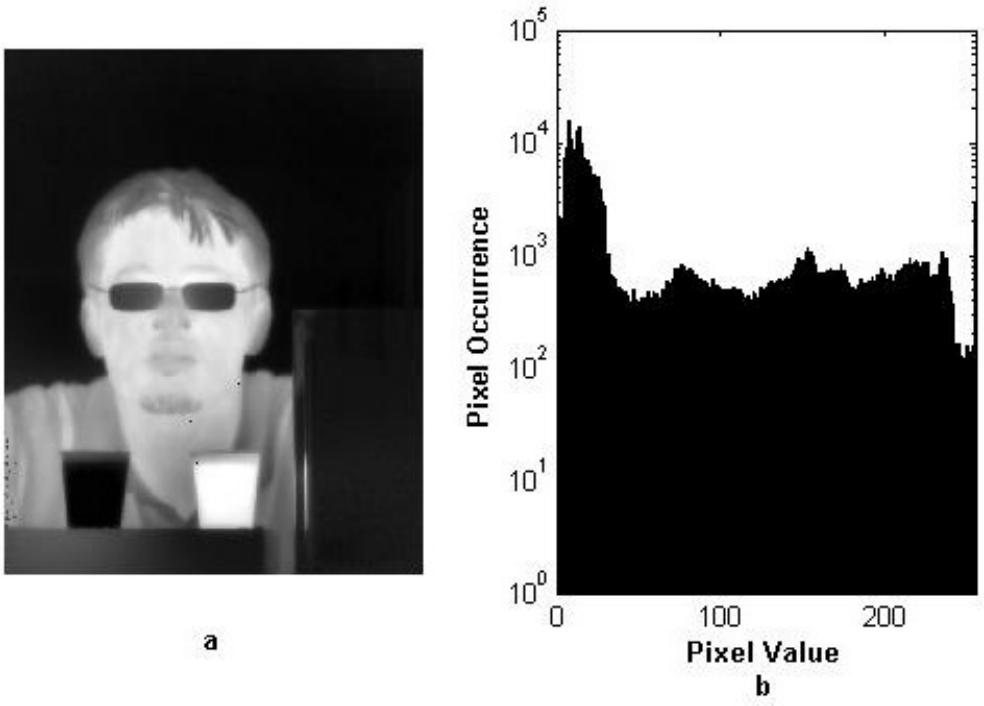

Figure 4-7 Output Image and Histogram for Modified Balanced CLAHE Method (a) Output Image with 9 Block, (b) Output Histogram with 9 Block

4.3 Problems in Detail Enhancement with Local Frequency Cues

Some modifications are necessary for the enhancement with local frequency cues method to decrease the computational load of operations. The main focus is to change the calculation of complex parts and make improvements to the algorithm. Modifications are proposed for the parts of the algorithm listed below. These are:

• Fourier Transform of each block,
• Cluster tree operations and distance transformation

The Fourier transform can be implemented with Field-Programmable Gate Array (FPGA) and has a fast implementation. However, clustering operation performed with Fourier coefficients has limited performance according to the experimental

results. In addition to this, cluster center and block weight calculations depends on the length of Fourier coefficients.

Cluster tree operations are complex due to the number of blocks, which image is separated. A distance matrix is constructed with the distances from one block to another. Thus, the size of the distance matrix is determined by the total number of blocks. For example, the size of the distance matrix is 20x20 for 20 blocks. Hence, the complexity of cluster tree operations is directly proportional to the block size. On the other hand, if the number of blocks is decreased, then the resulting clustering will have a poor performance. Because the small details blend to large blocks, they can be assigned to a cluster which it does not belong originally.

Distance values are calculated from one pixel to all cluster centers for gain matrix. This calculation is repeated for each pixel, and this brings excessive multiplications, square root, division and summation operations as described in the equation (3.52). The number of blocks must be reduced to decrease this excessive load. Thus, a better distance calculation performance is achieved by forsaking the clustering performance. The optimum number of blocks for image can be decided according to the experimental result. However, this is a very time-consuming process. Clearly, it is also very hard to implement the number of blocks determined for one image to other and achieve same performance.

In this thesis, two types of modifications are proposed. The first modification is performed for the cluster tree operations. Fourier coefficients are replaced with mean-standard deviation values and wavelet coefficients. Mean and standard deviation values are used to improve clustering performance of the algorithm. On the other hand, wavelet coefficients are used to experiment clustering operation based on edge similarity. The second modification is performed by adding K-Means clustering method to the algorithm.

4.3.1 Modifications for Cluster Tree Operations

The Fourier Transform is replaced with other processes to improve clustering performance. These are:

• Mean-Standard Deviation calculations
• Wavelet calculations

These calculations are repeated for each block, and then their outputs are used to set up a cluster tree. This thesis mainly focused on the clustering of image according to the target and texture. Hence, two clusters are sufficient for expected results.

4.3.1.1 Proposed Modification Based on Mean and Standard Deviation Calculations

The clustering tree approach of the original algorithm uses Fourier coefficients to perform clustering operation. The blocks at the same cluster have closer Fourier coefficients, and the distance between them will be smaller. However, the difference will increase for the blocks at different clusters. This concept can be implemented with the mean and standard deviation information of the blocks. The clustering is performed with these values instead of Fourier coefficients. Therefore, the mean and standard deviation of each block are calculated. These calculations have small computational loads.

The distance between the mean and standard deviation of each block is used for the distance matrix calculations. The resulted clustering has satisfying outputs. Besides of simplifying the distance matrix, this change also affects the gain matrix calculation. The new equations are:

$$TE_j = \sum_{n=1}^{2} [CC_j(n)]^2 \tag{4.1}$$

$$\overline{CC_j}(n) = \frac{[CC_j(n)]^2}{TE_j} \tag{4.2}$$

$$w_j = \sum_{n=1}^{2} \overline{CC_j}(n) \times n \tag{4.3}$$

There are only two parameters and the repetition is decreased from half block dimension ((B1×B2))⁄2 to two. It is also clear that the median filtering is not necessary. Output of this method for the images in Figure 3-1 and Figure 3-12 can be seen in Figure 4-8 and Figure 4-9. Parameters are selected same with Figure 3-11.

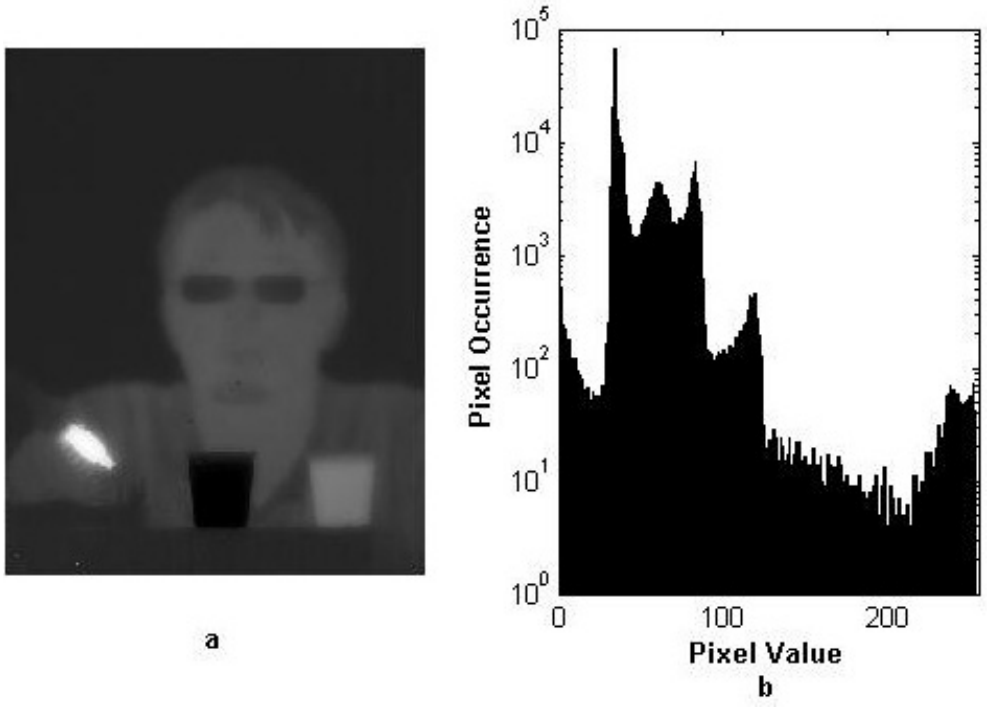

Figure 4-8 Output of Modification Based on Mean-Standard Deviation Calculations (a) Output Image, (b) Output Histogram

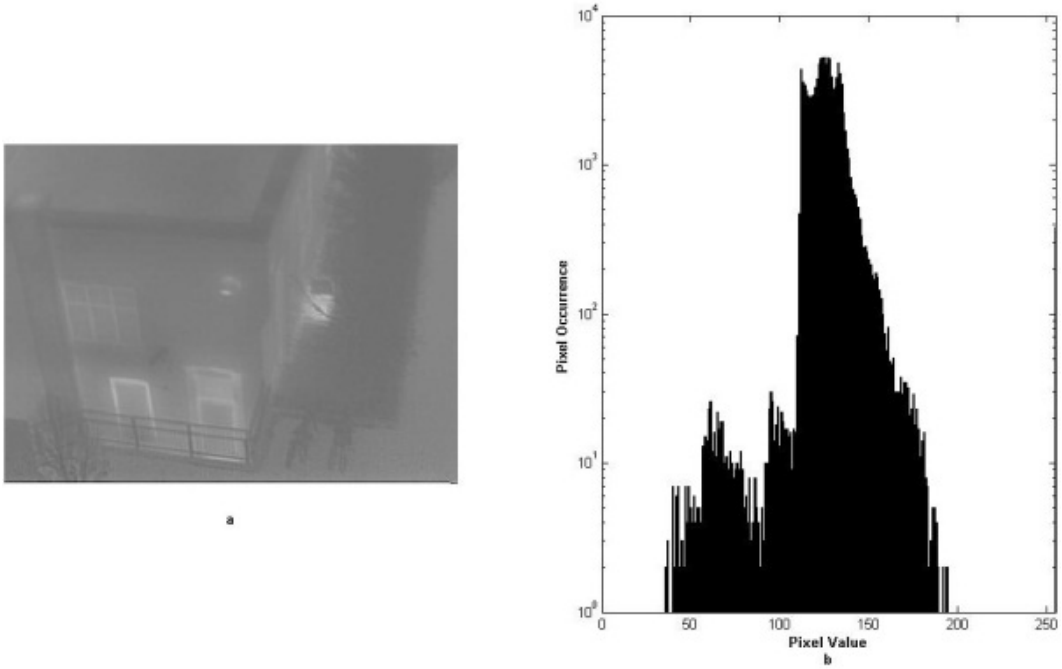

Figure 4-9 Output of Modification Based on Mean-Standard Deviation Calculations (a) Output Image, (b) Output Histogram

4.3.1.2 Proposed Modification Based on Wavelet Calculations

Wavelet transform was developed at 1980s, and 1990s as an alternative to the Fourier transform. In the aspect of the image processing, two-dimensional wavelet transform is used to decompose images to approximation and detail coefficients [6]. It constructs an image pyramid with continuously decreasing size of two from both dimensions. The bottom level consists of the original image while the top level is the final image of wavelet transform at level j. It is realized for an image as follows:

- h_φ is a half-band low pass filter ,and h_ψ is a half-band high pass filter.

- Columns of the image at level j+1 are filtered with digital filters $h_\varphi(-n)$ and $h_\psi(-n)$. Horizontal resolution of the image is reduced by factor 2 after this operation.
- Rows of resulted image at step 1 are filtered with digital filters $h_\varphi(-n)$ and $h_\psi(-n)$. Vertical resolution of the image is reduced by factor 2 after this operation.

The block diagram of the wavelet transform can be observed at Figure 4-10. $W_\varphi(j+1,m,n)$ and $W_\varphi(j,m,n)$ are the images at the level j+1 and j respectively. $W_\varphi(j,m,n)$ is the approximation image obtained by filtering an image at the level j+1 with both horizontal and vertical low pass filters. $W_\psi^D(j,m,n)$, $W_\psi^H(j,m,n)$ and $W_\psi^V(j,m,n)$ are diagonal, horizontal and vertical coefficients respectively. They correspond to the high-frequency details or variations alongside diagonals, columns and rows of image [6]. The depth of the image pyramid depends on the type of application. In our case, 1 or 2 depth is enough due to the real time computation and storage conditions.

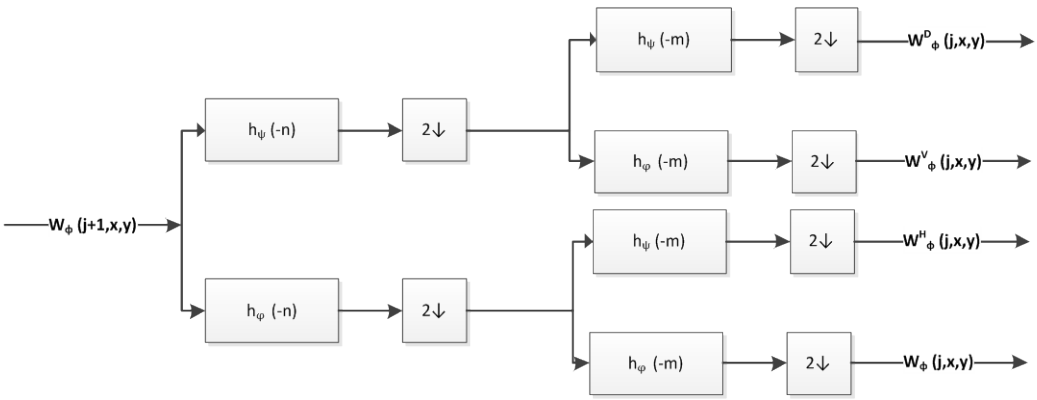

Figure 4-10 - 2D Wavelet Transform

The one-level wavelet transform is used instead of the Fourier transform as modification. If one of the three coefficients is used, then clustering performance

will be based on the selected coefficients. For example, if horizontal detail coefficients which contain the edge and corner details alongside the columns are selected, then clustering is affected by these edges. If all detail coefficients are used, then clustering performance will increase. The filter coefficients used for this application are based on the Haar and Symlet coefficients. Output of this method for the images in Figure 3-1 and Figure 3-12 (a) can be seen in Figure 4-11 and Figure 4-12 with same parameters.

This operation does not reduce the computation time and complexity. Therefore, high image pyramid depth causes problems for real time processes such as extra computational load and storage. It is also clear from the figures that this operation does not improve detail visibility for the images used in this thesis.

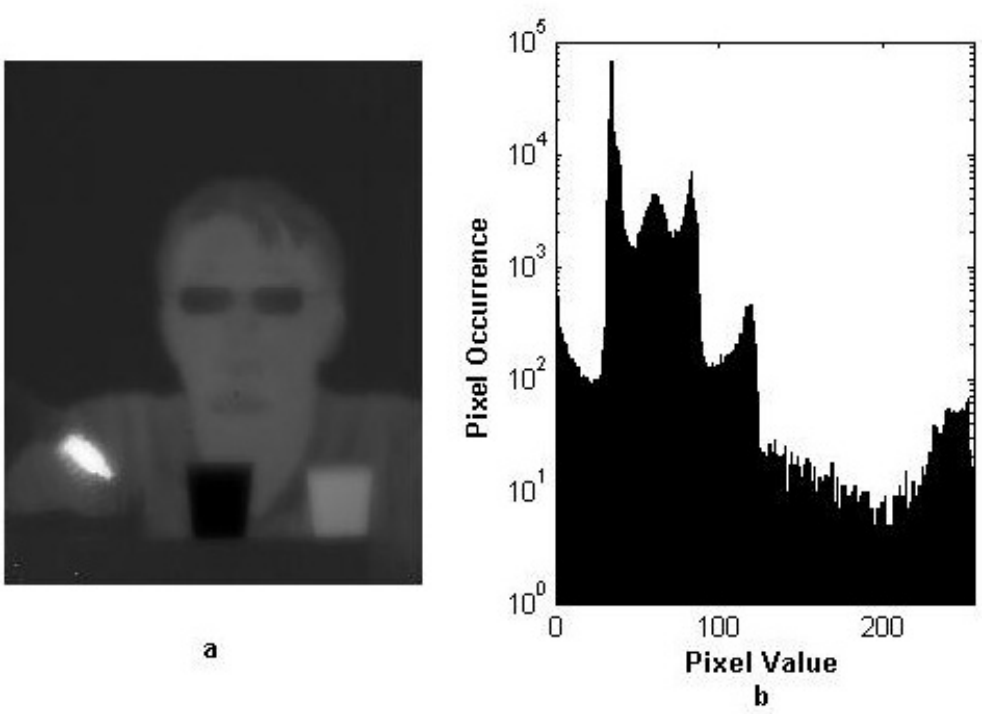

Figure 4-11 Output of Modification Based on Wavelet Calculations (a) Output Image, (b) Output Histogram

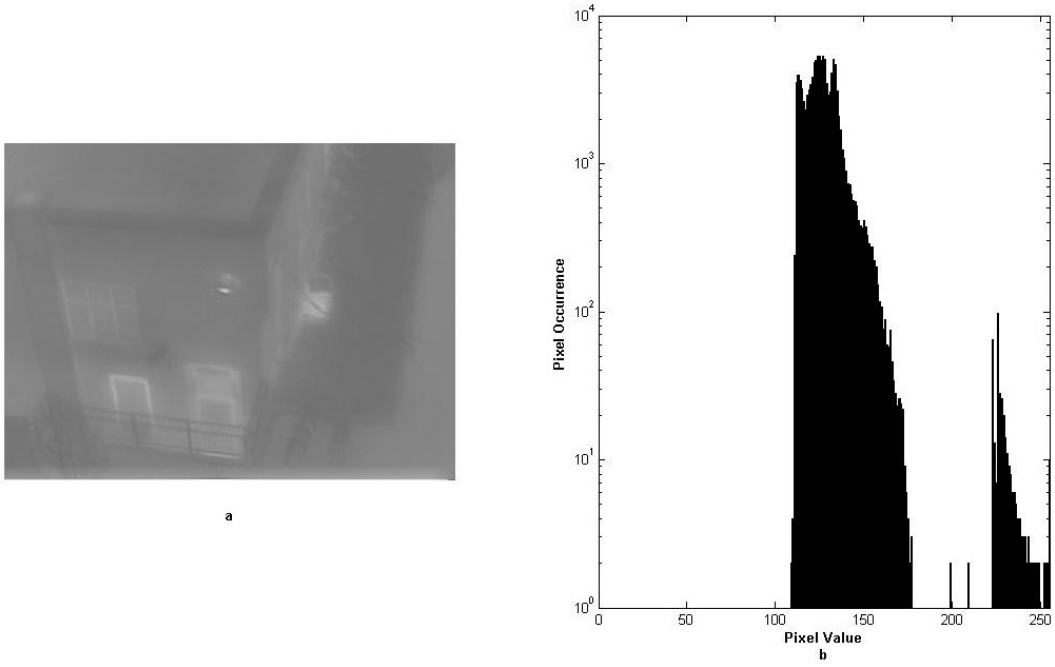

Figure 4-12 Output of Modification Based on Wavelet Calculations (a) Output Image, (b) Output Histogram

4.3.2 Proposed Modification for Clustering Based on the K-Means Algorithm

K-Means clustering is very popular for image and video-based applications due to its simplicity. The algorithm puts the input data points into classes according to their distance to the class centers [32]. The minimization of this distance is done as follows:

$$D = \sum_{l=1}^{k} \sum_{I(i,j)\epsilon S_l} (I(i,j) - \mu_l)^2 \tag{4.4}$$

In this equation, I(k,l) denotes the pixel value at cluster S_l; the constant k denotes the number of clusters, and μ_l denotes the center value at cluster l. This minimization is done using pixel intensity values at traditional K-Means

clustering algorithm. The algorithm stops when there is no change in the minimization function.

In this thesis, K-Means method is used to separate image into two clusters. There are two variations in the algorithm based on the K-Means clustering operations.

Firstly, Fourier transform is calculated for k blocks and the image is clustered using K-Means method instead of the cluster tree operation. K-Means algorithm is applied at the pixel level using intensity values, and so the upper limit of the block number can be increased. Each block is assigned to either target or background clusters depending on the dominant cluster. If most of the pixels in the block belong to background, then block is labeled as the background cluster. Otherwise, block is labeled as the target region. Random selection is performed for the equal distribution of clusters on the block members. Then, the gain matrix calculation is performed with Fourier coefficients and clustering data provided by K-Means method. In other words, the coefficients calculated by Fourier transform are used with the clustering results of K-Means algorithm. This method eliminates the cluster tree operation based on Fourier coefficients. Output of this method for the images in Figure 3-1 and Figure 3-12 (a) can be seen in Figure 4-13 and Figure 4-14.

The second case uses the mean and standard deviation information instead of Fourier transform. The K-Means clustering is also performed by using them. It has satisfying outputs. However, K-Means algorithm has high iteration levels to complete its clustering. Because of this, it can be performed at the block level. The block level application reduces the computational load of the algorithm. Output of this method for the images in Figure 3-1 and Figure 3-12 (a) can be seen in Figure 4-15 and Figure 4-16. Parameters are selected same with Figure 3-11.

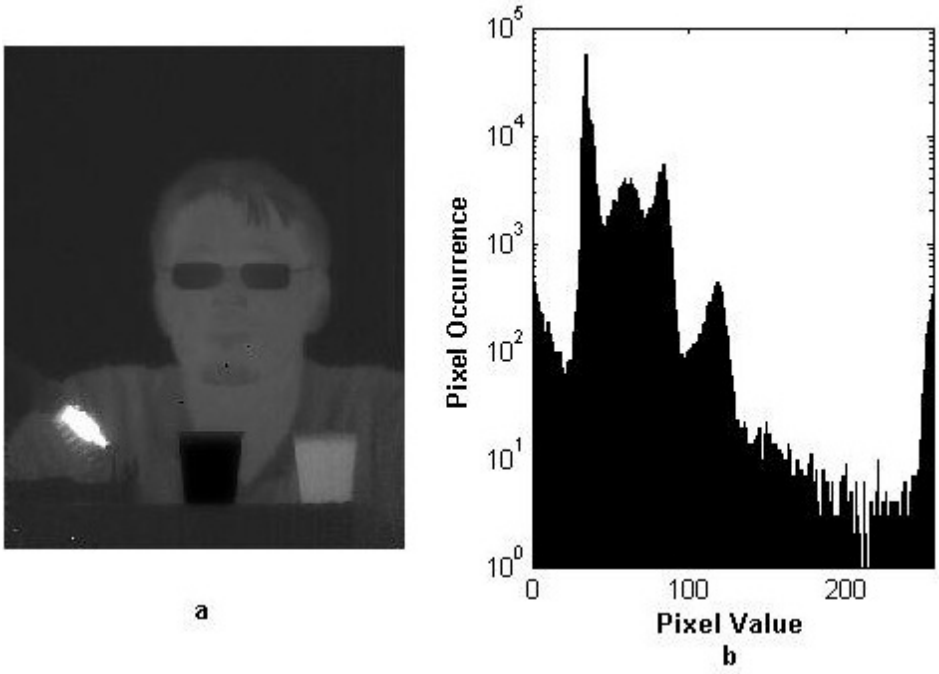

Figure 4-13 Output of the First Case (a) Output Image, (b) Output Histogram

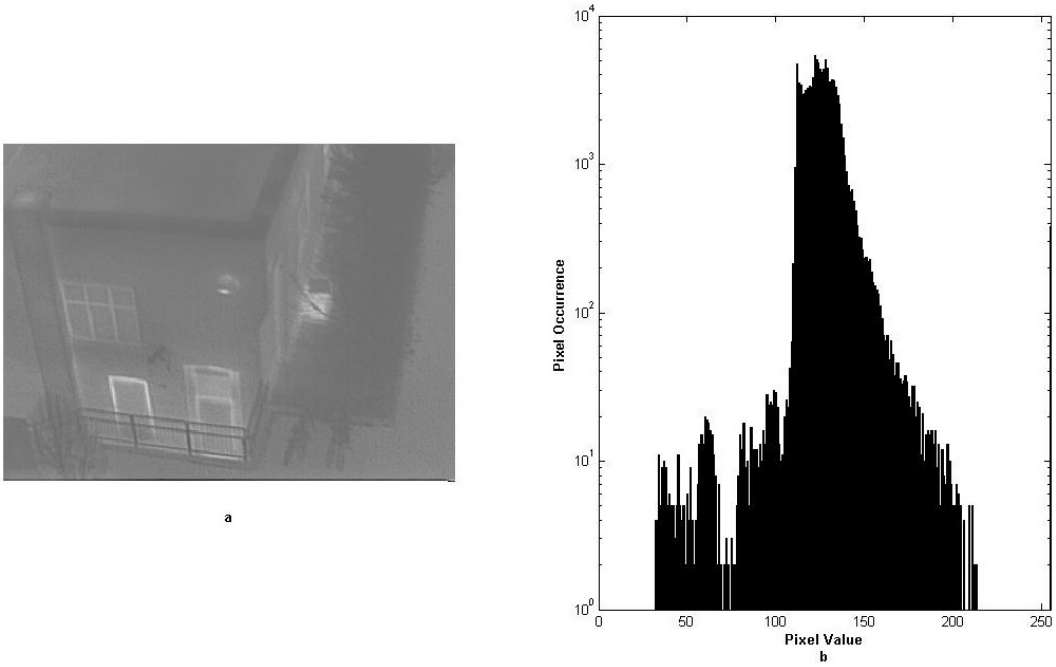

Figure 4-14 Output of the First Case (a) Output Image, (b) Output Histogram

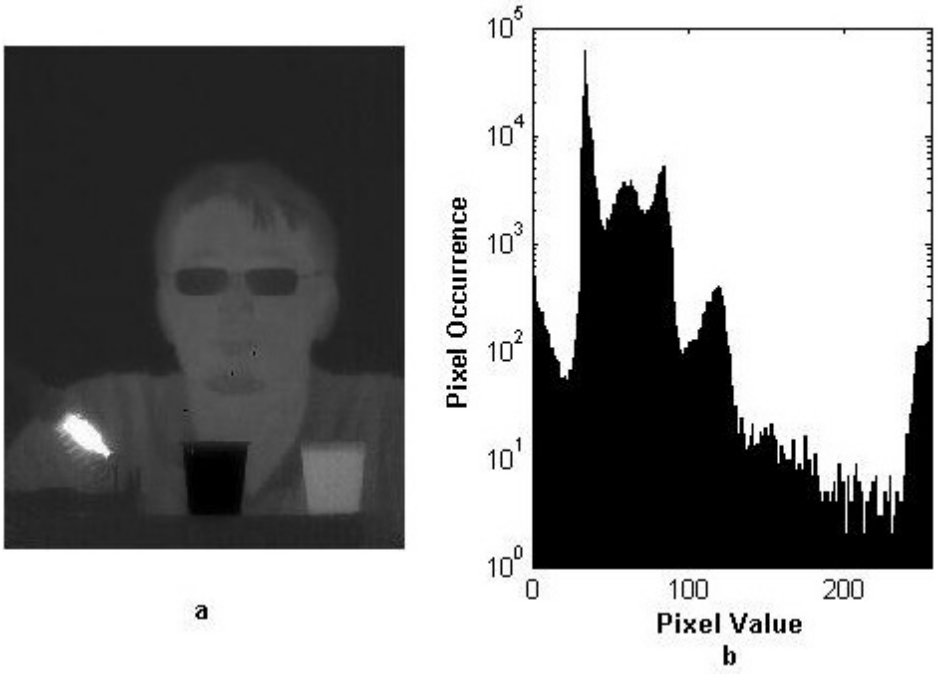

Figure 4-15 Output of the Second Case (a) Output Image, (b) Output Histogram

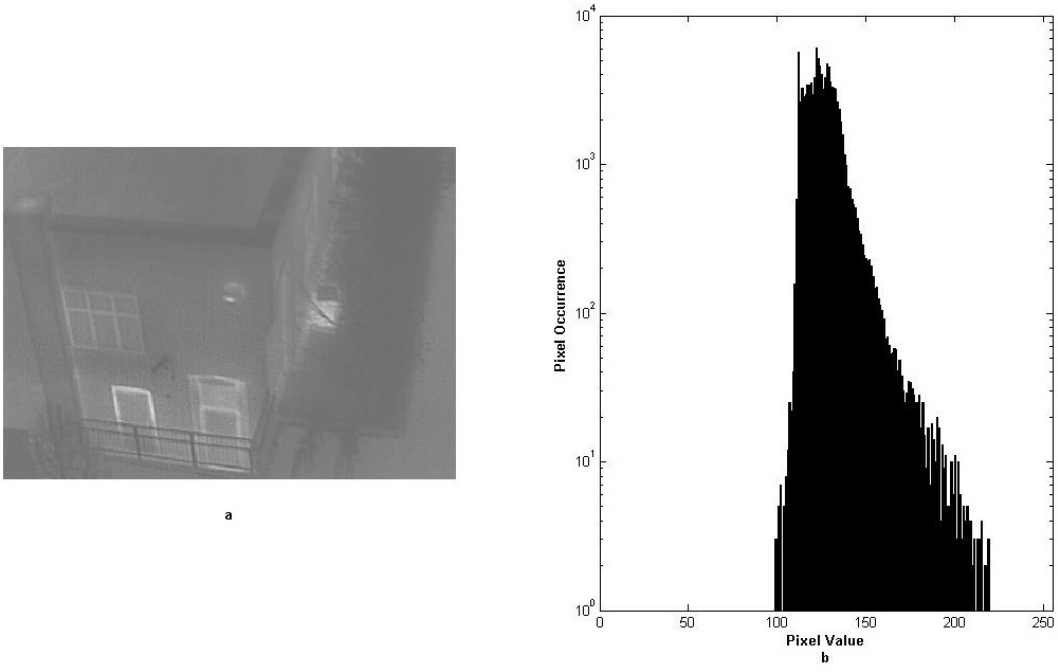

Figure 4-16 Output of the Second Case (a) Output Image, (b) Output Histogram

CHAPTER 5

RESULTS AND COMPARISONS

5.1 Introduction

Image quality measurement is a very important and challenging operation. It is used to determine usability of the images after they have undergone any kind of operation. The end users of these applications are human observers. Therefore, people are used to evaluate the performance of image or video processing operations. These performance evolution operations are called as subjective tests. They provide very accurate assessment of image quality. However, they are very time and resource consuming operations. Thus, test methods which evaluate the performance of any operation with automated operations are developed. They are named as objective tests. Most of these methods base on the human visual system (HVS), and they can consist of complex algorithms.

In this thesis, objective methods are used to evaluate the performance of contrast enhancement operations.

5.2 Objective Image Quality Metrics

The success rates of the quality measurement methods are limited to the specific types of operations. For example, the peak signal-to-noise ratio (PSNR) and mean square errors (MSE) methods are very good references for the applications which purpose the preservation of the original image. They are very popular for their low complexity. Mean square error measures the similarity between input and output images. This value shows how much output image deviates from the original one.

PSNR is the ratio between the power of signal and corrupting noise introduced by the applied method. Their structure makes them very suitable for applications such as video compression. Therefore, these two methods are unsuitable image quality metrics for contrast enhancement operation.

The main purpose of the contrast enhancement operations is to change the intensity distribution of an input image. The quality metrics used in literature for image quality are explained below. Some of these techniques are used in this thesis to measure quality of the contrast enhancement operations. The other metrics are not used, because they measure the similarity between input and output images. They are:

- Discrete Entropy
- Quality Metrics Used by Chen
- Universal Image Quality Index
- Absolute Mean Brightness Error
- Image Contrast

5.2.1 Discrete Entropy Function

Discrete entropy is the sum of the multiplication of probability distribution function (pdf) value and log of the inverse of pdf value [45, 46]. It is formulated as follows:

$$Entropy = \sum_{i=0}^{k} PDF(i) log_2 \left(\frac{1}{PDF(i)}\right), \quad k: maximum\ output\ value \tag{5.1}$$

$$Entropy = -\sum_{i=0}^{k} PDF(i) log_2 \big(PDF(i)\big), \quad k: maximum\ output\ value \tag{5.2}$$

It is clear from the equation (5.2) that discrete entropy value is always nonnegative. It does not give any information about the enhancement procedure. It rather shows the richness of the output image. This is accomplished by showing the number of bits which an image can be expressed. The minimum entropy value is zero. The maximum entropy value is obtained with an image with uniform histogram distribution. For example, if the output dynamic range is 8-bits, then the maximum discrete entropy value can be 8 as follows:

$$PDF(i) = \frac{1}{256}, \qquad 0 \leq i \leq 255 \tag{5.3}$$

$$Entropy = -\sum_{i=0}^{255} PDF(i) log_2\big(PDF(i)\big) = 8 \tag{5.4}$$

The discrete entropy produces values from 0 to log2(k+1), and k denotes the maximum intensity value at the output image.

5.2.2 Relative Entropy Function

Relative entropy function is also known as the Kullback-Leibler distance. It shows the relative distance of one image from the other one [45, 46]. If two discrete probability distribution functions of the input and output images are expressed with PDF_I and PDF_O, then the relative entropy is formulated as follows:

$$Entropy = \sum_{i=0}^{k} PDF_I(i) log_2\left(\frac{PDF_I(i)}{PDF_O(i)}\right), \qquad k: maximum\ output\ value \tag{5.5}$$

The equation (5.5) shows the distribution of the output image with respect to the input image. It is equal to zero for the same probability distribution functions. Its value will be closer to zero for the images with similar distribution, and it will increase for the distinct images. Therefore, it gives information about the

similarity between input and output images after contrast enhancement operation. There is also a limitation associated with this function. The relative entropy is not a symmetric function. If the values of PDF_O and PDF_I are replaced, then its value will be different.

5.2.3 Mutual Information Function

The mutual information between two variables is described as the reduction of uncertainty in one variable due to the other one [45, 46]. This same concept can be used in image quality measurement. It shows the connection and similarity between input and output images after image or video processing operations. It is formulated as follows:

$$I(X;Y) = \sum_{X,Y} PDF_X(X) log2\left(\frac{PDF_{XY}(X,Y)}{PDF_X(X)PDF_Y(Y)}\right) \tag{5.6}$$

$$I(X;Y) = -\sum_{X,Y} PDF_X(X) log2(PDF_X(X)) + \sum_{X,Y} PDF_X(X) log2\left(\frac{PDF_{XY}(X,Y)}{PDF_X(X)}\right) \tag{5.7}$$

$$I(X;Y) = H(X) - H(X|Y) \tag{5.8}$$

In this formulation, I(X;Y) denotes the mutual information; H(X) and H(X|Y) denote entropy and conditional entropy values, and PDF_{XY} denotes joint probability distribution. This function shows the similarity between the distribution functions. Therefore, the higher mutual information values indicate that the edge and structural information are preserved at the output images.

5.2.4 Quality Metrics Used by Chen

Qiang Chen proposed two methods to measure image quality [47]. The first method is named as intensity contrast. It is applied to both original and final image after image processing operations. The main purpose of this method is to

measure a local contrast difference for input and output images. This value shows the contrast improvement after image enhancement operation. The intensity contrast method calculates the gray level co-occurrence matrix. This matrix uses a pixel and its right-side neighbor with specified offset in a given image. In other words, it shows the local contrast change. It contains the frequency counts of the pixel differences, and it is calculated as follows.

$$\hat{p}(i,j) = \sum_{x=0}^{M-1} \sum_{y=0}^{N-1} \begin{cases} 1, & Img(x,y) = i \; and \; Img(x+\Delta x, y+\Delta y) = j \\ 0, & Otherwise \end{cases} \quad (5.9)$$

In this formulation, Img denotes the given image. The gray level co-occurrence matrix $\hat{p}(i,j)$ is used to calculate the intensity contrast as follows:

$$Con = \sum_{i,j} |i-j|^2 \hat{p}(i,j), \;\; 0 \le i,j \le k \;\; and \; k: maximum \; intensity \; value \quad (5.10)$$

The second method is the discrete entropy calculated with the gray level co-occurrence matrix. This method only replaces the probability distribution function with co-occurrence matrix. It shows the amount of information which the local contrast of the image holds. It is formulated as follows:

$$Entropy = -\sum_{i,j} \hat{p}(i,j) log_2\big(\hat{p}(i,j)\big), \quad 0 \le i,j \le k \quad (5.11)$$

Intensity contrast and discrete entropy values reflect the image enhancement quality. Therefore, the higher values represent better enhancement results.

5.2.5 Structural Similarity and Universal Image Quality Index

Structural similarity (SSIM) is another method for image quality assessment. It uses the assumption that human visual system is most sensitive to the structural

information in a given image [48, 49]. Therefore, the structure information is used as the quality metric to measure similarity between input and output images. This parameter is divided into three categories. These are the luminance, contrast and structure. They are formulated as follows:

$$l(x,y) = \frac{2\mu_x\mu_y + C_1}{{\mu_x}^2 + {\mu_y}^2 + C_1} \tag{5.12}$$

$$c(x,y) = \frac{2\sigma_x\sigma_y + C_2}{{\sigma_x}^2 + {\sigma_y}^2 + C_2} \tag{5.13}$$

$$s(x,y) = \frac{\sigma_{xy} + C_3}{\sigma_x\sigma_y + C_3}, \tag{5.14}$$

where μ_x and μ_y denote the mean values of the discrete nonnegative input and output images. ${\sigma_x}^2$ is the variance of the input image; ${\sigma_y}^2$ is the variance of the output image, and σ_{xy} is the covariance of the input and output images. They are calculated as:

$$\mu = \frac{1}{n}\sum_i\sum_j I(i,j) \tag{5.15}$$

$$\sigma^2 = \frac{1}{n-1}\sum_i\sum_j (I(i,j) - \mu)^2 \tag{5.16}$$

$$\sigma_{xy} = \frac{1}{n-1}\sum_i\sum_j (I_x(i,j) - \mu_x)(I_y(i,j) - \mu_y) \tag{5.17}$$

C_1, C_2 and C_3 are small constants, and they are calculated as follows:

$$C_1 = (K_1L)^2,\ K_1 \ll 1, \qquad L: maximum\ intensity\ value \tag{5.18}$$

$$C_2 = (K_2L)^2,\ K_2 \ll 1, \qquad L: maximum\ intensity\ value \tag{5.19}$$

$$C_3 = \frac{C_2}{2} \tag{5.20}$$

The First component in equation (5.12) is the luminance information between the two images. It measures the similarity between two images with their mean intensity values. The second component in equation (5.13) is the contrast. This part of the formula uses the standard deviation to compare contrast information of two images. The third component in equation (5.14) is the structure information. The covariance of the image is divided by the standard deviations of the input and output images. This produces a normalized output value. This value measures the degree of linear correlation between input and output image. It is named as structure information between two images. The structural similarity (SSIM) is set up with multiplication of these three components. The most important point is the independence of them. The structural similarity formula is set up as follows:

$$SSIM(x, y) = I(x, y)c(x, y)s(x, y) \tag{5.21}$$

The structural similarity is calculated with a sliding window. The window with a predefined size is passed on the both images at the same time and then a structure similarity value is calculated for each location. The mean of these values is assigned as a final structural similarity value. The value of the three components of structural similarity is in the range of [0, 1]. Hence, the final value of the SSIM is also in the range of [0, 1]. It is calculated for the image with horizontal and vertical dimension M and N as follows:

$$SSIM = \frac{1}{MN}\sum_{x=0}^{M}\sum_{y=0}^{N} SSIM(x, y) \tag{5.22}$$

The universal image quality index (UIQI) is proposed by the same authors, and it is a special case of structural similarity. The UIQI assumes C_1, C2 and C_3 constants as zero. The main concept is same with the SSIM. These three

coefficients work as limiting factors in the SSIM. Therefore, the SSIM is an improved version of the UIQI. It is given by:

$$UIQI = \frac{\sigma_{xy}}{\sigma_x \sigma_y} \frac{2\mu_x \mu_y}{{\mu_x}^2 + {\mu_y}^2} \frac{2\sigma_x \sigma_y}{{\sigma_x}^2 + {\sigma_y}^2} \tag{5.23}$$

5.2.6 Absolute Mean Brightness Error

Absolute Mean Brightness Error (AMBE) examines the loyalty of the output image to the input image in point of contrast enhancement. This method uses the difference between mean intensity values of the input and output images [51]. The difference is the absolute value, and it is always positive. The smaller difference means that the output image contains similar brightness information with the input image. The higher values indicate the distinction between input and output images. IR images have low contrast, and mean intensity value is generally shifted after contrast enhancement operation. However, higher value does not always improve the contrast. The natural appearance can be distorted by the output operation. This is the main drawback of this quality assessment method. The AMBE is formulated as follows:

$$AMBE = |E(X) - E(Y)| \tag{5.24}$$

In this formulation, E is the expected value, and it is calculated as follows:

$$E = \sum_{i=0}^{k} i \times PDF(i)\,, 0 \leq PDF(i) \leq 1\,, \tag{5.25}$$

where k is the maximum output value.

5.2.7 Image Contrast

Contrast of the image is simply its standard deviation [24]. It is calculated as follows:

$$Contrast = \sqrt{\frac{1}{MN}\sum_{i=1}^{M}\sum_{j=1}^{N}(I(i,j)-\mu)^2}\ , \tag{5.26}$$

where M and N are the image dimensions; μ is the mean of image. Higher value indicates better enhancement results.

5.3 Outputs of Contrast Enhancement Algorithms

Outputs of five image sets are presented in Figure 5-1 through Figure 5-5. Figures contain original images and outputs of the 9 contrast enhancement algorithms. Outputs of the improved methods, which contain proposed modifications for Balanced CLAHE and Enhancement with Local Frequency Cues methods, are also presented. First image set in Figure 5-1 contains an input image with 8-bit dynamic range. Second and third images in Figure 5-2 and Figure 5-3 contain input images with 14-bit dynamic range. These images are not visible due to very high dynamic range, and so they are converted to 8-bit with Linear Scaling operation. Image sets in Figure 5-4 and Figure 5-5 also contain 8-bit input images.

Experimented methods contain both global and local enhancement methods. Especially, CLAHE and Balanced CLAHE methods are implemented by using the local approach and appropriate threshold values. These threshold values are selected between 20% and 53.5% of the total pixels. In other words, CLAHE and Balanced CLAHE methods clip between 47.5% and 80% of the total pixels, and clipped values are treated as excess pixels. Same values are used for CLAHE and Balanced CLAHE operations to examine results under similar conditions. Other

parameters are selected according to the experiment results and preserved for all image sets. They are presented in Table 5-1. These values are selected according to the experiment results.

Table 5-1 Parameter Values Used in Experiments

Enhancement Method	Parameter	Value
HM	Lower Limit	30
	Upper Limit	220
TPHE	Clipping Percentage	5%
DPS	α	3
	β	3
BCLAHE	α	2
EWLFC	α_{mid}	0.5
	α_{high}	3
	β_{mid}	0.5
	β_{high}	0.5

Abbreviations of the contrast enhancement algorithms are listed in Table 5-2. Enhancement operations performed with local frequency clues, and its variations proposed in this thesis are also presented in this table. These methods are used only to improve target detail information, but there is no drastic change in the overall image contrast.

Table 5-2 Abbreviations of the Enhancement Algorithms

Abbreviation	Full Name
HE	Histogram Equalization
HM	Histogram Matching
PHE	Plateau Histogram Equalization
TPHE	Tail-Less Plateau Histogram Equalization
DPS	Detail Preserving Stretching
AHME	Adaptively Modified Histogram Equalization
CLAHE	Contrast Limited Adaptive Histogram Equalization
BCLAHE	Balanced Contrast Limited Adaptive Histogram Equalization
EWLFC	Enhancement with Local Frequency Cues
EWLFC-M-SD	Frequency information is replaced with Mean and Standard Deviation in EWLFC
EWLFC-KM	Distance matrix calculation is replaced with K-Means operation in EWLFC
EWLFC-WTC	Frequency information is replaced with Wavelet Transform Coefficient in EWLFC
EWLFC-KMMSD	Enhancement with Mean and Standard Deviation by using K-Means operation

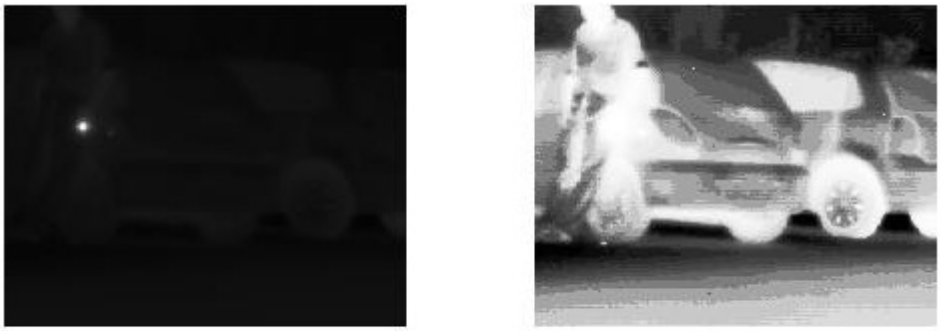

a b

Figure 5-1 Outputs of Contrast Enhancement Algorithms on Image Set 1 (a) Original Image, (b) Histogram Equalization Output

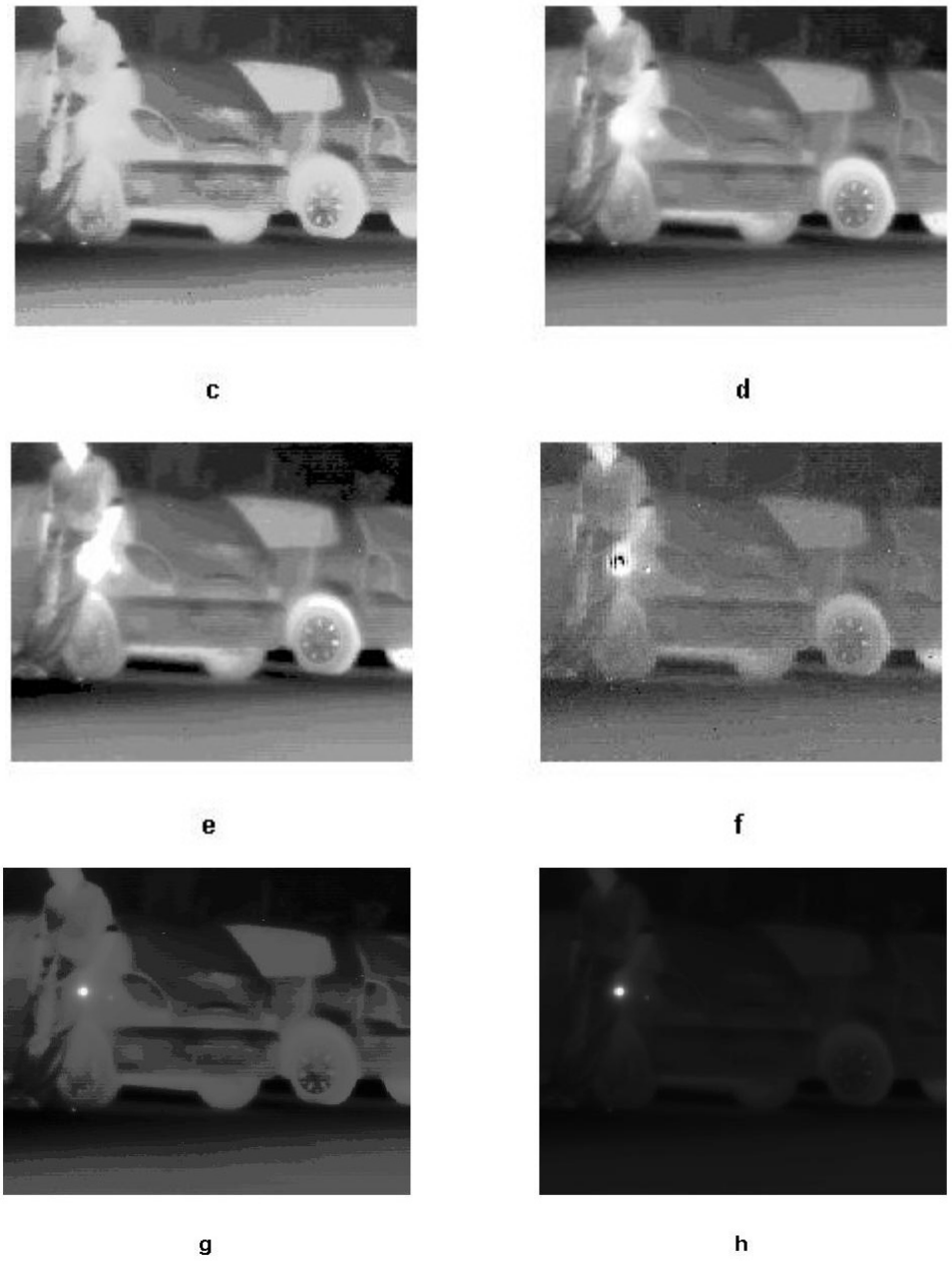

Figure 5-1 Outputs of Contrast Enhancement Algorithms on Image Set 1 (c) Histogram Matching Output, (d) Plateau Histogram Equalization Output, (e) Tail-Less Plateau Histogram Equalization Output, (f) Detail-Preserving Stretching Output, (g) AHME Output, (h) CLAHE Output with 4 blocks (continued)

i

j

k

l

m

n

Figure 5-1 Outputs of Contrast Enhancement Algorithms on Image Set 1 (i) CLAHE Output with 9 blocks, (j) Balanced CLAHE Output with 4 blocks, (k) Balanced CLAHE Output with 9 blocks, (l) Balanced CLAHE Output with PM1, (m) Balanced CLAHE Output with PM2, (n) EWLFC Output (continued)

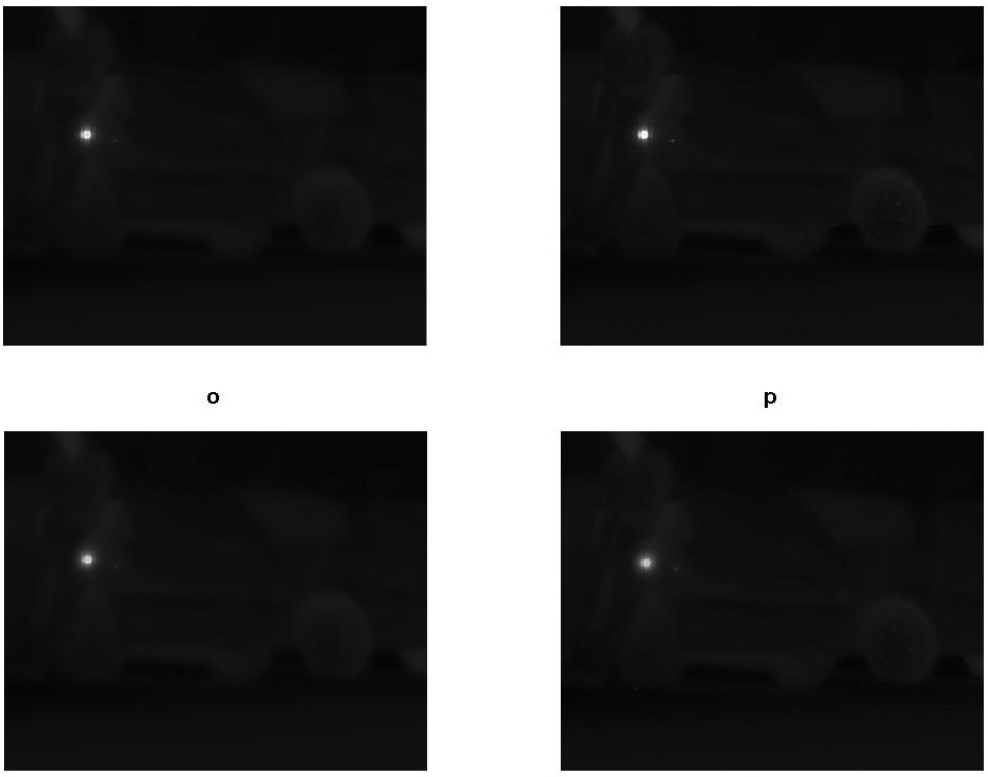

o p

r s

Figure 5-1 Outputs of Contrast Enhancement Algorithms on Image Set 1 (o) EWLFC-M-SD Output, (p) EWLFC-KM Output, (r) EWLFC-WTC Output, (s) EWLFC-KMMSD Output (continued)

a b

Figure 5-2 Outputs of Contrast Enhancement Algorithms on Image Set 2 (a) Original Image, (b) Histogram Equalization Output

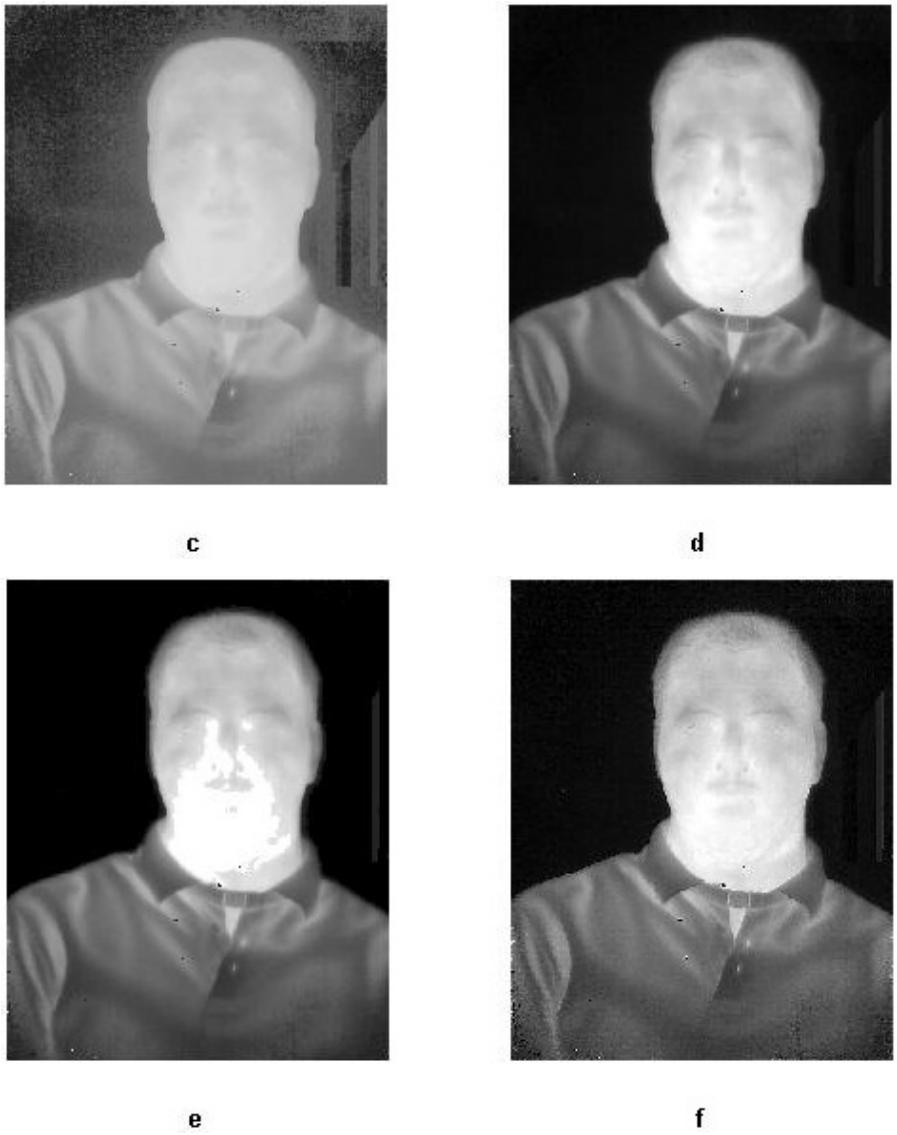

Figure 5-2 Outputs of Contrast Enhancement Algorithms on Image Set 2 (c) Histogram Matching Output, (d) Plateau Histogram Equalization Output, (e) Tail-Less Plateau Histogram Equalization Output, (f) Detail-Preserving Stretching Output (continued)

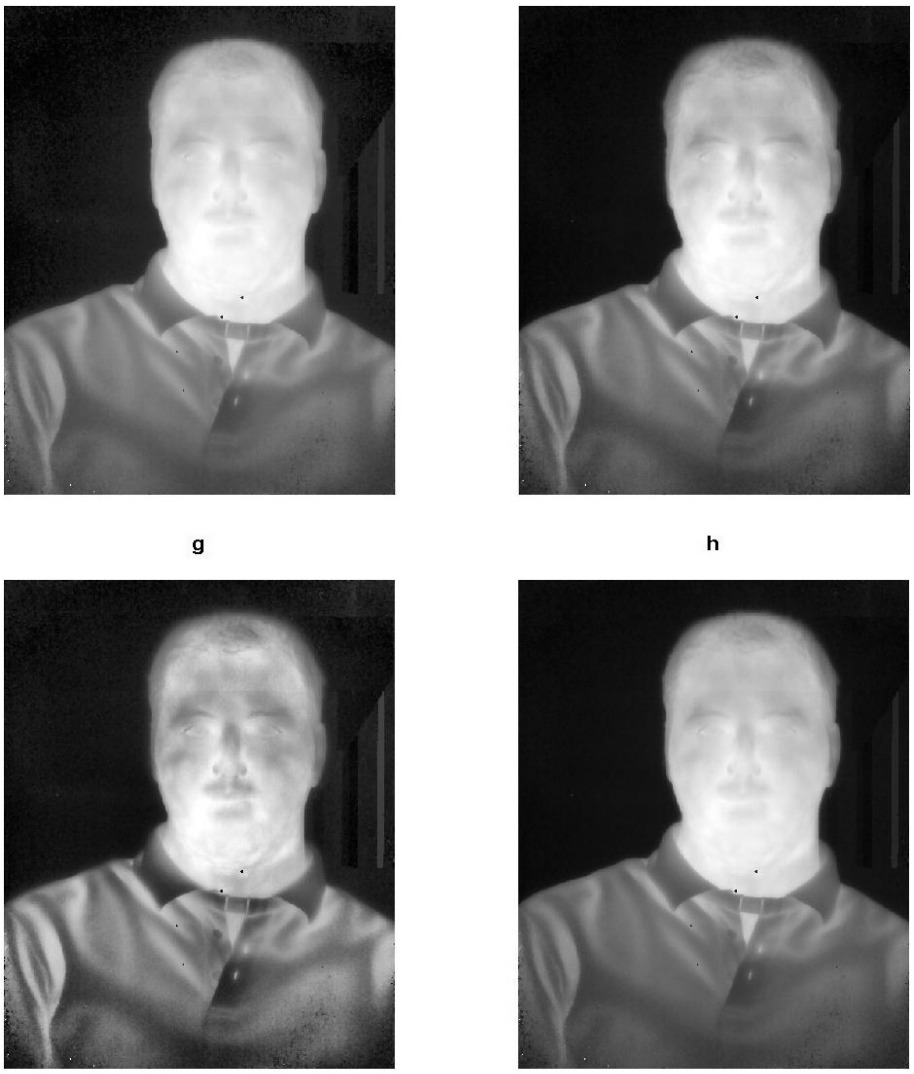

g h

i j

Figure 5-2 Outputs of Contrast Enhancement Algorithms on Image Set 2 (g) AHME Output, (h) CLAHE Output with 4 blocks, (i) CLAHE Output with 9 blocks, (j) Balanced CLAHE Output with 4 blocks (continued)

k

l

m

n

Figure 5-2 Outputs of Contrast Enhancement Algorithms on Image Set 2 (k) Balanced CLAHE Output with 9 blocks, (l) Balanced CLAHE Output with PM1, (m) Balanced CLAHE Output with PM2, (n) EWLFC Output (continued)

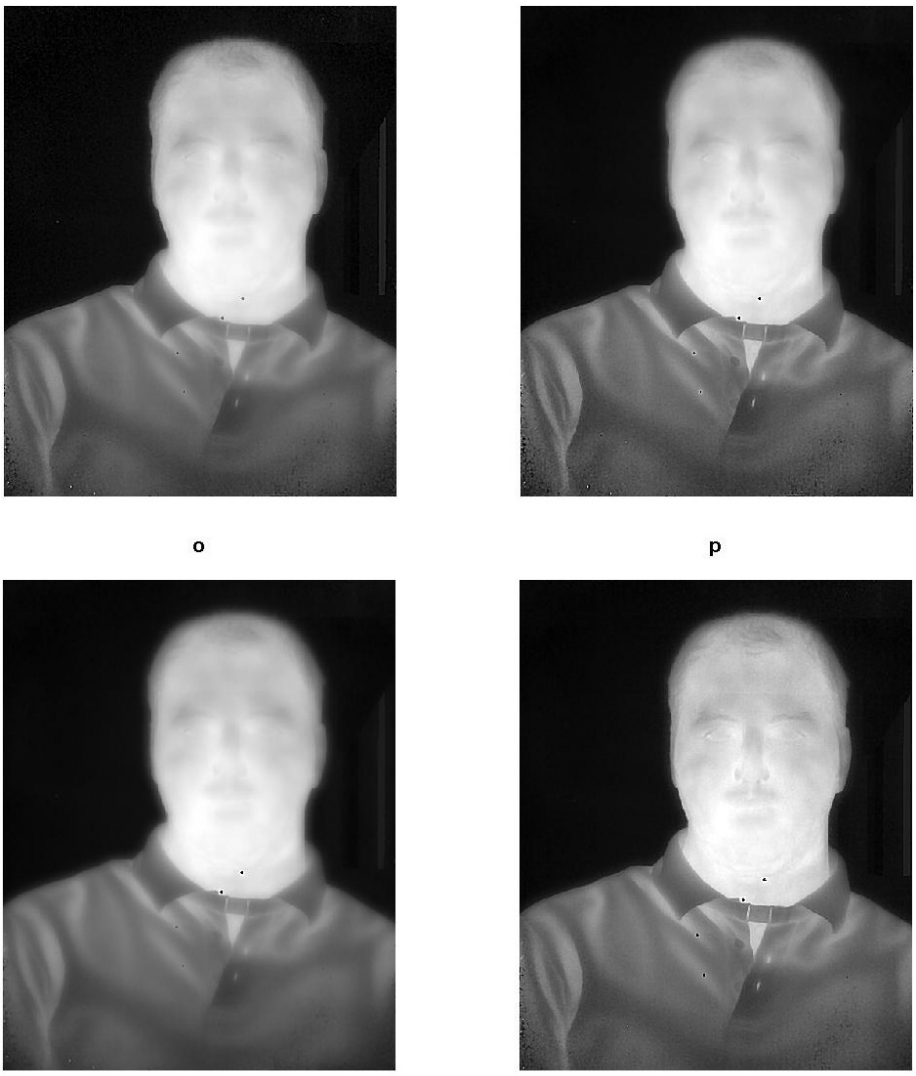

Figure 5-2 Outputs of Contrast Enhancement Algorithms on Image Set 2 (o) EWLFC-M-SD Output, (p) EWLFC-KM Output, (r) EWLFC-WTC Output, (s) EWLFC-KMMSD Output (continued)

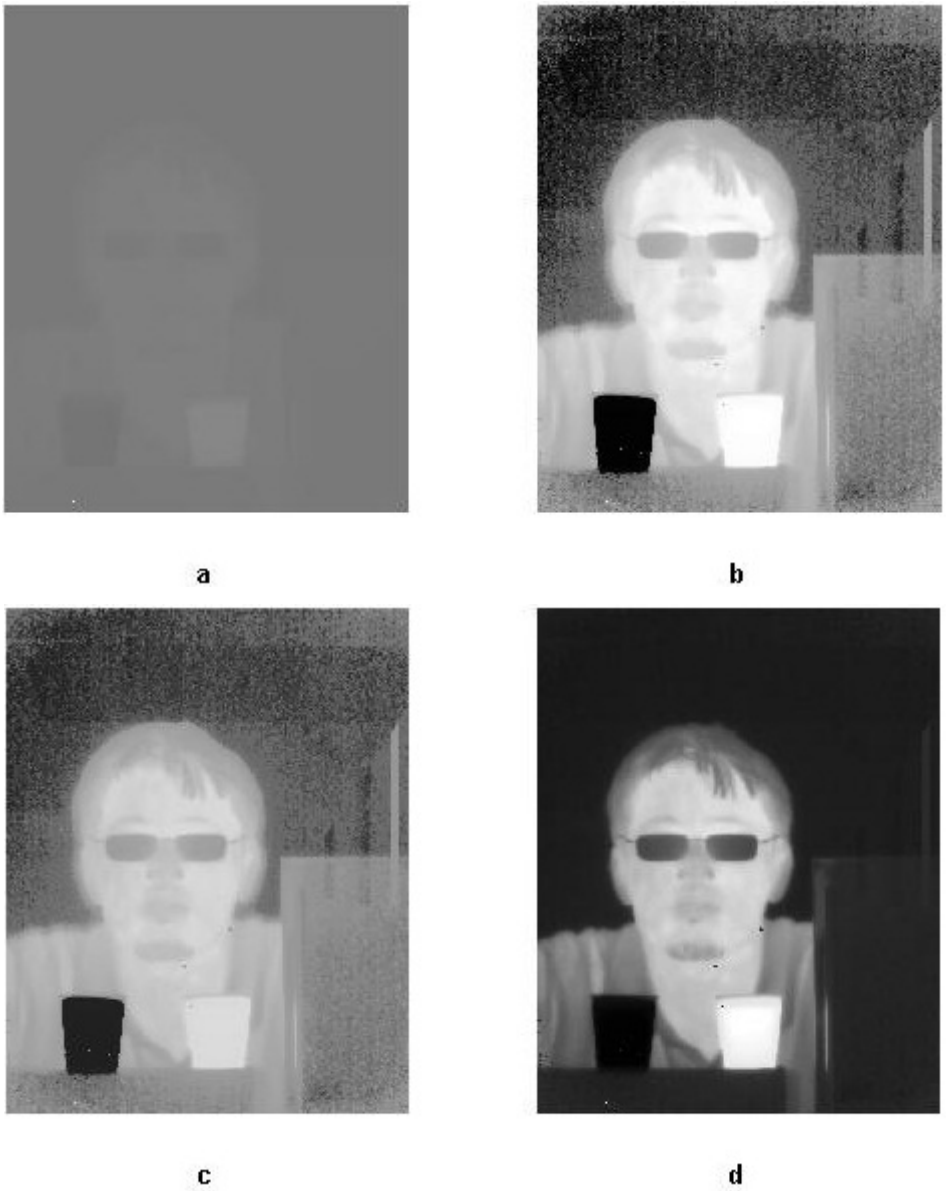

Figure 5-3 Outputs of Contrast Enhancement Algorithms on Image Set 3 (a) Original Image, (b) Histogram Equalization Output, (c) Histogram Matching Output, (d) Plateau Histogram Equalization Output

e

f

g

h

Figure 5-3 Outputs of Contrast Enhancement Algorithms on Image Set 3 (e) Tail-Less Plateau Histogram Equalization Output, (f) Detail-Preserving Stretching Output, (g) AHME Output, (h) CLAHE Output with 4 blocks (continued)

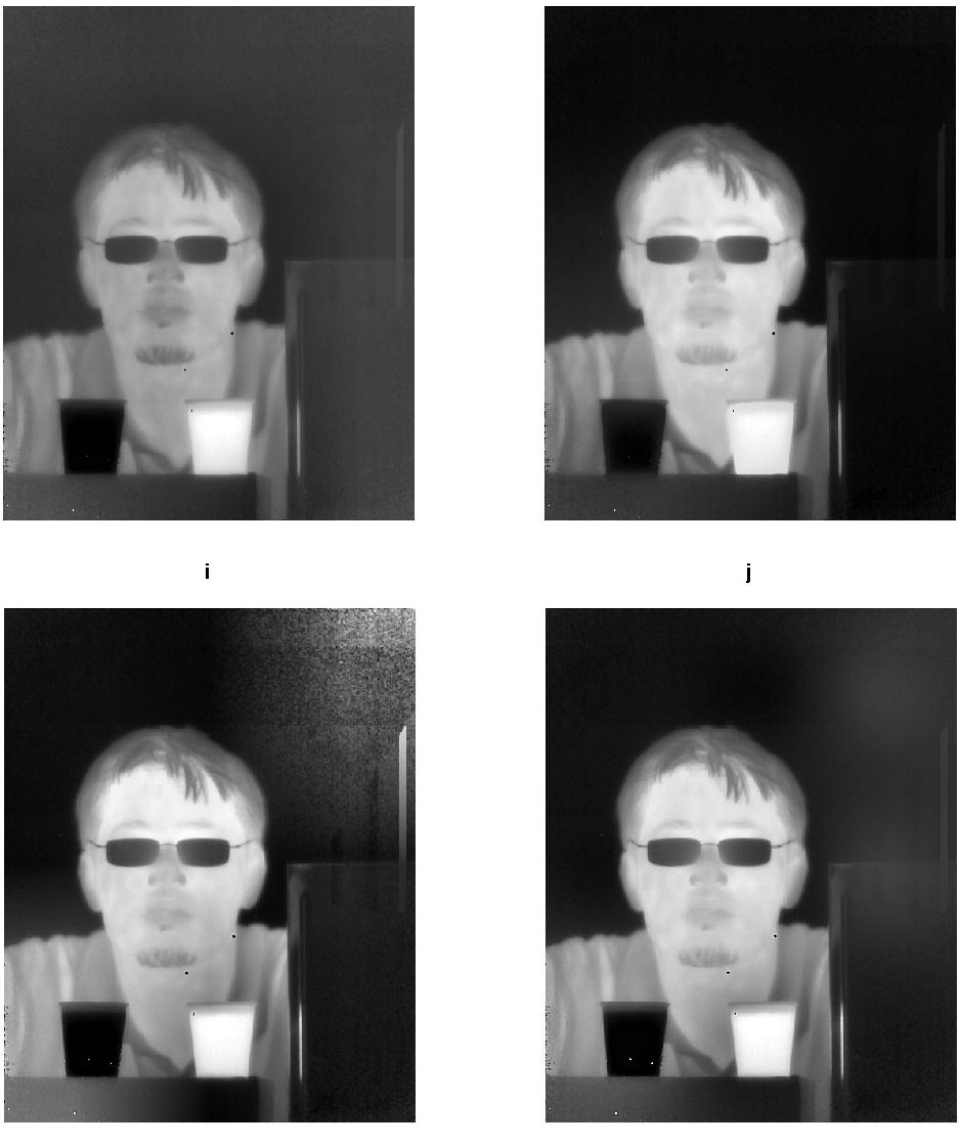

i j

k l

Figure 5-3 Outputs of Contrast Enhancement Algorithms on Image Set 3 (i) CLAHE Output with 9 blocks, (j) Balanced CLAHE Output with 4 blocks, (k) Balanced CLAHE Output with 9 blocks, (l) Balanced CLAHE Output with PM1 (continued)

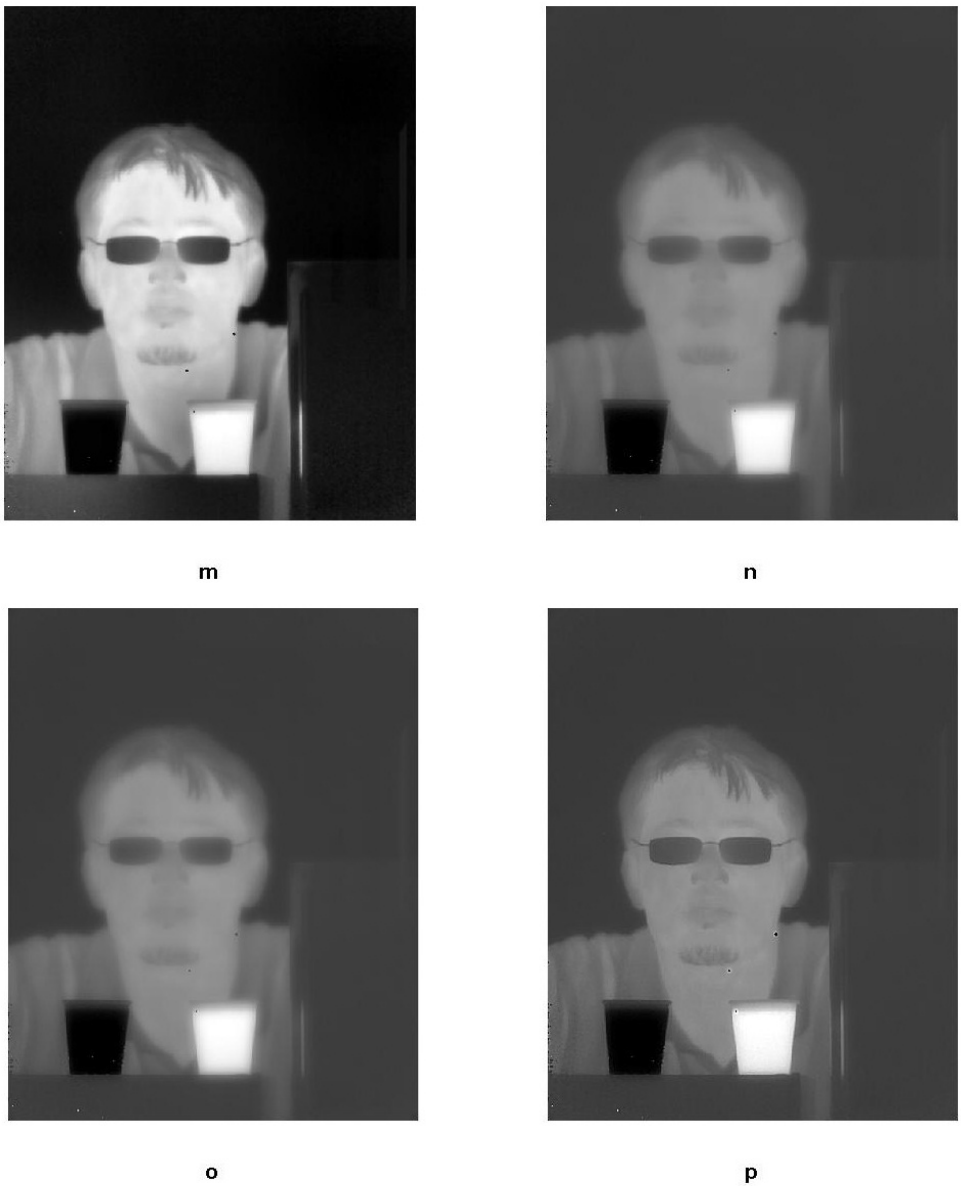

m n

o p

Figure 5-3 Outputs of Contrast Enhancement Algorithms on Image Set 3 (m) Balanced CLAHE Output with PM2, (n) EWLFC Output, (o) EWLFC-M-SD Output, (p) EWLFC-KM Output (continued)

r s

Figure 5-3 Outputs of Contrast Enhancement Algorithms on Image Set 3 (r) EWLFC-WTC Output, (s) EWLFC-KMMSD Output (continued)

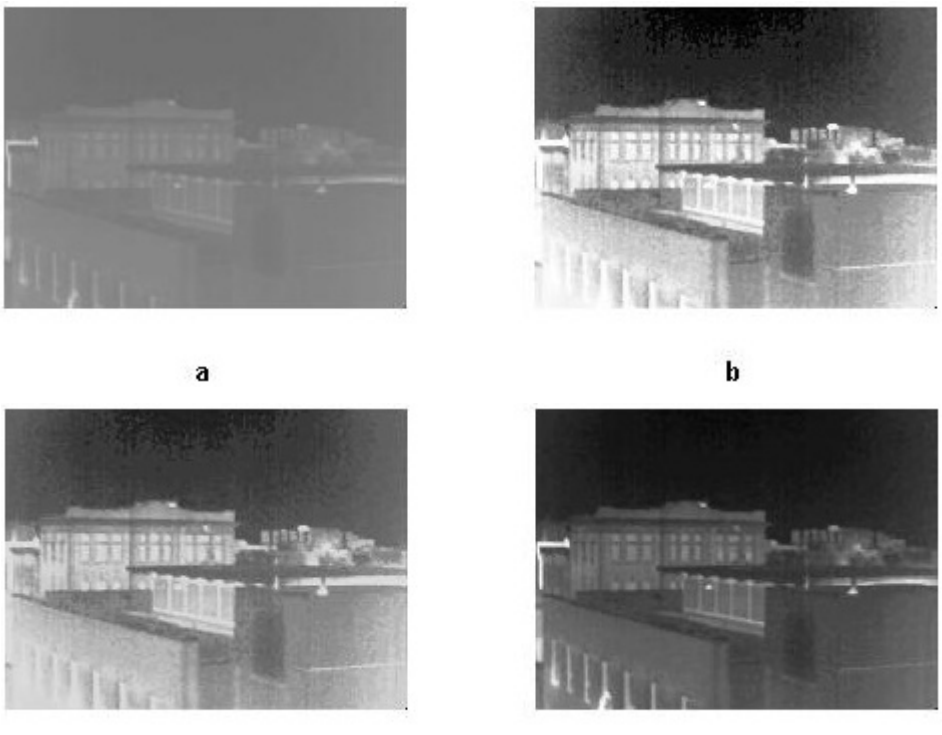

a b

c d

Figure 5-4 Outputs of Contrast Enhancement Algorithms on Image Set 4 (a) Original Image, (b) Histogram Equalization Output, (c) Histogram Matching Output, (d) Plateau Histogram Equalization Output

e

f

g

h

i

j

Figure 5-4 Outputs of Contrast Enhancement Algorithms on Image Set 4 (e) Tail-Less Plateau Histogram Equalization Output, (f) Detail-Preserving Stretching Output, (g) AHME Output, (h) CLAHE Output with 4 blocks, (i) CLAHE Output with 9 blocks, (j) Balanced CLAHE Output with 4 blocks (continued)

k

l

m

n

o

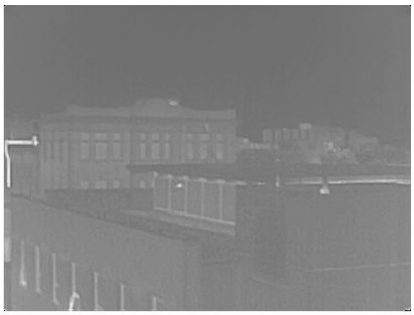

p

Figure 5-4 Outputs of Contrast Enhancement Algorithms on Image Set 4 (k) Balanced CLAHE Output with 9 blocks, (l) Balanced CLAHE Output with PM1, (m) Balanced CLAHE Output with PM2, (n) EWLFC Output, (o) EWLFC-M-SD Output, (p) EWLFC-KM Output (continued)

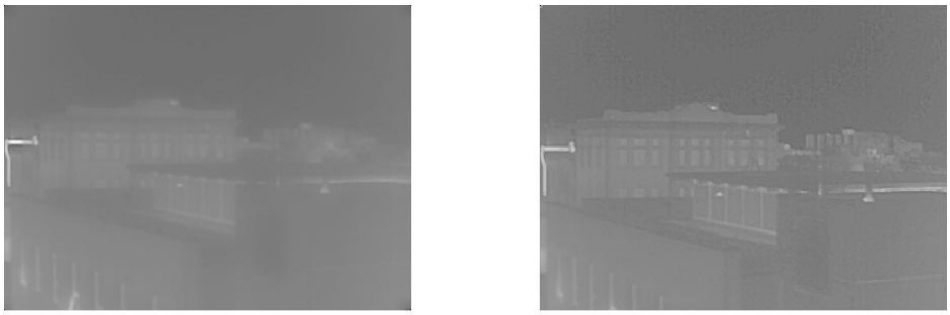

r s

Figure 5-4 Outputs of Contrast Enhancement Algorithms on Image Set 4 (r) EWLFC-WTC Output, (s) EWLFC-KMMSD Output (continued)

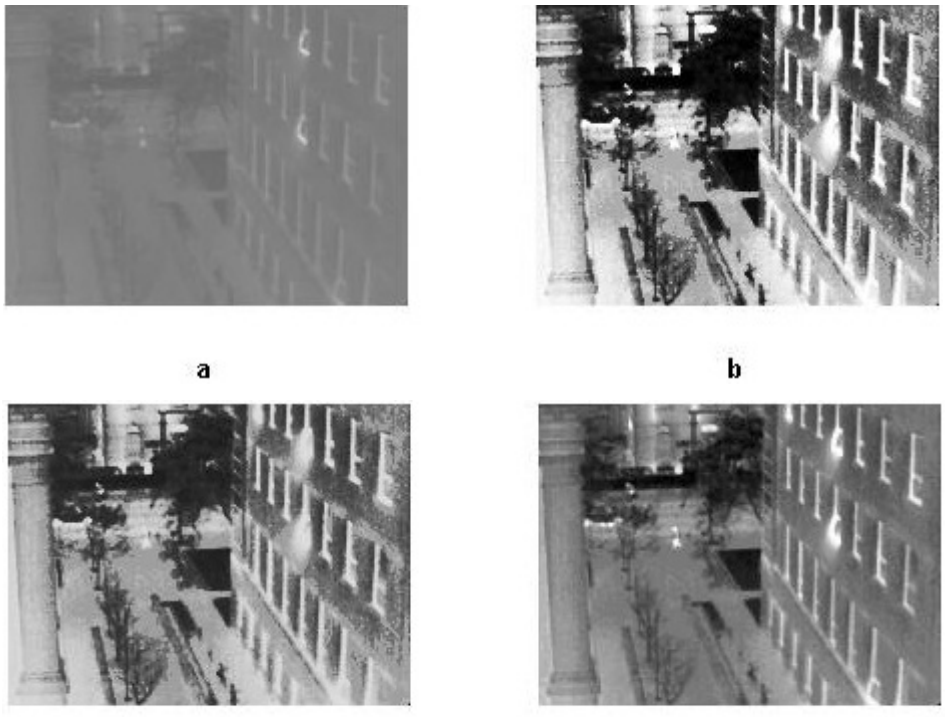

a b

c d

Figure 5-5 Outputs of Contrast Enhancement Algorithms on Image Set 5 (a) Original Image, (b) Histogram Equalization Output, (c) Histogram Matching Output, (d) Plateau Histogram Equalization Output

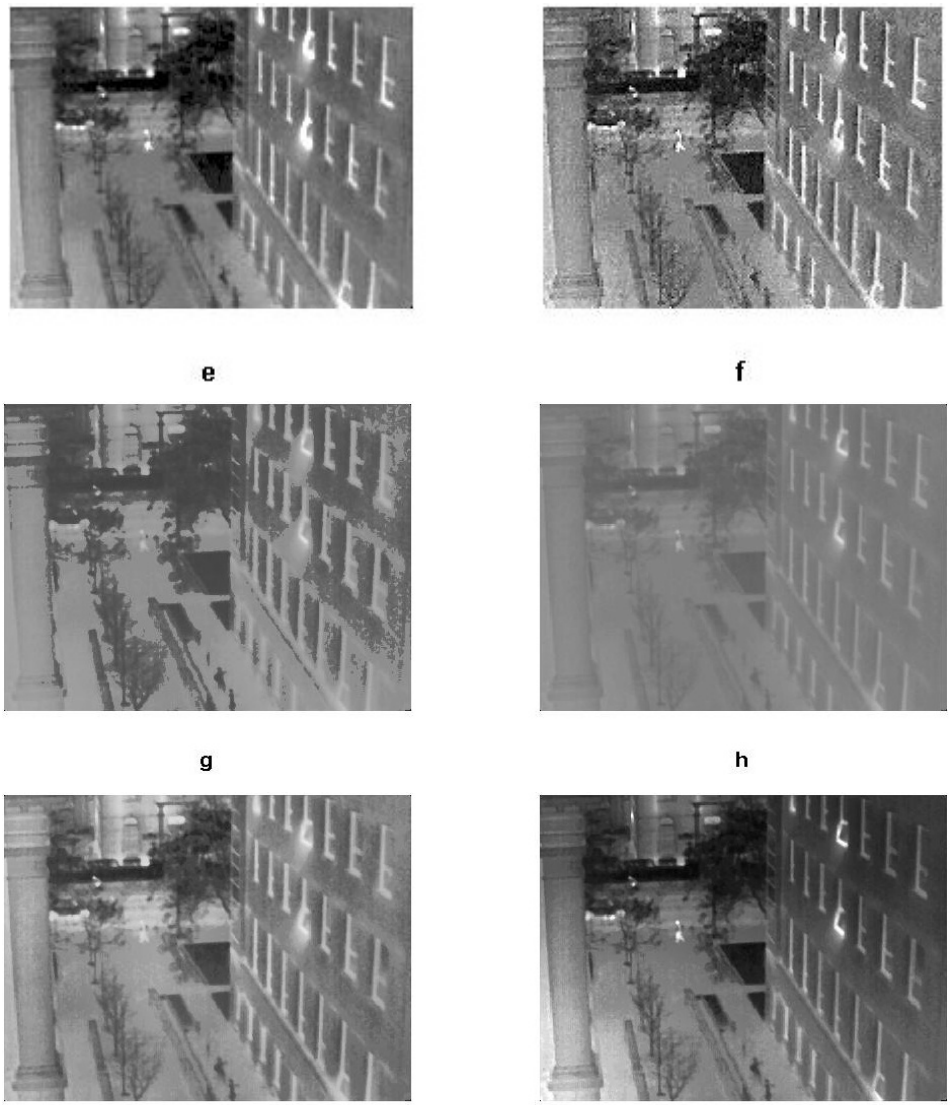

Figure 5-5 Outputs of Contrast Enhancement Algorithms on Image Set 5 (e) Tail-Less Plateau Histogram Equalization Output, (f) Detail-Preserve Stretching Output, (g) AHME Output, (h) CLAHE Output with 4 blocks, (i) CLAHE Output with 9 blocks, (j) Balanced CLAHE Output with 4 blocks (continued)

k

l

m

n

o

p

Figure 5-5 Outputs of Contrast Enhancement Algorithms on Image Set 5 (k) Balanced CLAHE Output with 9 blocks, (l) Balanced CLAHE Output PM1, (m) Balanced CLAHE Output PM2, (n) EWLFC Output, (o) EWLFC-M-SD Output, (p) EWLFC-KM Output (continued)

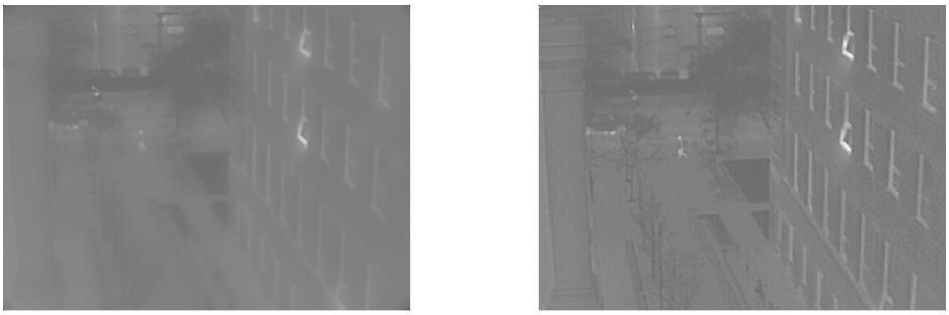

r s

Figure 5-5 Outputs of Contrast Enhancement Algorithms on Image Set 5 (r) EWLFC-WTC Output, (s) EWLFC-KMMSD Output (continued)

5.4 Results of The Objective Quality Metrics

Objective test results are obtained in order to evaluate performances of contrast enhancement methods. Gray scale images and their enhanced versions are used as test images. There are about 12 image sets used throughout this thesis. However, only the results of five image sets are given for visual comparison due to space drawback. Some quality metrics are also calculated for the original test images in order to compare them with the results of enhanced images.

All objective quality metrics used to evaluate performances of the contrast enhancement operations produce higher values for better enhancement results. Two image sets contain 14-bit images, and DRC methods are applied them to obtain 8-bit images. These low dynamic range images are used for contrast enhancement operations. Thus, contrast of the original image is measured with these 8-bit images to compare performance of the enhancement method with its true input.

Abbreviations of the objective quality metric methods are listed in Table 5-3. Table 5-2 and Table 5-3 are used in order to explain enhancement and quality metric names used in this thesis.

Table 5-3 Abbreviations of the Objective Quality Metrics

Abbreviation	Full Name
DE	Discrete Entropy
RE	Relative Entropy
MI	Mutual Information
ICUBC	Intensity Contrast Used by Chen
EUBC	Entropy Used by Chen
SSIM	Structural Similarity
UIQI	Universal Image Quality Index
AMBE	Absolute Mean Brightness Error

The first quality results are obtained from the images in Figure 5-1. Image (a) is the original image with 8-bit dynamic range. It was taken by a midwave detector with 3-5 μm spectral band. It has very low contrast and target information is not visible. Images in (b) through (s) are the enhanced versions obtained with different methods. Objective quality values of the image set in Figure 5-1 are presented in Table 5-4. This table gives the performance values according to different enhancement methods. For each quality metric column, the best and worst three methods are marked with yellow and red colors respectively.

The second and third quality results are obtained from the images in Figure 5-2 and Figure 5-3. The original images have 14-bit dynamic range. These images were also taken by a midwave detector with 3-5 μm spectral band in laboratory environment. The target information is not visible due to the very high dynamic range of the infrared system. Enhancement algorithms suppress this high dynamic range to the standard display level. Objective quality values of the original and enhanced images are presented in Table 5-5 and Table 5-6 respectively.

The fourth and fifth quality results are obtained from the images in Figure 5-4 and Figure 5-5. Original images have 8-bit dynamic range and washout appearance. They were taken by a midwave detector with 3-5 µm spectral band in a real-world environment. Image quality values of the original and enhanced images are presented in Table 5-7 and Table 5-8 respectively.

Results of quality metrics are also drawn in Figure 5-6 through Figure 5-11. In these plots, each line represents the objective quality results of an enhancement method according to different image sets.

Table 5-4 Outputs of the Quality Metrics for Images in Figure 5-1

Method Name	DE	ICUBC	EUBC	UIQI	AMBE	Contrast
Org Img	3,9334	0,7653	4,4784	-	-	6,5137
HE	3,8951	50,7169	4,4255	0,0779	124,1224	74,4275
HM	3,8824	27,9148	4,4090	0,0755	119,1857	55,4072
PHE	3,9179	17,8980	4,4583	0,0821	101,4893	50,8972
TPHE	3,7908	24,7642	4,2954	0,0735	100,6672	53,8464
DPS	6,2614	187,4994	9,1585	0,0476	92,4963	33,9203
AHME	3,9308	10,1850	4,4754	0,2856	39,2263	30,3764
CLAHE (4 block)	4,4893	0,8787	5,1008	0,8565	5,3074	8,1828
CLAHE (9 block)	6,2957	4,1582	7,0762	0,2085	31,6932	22,0832
BCLAHE (4 block)	7,3925	25,2238	9,4916	0,1131	78,5053	49,0748
BCLAHE (9 block)	7,5439	19,5264	10,5106	0,0283	102,1772	49,1636
BCLAHE (PM1)	5,6249	3,4614	7,2929	0,2299	17,4154	14,5342
BCLAHE (PM2)	7,0175	4,5444	8,8865	0,1322	46,1288	39,7839
EWLFC	3,8968	1,5433	4,4260	0,8436	0,0067	6,3142
EWLFC-M-SD	3,8968	1,7448	4,4293	0,8456	0,0066	6,3686
EWLFC-KM	3,9712	2,8358	5,0846	0,7701	0,0003	6,6611
EWLFC-WTC	3,8968	0,8354	4,4094	0,8292	0,0059	6,0668
EWLFC-KMMSD	3,9809	0,8615	5,0500	0,2014	0,0567	6,1218

Table 5-5 Outputs of the Quality Metrics for Images in Figure 5-2

Method Name	DE	ICUBC	EUBC	UIQI	AMBE	Contrast
Org Img	7,1029	15,4031	9,9928	-	-	75,0354
HE	6,7707	64,7583	9,3877	0,5647	42,8266	72,2268
HM	6,5826	35,4500	9,0544	0,5399	40,3893	53,8126
PHE	7,0873	15,7471	9,9665	0,9894	0,7106	74,6187
TPHE	5,3721	20,1341	7,2331	0,5765	4,6007	80,8787
DPS	7,3587	85,1600	11,8668	0,6226	0,2073	75,4819
AHME	7,0419	21,8079	9,8833	0,8103	11,5066	73,0063
CLAHE (4 block)	7,2978	16,9688	10,3940	0,9634	1,5474	73,4343
CLAHE (9 block)	7,5255	32,4608	11,1350	0,7079	5,4463	69,2223
BCLAHE (4 block)	7,1120	14,4845	10,0140	0,9498	0,4993	71,6525
BCLAHE (9 block)	7,8092	154,8407	12,2429	0,4251	18,5479	72,5434
BCLAHE (PM1)	7,4439	41,0621	11,3480	0,5486	7,6966	79,6370
BCLAHE (PM2)	7,4500	20,5955	10,7912	0,6607	6,9461	79,9412
EWLFC	7,3215	16,4392	10,5537	0,8390	0,0673	74,5185
EWLFC-M-SD	7,3221	20,4263	10,7371	0,8516	0,0667	74,5148
EWLFC-KM	7,2204	28,7146	10,4684	0,8429	0,0245	74,6583
EWLFC-WTC	7,2051	8,1906	9,6208	0,7923	0,0414	74,1406
EWLFC-KMMSD	7,2016	26,3386	10,5711	0,1627	1,9033	75,9213

Table 5-6 Outputs of the Quality Metrics for Images in Figure 5-3

Method Name	DE	ICUBC	EUBC	UIQI	AMBE	Contrast
Org Img	5,4811	5,5153	7,3684	-	-	38,3418
HE	5,2887	177,2458	7,0568	0,3418	53,2116	68,8341
HM	5,1944	98,4246	6,8938	0,3746	49,6362	51,2467
PHE	5,4432	13,7362	7,3106	0,6809	7,3659	65,9549
TPHE	5,2375	30,5910	7,0475	0,5929	8,1093	67,2815
DPS	6,1330	59,2344	9,9510	0,4599	23,9266	46,5444
AHME	5,4585	31,0504	7,3338	0,5538	30,8551	48,2600
CLAHE (4 block)	5,7301	6,7677	7,8219	0,9312	1,4873	44,0943
CLAHE (9 block)	6,7258	11,4959	9,2843	0,7003	3,9313	48,5312
BCLAHE (4 block)	6,6218	15,2249	9,4686	0,4458	14,7782	75,1503
BCLAHE (9 block)	7,4280	52,2791	11,0442	0,2832	0,2050	72,0340
BCLAHE (PM1)	7,2734	25,1769	10,3705	0,3429	3,1314	68,4919
BCLAHE (PM2)	6,9718	16,7715	9,8261	0,3253	13,3410	76,3943
EWLFC	5,4950	3,9954	7,1359	0,7681	0,0411	37,7297
EWLFC-M-SD	5,4947	4,0748	7,1392	0,7698	0,0402	37,7399
EWLFC-KM	5,5186	9,0828	7,6048	0,8489	0,0106	38,1485
EWLFC-WTC	5,5099	3,6629	7,0831	0,7397	0,0237	37,6199
EWLFC-KMMSD	5,5720	8,0358	7,6196	0,1260	0,9072	38,7381

Table 5-7 Outputs of the Quality Metrics for Images in Figure 5-4

Method Name	DE	ICUBC	EUBC	UIQI	AMBE	Contrast
Org Img	4,8587	3,8882	6,6523	-	-	11,0525
HE	4,8062	91,6769	6,5705	0,2452	6,6712	72,7463
HM	4,7780	50,6757	6,5211	0,3357	3,2213	54,1925
PHE	4,8584	31,1194	6,6520	0,4174	57,2105	36,2362
TPHE	4,6588	46,9632	6,3429	0,3755	60,1331	40,7639
DPS	7,1216	300,9483	12,3418	0,1917	1,3472	43,9300
AHME	4,8552	20,7016	6,6487	0,5975	0,4655	29,2402
CLAHE (4 block)	5,6722	7,5179	7,8336	0,8569	4,3699	14,9193
CLAHE (9 block)	6,7055	50,5696	9,6968	0,3316	1,4829	27,5573
BCLAHE (4 block)	6,4941	45,8349	9,4128	0,3484	69,3251	27,5867
BCLAHE (9 block)	7,1044	87,7990	10,6651	0,2578	39,3131	39,1604
BCLAHE (PM1)	6,8907	63,4574	10,4373	0,3037	42,0107	32,9389
BCLAHE (PM2)	7,2438	52,0278	10,3755	0,2476	64,6442	43,7826
EWLFC	5,0733	5,3014	6,7659	0,8033	0,0282	10,8386
EWLFC-M-SD	5,0736	5,3466	6,7753	0,8059	0,0282	10,8442
EWLFC-KM	5,1815	12,5143	7,8246	0,7885	0,0014	11,7588
EWLFC-WTC	5,0740	2,2266	6,5108	0,7269	0,0380	10,5570
EWLFC-KMMSD	5,2121	6,8853	7,9955	0,0365	0,6382	10,9507

Table 5-8 Outputs of the Quality Metrics for Images in Figure 5-5

Method Name	DE	ICUBC	EUBC	UIQI	AMBE	Contrast
Org Img	4,3643	5,2824	6,6034	-	-	7,4372
HE	4,3291	580,0714	6,5503	0,1578	10,4565	74,5056
HM	4,3133	320,8815	6,5227	0,2371	5,9057	55,5312
PHE	4,3586	127,2075	6,5987	0,3373	11,3996	38,3410
TPHE	4,2981	138,0254	6,5021	0,3311	11,6123	39,5210
DPS	7,3043	722,6384	13,2288	0,1534	1,2501	46,9530
AHME	4,3623	126,9541	6,6018	0,4621	4,0014	31,0330
CLAHE (4 block)	5,2843	12,6056	7,8551	0,8710	0,2086	11,8330
CLAHE (9 block)	6,9733	97,0107	10,3625	0,3466	4,1479	32,2792
BCLAHE (4 block)	7,2937	87,5316	11,1200	0,3748	31,1053	43,3820
BCLAHE (9 block)	7,3059	121,1893	11,2200	0,2882	45,1640	44,9003
BCLAHE (PM1)	7,2907	122,3606	11,1999	0,2926	45,0484	41,7829
BCLAHE (PM2)	7,2812	101,8669	10,9342	0,3068	45,1984	41,3364
EWLFC	4,4584	2,9390	6,4432	0,7719	0,0315	6,3747
EWLFC-M-SD	4,4584	2,9384	6,4416	0,7714	0,0319	6,3743
EWLFC-KM	4,6333	6,8818	7,3096	0,8498	0,0308	7,1297
EWLFC-WTC	4,4625	2,2716	6,4706	0,7786	0,0321	6,2702
EWLFC-KMMSD	4,8488	17,6166	8,1909	0,0833	0,1969	8,4365

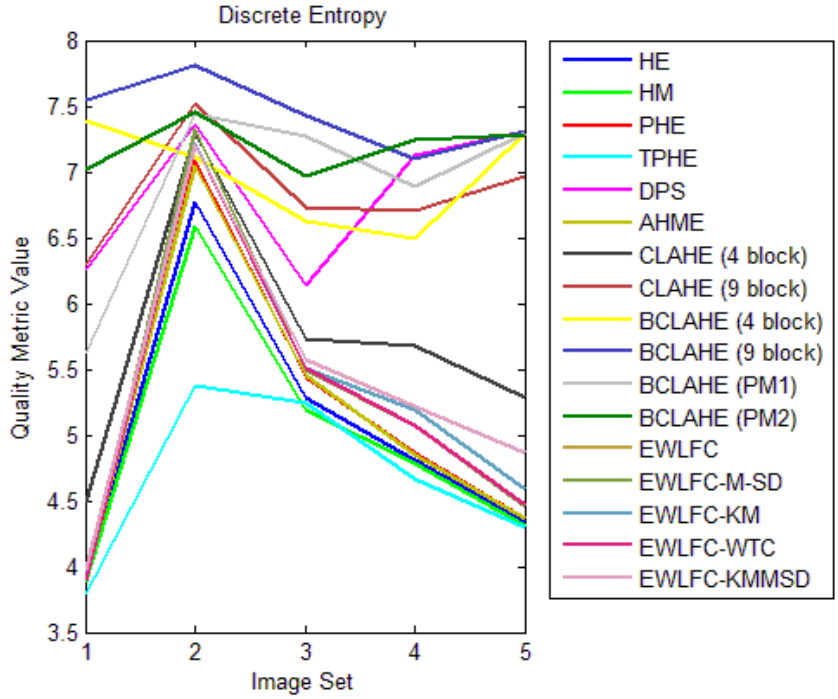

Figure 5-6 Discrete Entropy Results of Enhancement Methods With Different Image Sets

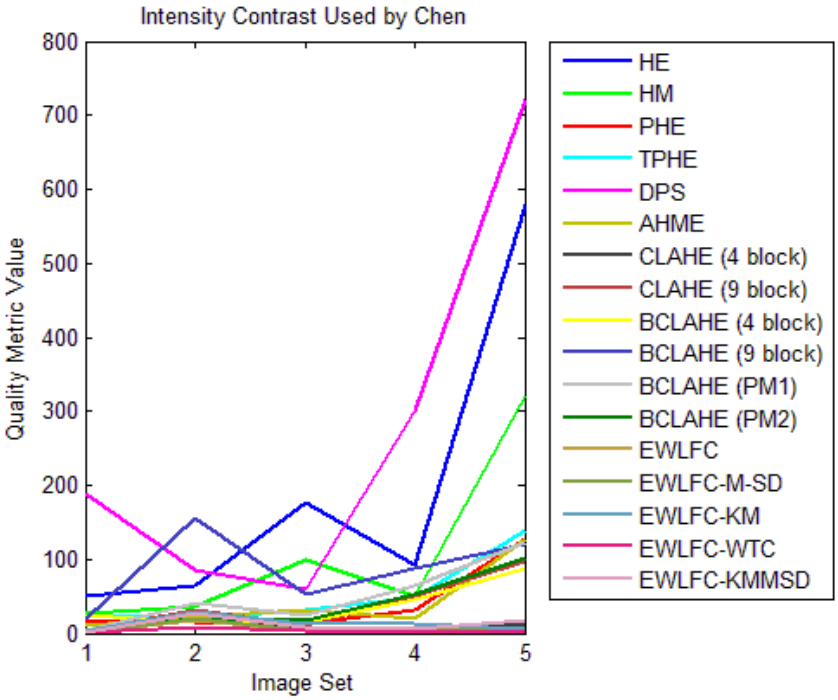

Figure 5-7 Intensity Contrast Results of Enhancement Methods With Different Image Sets

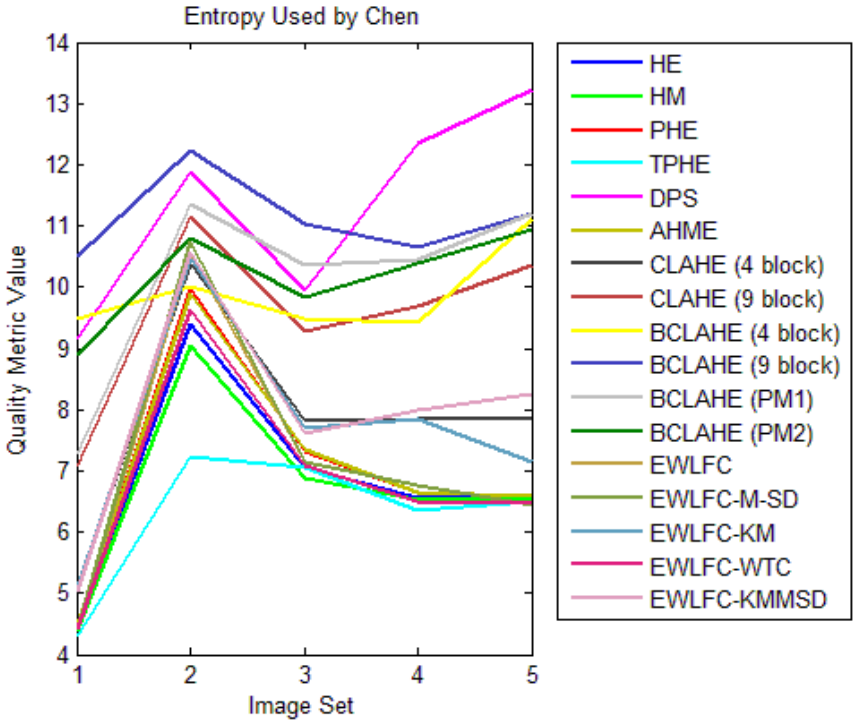

Figure 5-8 Entropy Results of Enhancement Methods With Different Image Sets

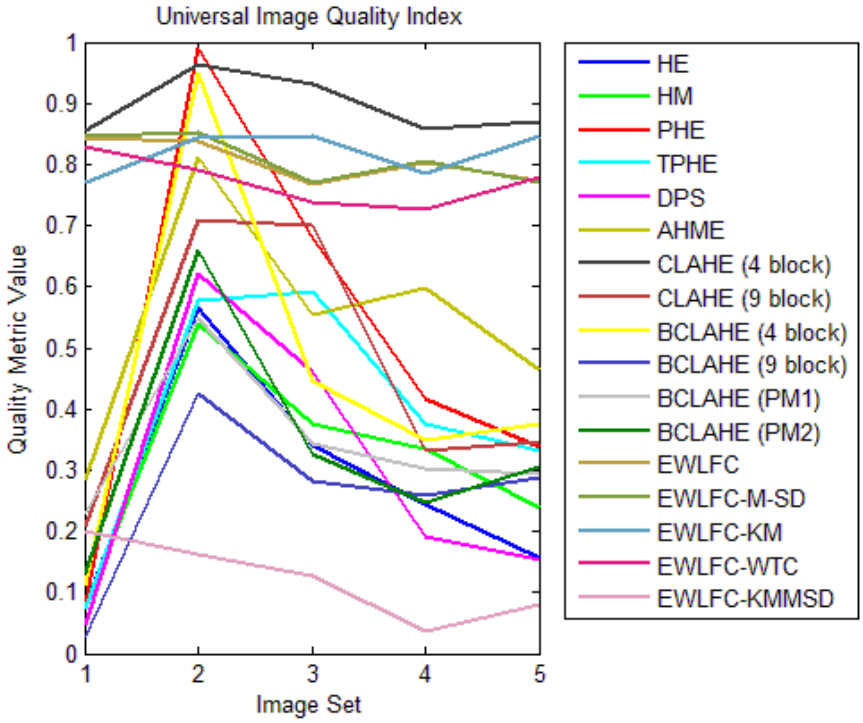

Figure 5-9 UIQI Results of Enhancement Methods With Different Image Sets

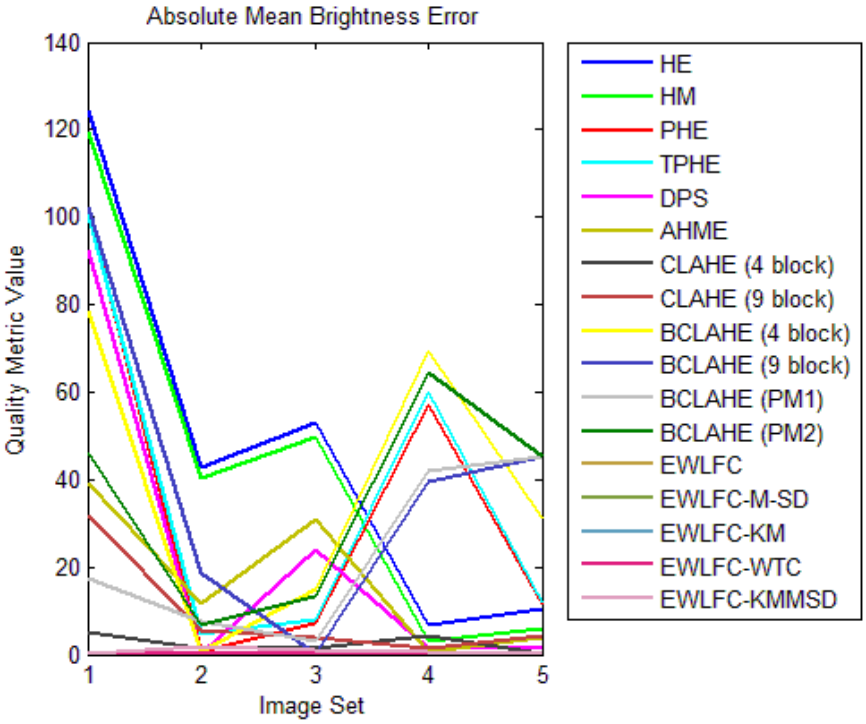

Figure 5-10 AMBE Results of Enhancement Methods With Different Image Sets

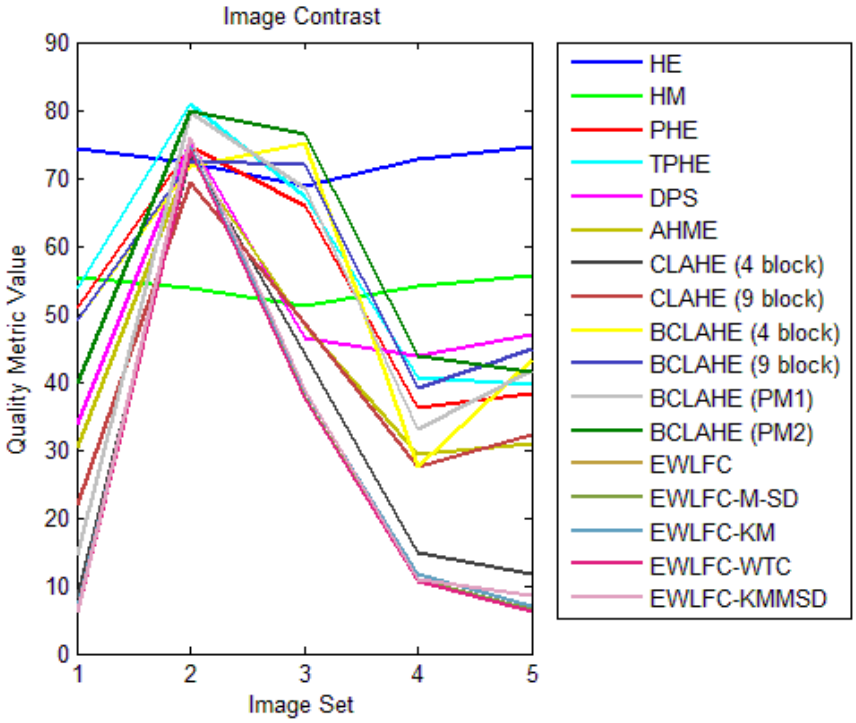

Figure 5-11 Image Contrast Results of Enhancement Methods With Different Image Sets

5.5 Summary of Objective Quality Metric Results

First image set contains an 8-bit original image with narrow gray level interval. The target information is almost invisible. Outputs of the contrast enhancement methods are presented in Figure 5-1. Histogram equalization method produces an over enhanced output image. The detail information is mostly saturated. Histogram matching method also gives a close result to the histogram equalization method. PHE and TPHE with tail value of 5% have similar outputs, and their outputs have better visibility compared to the previous two methods. It is clear from the results that DPS and AHME methods produce unnatural looking images. DPS particularly damages the output image and gives an image with granular parts. CLAHE method is used with 4 and 9 blocks. An appropriate threshold value is also selected. It gives better enhancement results compared to the other ones. Especially, CLAHE method with 9 blocks has improved overall contrast. Balanced CLAHE method is also applied with a local approach by using 4 and 9 blocks. This method produces a darker part at the top left of image for local implementation with 4 blocks. This problem associated with Balanced CLAHE method is mentioned in Chapter 4. The other parts are fairly satisfying. Balanced CLAHE with 9 blocks and proposed modifications for this method produce better results. The method based on the local frequency clues, and its modified versions produce an image with enhanced detail information. However, they do not improve overall contrast as mentioned before.

Quality metric results for image set 1 are presented in Table 5-4. Discrete entropy values show that Balanced CLAHE method with 9 blocks produces an image with highest bit rate. Balanced CLAHE method with 4 blocks and proposed modification 2 for this method also have higher values. The other histogram based methods does not improve visibility according to the discrete entropy metric, although they improve the contrast.

The method based on the local frequency clues enhances edge information, and so output bit rate does not change excessively. Its modified versions have the same effect. Entropy used by Chen also gives a similar result to discrete entropy metric. Intensity contrast metric shows that DPS has better contrast while HE has better contrast with respect to AMBE and Contrast metrics. However, visual results show that these methods produce unnatural looking and saturated images.

Second image set in Figure 5-2 contains a 14-bit original image with narrow gray level interval. The image is invisible due to very high dynamic range. Balanced CLAHE method converts this high dynamic range to 8-bit display format with its algorithm. However, other methods do not have this type of operation. Therefore, input dynamic range is compressed with linear scaling to produce 8-bit input images for these algorithms. Once again, HE and HM methods produce over enhanced output images. The detail information is mostly saturated. PHE output has a better visibility compared to the previous two methods. TPHE method with tail value of 5% produces a saturated image, and DPS gives an image with granular parts. Balanced CLAHE method with 4 blocks and proposed modifications produce good enhancement results compared to the other ones. Balanced CLAHE with 9 blocks suffers from the problem mentioned in Chapter 4. However, it is suppressed with proposed modifications. CLAHE method also has a satisfying output. The method based on the local frequency clues, and its modified versions proposed in this thesis produce an image with enhanced detail information except EWLFC-WTC. These methods also use 8-bit input image obtained from HDR image with gamma and linear transforms. Therefore, outputs have better contrast compared to the original image. EWLFC-WTC method has a washout appearance with respect to the other four outputs in Figure 5-2 (j), Figure 5-2 (k), Figure 5-2 (l) and Figure 5-2 (n).

Quality metric results for image set 2 are presented in Table 5-5. It is very clear from this table that objective quality metrics favor Balanced CLAHE and proposed modifications for this method.

Third image set in Figure 5-3 also contains a 14-bit original image with narrow gray level interval. HE and HM methods have unsatisfying output images, and the detail information is mostly saturated. PHE output has a better visibility compared to the previous two methods. TPHE method saturates 5% of frequency counts from the beginning and end of the histogram. Therefore, other pixel intensities get more gray level. This produces a granular background. Higher tail values produce unnatural looking output images while lower tail values produce results close to PHE method. DPS and AHME produce images with washout appearances. AHME method also has rough appearance. This gives a bad impression. Balanced CLAHE method and proposed modifications produce better enhancement results compared to the other ones. Proposed modification 2 for Balanced CLAHE method corrects the problem in 9 blocks approach. It has a satisfying contrast and edge details between all enhancement methods according to the visual inspection. CLAHE method also has a satisfying output. Images in Figure 5-3 (l) and Figure 5-3 (n) have very good edge details, but they have a washout appearance due to the lack of contrast improvement of this method.

Quality metric results for the image set in Figure 5-3 are presented in Table 5-6. Metric values which depend on the contrast difference between neighbor pixels favor HE method while entropy based methods favors Balanced CLAHE, Balanced CLAHE PM1, Balanced CLAHE PM2 and DPS methods. However, high-contrast difference does not always give good enhancement results. This was seen in the experiments.

Fourth and fifth image sets contain 8-bits original images with narrow gray level interval and washout appearance. They are presented in Figure 5-4 and Figure 5-5. Clearly, PHE and Balanced CLAHE with 4 blocks have best enhancement results for visual inspection. Discrete entropy and quality metrics used by Chen favor the DPS methods for these two images. Balanced CLAHE with 9 blocks also has better enhancement results according to the quality metrics. Quality metric results for these two image sets are presented in Table 5-7 and Table 5-8 respectively.

Experiments showed that Balanced CLAHE is the best enhancement method for the most of the image sets. It has satisfying results according to the visual inspection. Entropy based quality metrics also supports these results. These quality metrics have consistent results with visual results. It is also clear that proposed methods EWLFC-KM and EWLFC-KMMSD have superior performance compared to the original method EWLFC according to both visual inspection and quality metrics. In addition to these, proposed modifications 1 and 2 for Balanced CLAHE method improve the visual quality and solve the problem with 9 blocks approach. This can be seen in images sets 2 and 3.

CHAPTER 6

CONCLUSIONS AND FUTURE WORK

Infrared imaging systems have wide application area from target acquisition to tracking operations. They operate at different spectral bands and provide information, which is impossible for human perception. However, they have high dynamic range outputs, and they generally use only a small partition of this dynamic range. Therefore, careful attention is required to display these images. This is achieved with high dynamic range compression and contrast enhancement operations. In the literature, there are approaches for infrared image enhancement. Even so, most of these methods are limited to specific applications.

This thesis investigates histogram based enhancement methods and enhancement with local frequency cues for infrared image enhancement. Different image sets with 8-bit and higher dynamic range are used to experiment on these techniques, and results are compared according to the objective quality metrics. Experiments showed that contrast enhancement operation performs better on low dynamic range images because the histogram based methods spreads all available dynamic range. Therefore, dynamic range compression method is applied to infrared images with high dynamic range to reduce noise component and obtain 8-bit images for contrast enhancement operations. Some of the contrast enhancement techniques use block based approach. Appropriate block size must be defined to obtain better results. Some modifications are proposed and experimented to select higher block dimensions to obtain better local enhancement.

Results show that Balanced CLAHE and proposed modifications for this method are the best techniques for enhancement of infrared images. Balanced CLAHE

method extracts details better than the other enhancement methods and uses all available output dynamic range. Enhancement method based on local frequency cues is also investigated. Some modifications are proposed and experimented for this technique in order to reduce computational complexity. They show better performance to improve target and edge details. However, quality metrics and visual results showed that overall contrast does not improve with these methods at all.

As future work, hardware implementation of the Balanced CLAHE algorithm can be implemented. Although it is a histogram based method, its excess pixel redistribution and dynamic range compression operations are limiting factors for real time applications. These operations can be modified to decrease hardware resource consumption. Thus, this method can be realized with FPGA and other storage resources. FPGA is considered as the main implementation platform for its timing accuracy. This platform is also very ideal for experimenting on the final behavior of the system with its advanced pre and post layout simulations. In addition to the real time implementation of Balanced CLAHE algorithm, subjective tests will be conducted.

This thesis uses TRC based dynamic range compression algorithms for their simplicity. More complex algorithms can be implemented to improve detail preservation after DRC operations. These methods will improve visual quality of the investigated contrast enhancement algorithms.

REFERENCES

[1] M. Vollmer and K.-P. Möllmann, “Infrared Thermal Imaging: Fundamentals, Research and Applications,” WILEY-VCH Verlag GmbH & Co. KGaA, Germany, 2010.

[2] G. C. Holst, Common Sense Approach to Thermal Imaging , JCD Publishing and SPIE Press, Florida and Washington USA, 2000.

[3] R. Highnam and M. Brady, “Model-Based Image Enhancement of Far Infrared Images,” IEEE Transactions on Pattern Analysis and Machine Intelligence, vol. 19, no. 4, pp. 410-415, 1997.

[4] J. M. DiCarlo and B. A. Wandella, “Rendering high dynamic range images,” Proc. SPIE, vol. 3965, pp. 392-401, 2000.

[5] J. Duan, G. Qiu, and M. Chen, “Comprehensive Fast Tone Mapping for High Dynamic Range Image Visualization,” Proc. Conf. Pacific Graphics, 2005.

[6] R. C. Gonzales and R. E. Woods, Digital Image Processing, 2nd Ed., Prentice Hall, 2002.

[7] E. Reinhard, G. Ward, S. Pattanaik, P. Debevec, W.Heidrick, and K. Myszkowski, High Dynamic Range Imaging: Acquisition, Display and Image-Based Lighting, 2nd Ed., Morgan Kaufmann Publishers, 2010.

[8] G. W. Larson, H. Rushmeier, and C. Piatko, “A Visibility Matching Tone Reproduction Operator for High Dynamic Range Scenes,” IEEE Transactions on Visualization and Computer Graphics, vol. 3, no. 4, pp. 291-306, 1997.

[9] R. Fattal, D. Lischinski, and M. Werman, ‘”Gradient domain high dynamic range compression,” Proc. 29th Annu. Conf. on Computer Graphics and Interactive Techniques, pp. 249-256, 2001.

[10] Y. Monobe, H. Yamashita, T. Kurosawa, and H. Kotera, “Dynamic range compression preserving local image contrast for digital video camera,” IEEE Trans. on Consumer Electronics, vol. 51, pp. 1-10,2005.

[11] F. Durand and J. Dorsey, “Fast bilateral filtering for the display of high-dynamic-range images,” Proc. 29th Annu. Conf. on Computer Graphics and Interactive Techniques, pp. 257-266, 2002.

[12] S. Weith-Glushko and C. Salvaggio, “Quantitative analysis of infrared contrast enhancement algorithms,” Proc. SPIE, Infrared Imaging Systems: Design, Analysis, Modeling, and Testing XVIII, vol. 6543, pp. 1-11, 2007.

[13] A. Polesel, G. Ramponi, and V. J. Mathews, “Image Enhancement via Adaptive Unsharp Masking,” IEEE Trans. on Image Processing, vol. 9, no. 3, pp. 505-510, 2000.

[14] W. Bing-jian, L. Shang-qian, L. Qing, and Z. Hui-xin, “A real-time contrast enhancement algorithm for infrared images based on plateau histogram,” Infrared Physics & Technology, vol. 48, no. 1, pp. 77-82, 2006.

[15] H. J. Kim, J. M. Lee, J. A. Lee, S. G. Oh, and W.-Y. Kim, “Contrast Enhancement Using Adaptively Modified Histogram Equalization,” Lecture Notes in Computer Science, vol. 4319, pp. 1150-1158, 2006.

[16] A. R. Jiménez-Sánchez, J. D. Mendiola-Santibañez, I. R. Terol-Villalobos, G. Herrera-Ruíz, D. Vargas-Vázquez, J. J. García-Escalante, and A. Lara-Guevara, “Morphological Background Detection and Enhancement of Images With Poor Lighting,” IEEE Trans. on Image Processing, vol. 18, no. 3, pp. 613-623, 2009.

[17] J.-H. Kim, J.-H. Kim, S.-W. Jung, S.-J. Ko, C.-K. Noh, “Novel contrast enhancement scheme for infrared image using detail-preserving stretching,” Proc. SPIE, Opt. Eng., vol. 50, 2011.

[18] A. M. Reza, “Realization of the Contrast Limited Adaptive Histogram Equalization (CLAHE) for Real-Time Image Enhancement,” The Journal of VLSI Signal Processing, vol. 38, no. 1, pp. 35-44, 2004.

[19] F. Branchitta, M. Diani, G. Corsini and A. Porta, “Dynamic-range compression and contrast enhancement in infrared imaging systems,” Proc. SPIE, Opt. Eng., vol. 47, 2008.

[20] J. A. Stark, “Adaptive image contrast enhancement using generalizations of histogram equalization,” IEEE Trans. Image Processing , vol. 9, no. 5, pp. 889-896, 2000.

[21] Y.-T. Kim, “Contrast enhancement using brightness preserving bi-histogram equalization,” IEEE Trans. Consumer Electronics, vol. 43, no. 1, pp. 1–8, 1997.

[22] M. Ogata, T. Tsuchiya, T. Kubozono, and K. Ueda, “Dynamic range compression based on illumination compensation,” IEEE Trans. on Consumer Electronics, vol. 47, no. 3, pp. 548-558, 2001.

[23] T. Arici, S. Dikbas, and Y. Altunbasak, "A Histogram Modification Framework and Its Application for Image Contrast Enhancement," IEEE Trans. Image Processing , vol. 18, no. 9, pp. 1921-1935, 2009.

[24] A. O. Karali, O. E. Okman, and T. Aytac, “Adaptive enhancement of sea-surface targets in infrared images based on local frequency cues,” JOSA: Optics, Image Science, and Vision, vol. 27, no. 3, pp. 509-517, 2010.

[25] S. F. F. Gibson, “Calculating distance maps from binary segemented data,” MERL A Mitsubishi Electric Research Laboratory, 1998.

[26] F. Y. Shih and O. R. Mitchell, “A mathematical morphology approach to Euclidean distance transformation,” IEEE Trans. on Image Processing, vol. 1, no. 2, pp. 197-204, 1992.

[27] P. Scheunders, “Multispectral image fusion using local mapping techniques,” International Conference on Pattern Recognition, Barcelona, Spain, 2000.

[28] P. Scheunders, “Local mapping for multispectral image visualization,” Image and Vision Computing, 2001.

[29] J. Y. Kim, L. S. Kim, and S. H. Hwang, “An Advanced Contrast Enhancement Using Partially Overlapped Sub-Block Histogram Equalization,” IEEE Trans. on Circuits and Systems for Video Technology, vol. 11, no. 4, pp. 475-484, 2001.

[30] J. C. Russ, The Image Processing Handbook, 6th Ed., CRC Press, 2011.

[31] T. Saegusa and T. Maruyama, “Real-time segmentation of color images based on the K-means clustering on FPGA,” International Conference on Field-Programmable Technology, 2007.

[32] T. Kanungo, D. M. Mount, N. S. Netanyahu, C. D. Piatko, R. Silverman, and A. Y. Wu, “An Efficient k-Means Clustering Algorithm: Analysis and Implementation,” IEEE Trans. on Pattern Analysis and Machine Intelligence, vol. 24, no 7, 2002.

[33] A. Zaric, M. Loncaric, D. Tralic, M. Brzica, E. Dumic, and S. Grgic, “Image Quality Assessment - Comparison of Objective Measures with Results of Subjective Test,” 52nd International Symposium ELMAR, pp. 113-118, 2010.

[34] V. S. Petrovic´, and C. S. Xydeas, “Gradient-based multiresolution image fusion,” IEEE Trans. Image Processing , vol. 13, no. 2, pp. 228-237, 2004.

[35] V. Petrović, “Subjective tests for image fusion evaluation and objective,” International Journal of Information Fusion, pp. 208-216, 2004.

[36] L. Tian and S. I. Kamata, “An iterative image enhancement algorithm and a new evaluation framework,” IEEE International Symposium on Industrial Electronics, pp. 992-997, 2008.

[37] Y. Hu and P. C. Loizou, “Subjective comparison and evaluation of speech enhancement algorithms,” Speech Commun., vol. 49, pp. 588-601, 2007.

[38] W. S. Lin, Y. L. Gai and A. A. Kassim, “Perceptual impact of edge sharpness in images,” IEE Proceedings-Vision, Image and Signal Processing, vol. 153, no. 2, pp. 215-223, 2006.

[39] D. M. Ryan and R. D. Tinkler, “Night pilotage assessment of image fusion,” Proc. SPIE, vol. 2465, pp. 50-67,1995.

[40] P. Steele and P. Perconti, “Part task investigation of multispectral image fusion using gray scale and synthetic color night vision sensor imagery for helicopter pilotage,” Proc. SPIE, vol. 3062,1997.

[41] K. Kipli, S. Krishnan, N. Zamhari, M. S. Muhammad, Sh. M. W. Masra, K. L. Chin, and K. Lias, “Full reference image quality metrics and their performance,” IEEE 7th International Colloquium on Signal Processing and its Applications, pp. 33-38, 2011.

[42] University of Toronto, http://www.dgp.toronto.edu/~nmorris/data/IRData/, 02.10.2011

[43] Uni. of South Florida, http://marathon.csee.usf.edu/range/DataBase.html, 15.09.2011

[44] D. C. Gil, R. Farah, J. M. P. Langlois, G.-A. Bilodeau, Y. Savaria, “Comparative analysis of contrast enhancement algorithms in surveillance imaging,” IEEE International Symposium on Circuits and Systems (ISCAS), pp. 849-852, 2011.

[45] Z. Ye, H. Mohamadian, and H. Majlesein, “Adaptive Enhancement of Gray Level and True Color Images with Quantitative Measurement Using Entropy and Relative Entropy,” 40th Southeastern Symposium on System Theory, pp. 127-131, 2008.

[46] Z. Ye, H. Mohamadian, and Y. Ye, “Gray level image processing using contrast enhancement and watershed segmentation with quantitative evaluation,” CBMI, pp. 470-475, 2008.

[47] Q. Chen, X. Xu, Q. Sun, and D. Xia, “A solution to the deficiencies of image enhancement,” Signal Processing, vol. 90, no. 1, pp. 44-56, 2010.

[48] Z. Wang, A. C. Bovik, H. R. Sheikh, and E. P. Simoncelli, “Image quality assessment: from error visibility to structural similarity,” IEEE Trans. on Image Processing, vol. 13, no.4, pp. 600-612, 2004.

[49] Z. Wang and A. C. Bovik, “A Universal Image Quality Index,” IEEE Signal Processing Letters, vol. 9, no. 3, pp. 81-84, 2002.

[50] E. Blasch, X. Li, G. Chen, and W. Li, “Image quality assessment for performance evaluation of image fusion,” 11th International Conference on Information Fusion, pp. 1-6, 2008.

[51] S.-D. Chen and Abd. R. Ramli, “Minimum mean brightness error bi-histogram equalization in contrast enhancement,” IEEE Trans. on Consumer Electronics, vol. 49, no. 4, pp. 1310-1319, 2003.